UNIVERSITAT DE BARCELONA

Effective field theory methods at high temperature and chemical potential

Marc Comadran

Effective field theory methods at high temperature and chemical potential

Marc Comadran

Cristina Manuel

Universitat de Barcelona

Effective field theory methods at high temperature and chemical potential

Memòria presentada per optar al grau de doctor per la Universitat de Barcelona

Programa de doctorat en Física

Autor: Marc Comadran

Directora: Cristina Manuel

Tutor: Joan Soto

Universitat de Barcelona

Acknowledgments

Scientific research could not be without the existence of a community, a society that makes it possible. I often think that scientific discoveries can be attributed not only to the efforts of the authors themselves, but also to the entire social structure necessary so that these can be fully dedicated to research. In this sense, I feel deeply grateful to society for having given me everything I need to be able to study, and well, one could say that I am grateful and proud of humanity. For this reason, I would like to thank all the teachers I have had during my life, because, being more or less aware, they aroused in me the passion for knowledge and without them it is quite certain that I would not be writing these lines today. It has also been important to have a fantastic family, with whom I would also like to share this gratitude. I am very grateful to my parents, who have always worked hard so that we could all study and from whom I have learned a lot in this life, much more than they surely think. I could not forget my three beloved sisters, the soul of our family, who bring us joy, pride and wisdom in our home, thank you. I have to confess that I have never been the best student. When I finished my university studies, I felt that the stage of my life in contact with the academic world was coming to an end. That is why I am deeply grateful to the advisor of this thesis, Cristina Manuel, for having believed in me and in this project, also for her valuable tutelage and leadership. Not only have I learned a lot of physics from her, but also to work with rigor and critical thinking. I feel honored to have been able to work with a great researcher like her, and I hope we can continue working together in the future. I would also like to thank all the people with whom I have interacted during these years, especially, I would like to mention Stefano Carignano and Juan Torres Rincon for their advice and for the debates we have had, also Joan Soto, tutor of this thesis, for the same reasons. On the other hand, this gratitude would not be complete without thanking the organizers and participants of the schools and conferences I have attended during these years. In particular, I would like to thank the people with whom friendship has arisen, I think we have had good moments together, and I hope we can enjoy many more. Finally, I would also like to mention all my friends, for their valuable friendship, and my partner, for the pleasant company that has given me since we met.

Abstract

This thesis applies and develops effective field theory (EFT) methods for the study of high temperature and/or very dense plasmas. In a first stage of the thesis, we investigate small plasma constituent mass effects on the properties of high temperature and/or density plasmas, specifically quark-gluon plasma (QGP) and electron-positron plasma (EPP). These effects could be relevant when the fermionic masses are not extremely small compared to the plasma temperature T and/or chemical potential μ. Our study provides a first step toward addressing its impact by computing small mass ($m \ll T, \mu$) corrections to the hard thermal loop (HTL) photon polarization tensor. In order to evaluate the mass corrections, we show the usefulness of effective field theory methods, in particular, the on-shell effective field theory (OSEFT) for fermions. We compare the mass corrections with both the power and two-loop corrections, and claim that they are equally important if the mass is soft, that is, $m \sim eT$ (or $m \sim e\mu$), where e is the gauge coupling constant, but are dominant if the mass obeys $eT < m \ll T$ (or $e\mu < m \ll \mu$). Importantly, the result also applies to the HTL gluon polarization tensor, differing only by color factors. Following this, we analyzed the impact of the mass corrections in the context of collisional energy loss of a heavy and highly energetic fermion ($E, M \gg T$) traversing the QGP or EPP. Using dimensional regularization, we effectively managed the new divergences arising from the small mass expansion and demonstrated a consistent cancellation of divergences between hard and soft contributions, yielding a finite result. The mass corrections to the energy loss are determined at leading logarithmic accuracy $\sim \frac{m^2}{T^2} \ln(\frac{1}{e})$ in the regime $E \ll \frac{M^2}{T^2}$, extending the foundational work of Braaten and Thoma for massless fermions.

In a second stage of the thesis, we developed an OSEFT framework for abelian gauge fields. The final Lagrangian can be formulated in terms of a gauge invariant vector field without the need to introduce gauge fixing. We demonstrated the reparametrization invariance (RI) of the theory, which means that the Lorentz symmetry is maintained. Exploiting the RI symmetry of the EFT, we provided a first principles derivation of the side-jump effect for photons. Applications of the OSEFT in the context of EPP are presented, for instance, in quantum kinetic theory and perturbative, quantum field theory computations. In addition, we showed that when small quantum effects are considered ($\sim \hbar$), the classical definition of the polarization ratios, given in terms of the Stokes parameters, lose their Lorentz invariance. Thus, we proposed a modified definition of the polarization ratios which is Lorentz invariant when those small quantum effects are present, relevant

in non-rest frames and with potential applications in astrophysics and cosmology, where such conditions are common.

Finally, we constructed a quantum kinetic theory for photons in the presence of an axion background and in the collisionless limit, from the full theory of quantum electrodynamics (QED). We demonstrated that in the classical regime, our kinetic equations capture well-known features of axion electrodynamics. Furthermore, we addressed the impact of the axion background on the photon collective modes within an EPP at thermal equilibrium. Notably, the axion background breaks the otherwise degenerate transverse collective modes at order $eg_{a\gamma}T(\partial a)$, where e represents the electron charge, $g_{a\gamma}$ denotes the photon-axion coupling, and ∂a represents the scale associated with variations in the axion field.

Resum

Mètodes de teories efectives de camp a alta temperatura i potencial químic

Aquesta tesi aplica i desenvolupa mètodes de teories efectives de camps per a l'estudi de plasmes a alta temperatura i/o densitat. Als anys 90 es van desenvolupar els marcs teòrics necessaris per estudiar l'electrodinàmica quàntica (QED) i la cromodinàmica quàntica (QCD) en aquestes condicions extremes. Les eines desenvolupades assumien que es podia negligir la massa dels constituents del plasma. En una primera etapa de la tesi, investiguem els efectes d'incorporar masses petites associades als constituents fermiònics del plasma en els càlculs pertorbatius, rellevants quan aquestes no són extremadament petites en comparació amb la temperatura i/o el potencial químic que caracteritza el plasma. El nostre estudi proporciona un primer pas per abordar aquest impacte, calculant petites correccions massives tant al tensor de polarització dels fotons com al dels gluons, sota l'aproximació del bucle tèrmic dur. Per avaluar aquestes correccions de massa, mostrem la utilitat de les teories efectives de camps, en particular, la "on-shell effective field theory" (OSEFT) per a fermions. A continuació, analitzem l'impacte de les correccions de massa en el context de la pèrdua d'energia per col·lisió d'un fermió altament massiu i energètic, que travessa un plasma a alta temperatura i/o densitat. Considerem els dos casos següents: quan els constituents del plasma són electrons, positrons i fotons, i també quan aquests són quarks, antiquarks i gluons. Utilitzant regularització dimensional, gestionem de manera efectiva les noves divergències sorgides de l'expansió per masses petites i demostrem una cancel·lació consistent de divergències entre les contribucions dures i suaus, obtenint un resultat finit. Les correccions de massa a la pèrdua d'energia es determinen a primer ordre amb precisió logarítmica, ampliant el treball fundacional de Braaten i Thoma per a fermions sense massa. En una segona etapa de la tesi, desenvolupem una nova teoria efectiva de camps, la OSEFT per als camps de gauge abelians. La Lagrangiana final es pot formular en termes d'un camp vectorial invariant de gauge sense la necessitat d'introduir un terme de fixació de gauge. Demostrem la invariància sota reparametrització (RI) de la teoria, el qual significa que la simetria de Lorentz es respectada. Explotant la simetria RI, proporcionem una derivació des de primers principis de l'efecte de desplaçament lateral ("side-jump") per als fotons. Presentem també aplicacions de l'OSEFT de fotons en el context dels plasmes d'electrons i positrons, per exemple, en la teoria cinètica quàntica i en càlculs pertorbatius de teoria quàntica de camps. A més, demostrem que quan es consideren petits efectes purament quàntics, la

definició clàssica dels ràtios de polarització, donada en termes dels paràmetres de Stokes, perd la seva invariància de Lorentz. Proposem doncs una definició nova dels ràtios de polarització, que és invariant de Lorentz quan aquests petits efectes quàntics són presents, rellevant en sistemes de referència que no estiguin en repòs respecte el medi i amb possibles aplicacions en astrofísica i cosmologia, on aquestes condicions són habituals. Finalment, construïm una teoria cinètica quàntica per a fotons en presència d'un fons d'axions, en l'anomenat límit sense col·lisions, a partir de la teoria completa de l'electrodinàmica quàntica. Demostrem que, en el règim clàssic, les equacions cinètiques exhibeixen característiques ben conegudes de l'electrodinàmica amb axions. El formalisme que presentem permet calcular de forma sistemàtica com el límit clàssic es corregeix degut a petits efectes quàntics. A més, abordem l'impacte del fons d'axions en els modes col·lectius dels fotons que ocorren en els plasmes d'electrons i positrons en equilibri tèrmic. Notablement, el fons d'axions trenca la degeneració dels modes col·lectius transversos, mentre que el mode col·lectiu longitudinal, anomenat plasmó, no es veu afectat.

Paraules clau:

229000 FISICA ALTAS ENERGIAS,
220807 FISICA DE PARTICULAS.

Contents

Chapter content

1. **Introduction:** In Sec.(1) we give a general motivation for the thesis and introduce the theoretical methods employed. An overview of the thesis works is provided in Sec.(2). The remaining Sec.(3) of the introduction is devoted to briefly discuss the necessary theoretical background to understand the content of the thesis and may be completely skipped by the expert reader.

2. **Publications:** In this chapter one can find the works presented in this thesis.

3. **Results and discussion:** We give and discuss there the main results obtained in our works.

4. **Conclusions:** We present our final thoughts and conclusions.

Chapter 1

Introduction

1 Motivation and theoretical methods

Our current understanding of nature based on the standard model of particle physics indicates that hadronic matter in extreme conditions of temperature and/or density undergoes a phase transition into a new state of matter, in which the quarks and gluons that form the hadrons become deconfined, the so called quark-gluon plasma (QGP). Lattice simulations predict that the crossover temperature required for the phase transition to occur is around $T_c \sim 155$ MeV [1]. A high temperature drop of QGP is believed to be produced for a short time in heavy-ion collision experiments at RHIC and CERN, where temperatures above T_c can be reached. Due to the sign problem, which does not allow to easily incorporate a chemical potential on the lattice [2], the value for the critical density is not known, but it is expected to be a relevant factor of the nuclear saturation density $n_0 \sim 0.15$ fm^{-3}. As those high densities can not be reproduced in laboratory conditions with current technology, the experimental access to the high density regime of the QGP is limited. Nevertheless, a very dense and low temperature QGP is one of the candidates for the phase of matter in the core of neutron stars (see e.g [3]), where densities several times n_0 can occur. On the other hand, electron/positron plasmas (EPP) are generated by highly energetic processes in many astrophysical scenarios, such as supernovae explosions, black holes, neutron stars and quasars. The generation of high temperature EPP in the laboratory is possible although complicated [4]. In addition, the properties of QGP, EPP and electroweak plasmas are essential for comprehending the evolution of the early universe [5]. In summary, understanding the properties of plasmas in extreme conditions is essential in many areas of physics, thus, a precise theoretical determination of their physical properties is desirable. This thesis is mainly devoted to develop and apply different theoretical methods for their study.

The quantum field theories necessary for the study of QGP and EPP are quantum chromodynamics (QCD) and quantum electrodynamics (QED) respectively. A well known peculiarity shared by both theories is the running of the coupling constant g, which means that the interaction strength between the quantum fields depends on the energy scale. Let us assume zero chemical potential ($\mu = 0$) for the following discussion. In the QCD case, as the temperature increases far beyond the critical temperature ($T \gg T_c$), the coupling between quarks and gluons becomes small ($g \ll 1$), so in the high temperature regime the overall picture is a weakly interacting gas of quarks and gluons. For QED, the coupling between electrons and photons becomes stronger as the temperature rises but slowly [6], so that for most practical scenarios one can also assume that it is small. Consequently, in the high temperature regime of a thermally equilibrated QGP or EPP, Bose-Einstein and Fermi-Dirac statistics imply that most of the plasma constituents have momenta of the order of the plasma temperature (T), which then govern the physics at the *hard* scale ($\sim T$). Due to the weak interactions between the plasma constituents, one expects the generation of perturbative or *soft* scales, e.g gT, $g^2T\ldots$, in the plasma. The appearance of a strong hierarchy of scales is the perfect scenario for the application of effective field theory (EFT) techniques. The concept of EFT is a powerful one in theoretical physics. It relies on the idea that in order to describe the physics of the system at a given energy scale, it is sufficient to consider the effective degrees of freedom that operate at that scale, integrating out from the theory the higher energetic modes. One then obtains an EFT that describes the low energy physics of the system. An introduction to EFT and the mathematical techniques employed in their construction can be found in the excellent reviews of Manohar [7, 8]. A general, although incomplete, landscape of different EFT used in the study of high temperature plasmas is sketched in Fig.(1.1). As can be seen there, nowadays there exist a vast number of EFT that provide an adequate framework to study the diverse phenomenology of the high temperature regime of plasmas. During

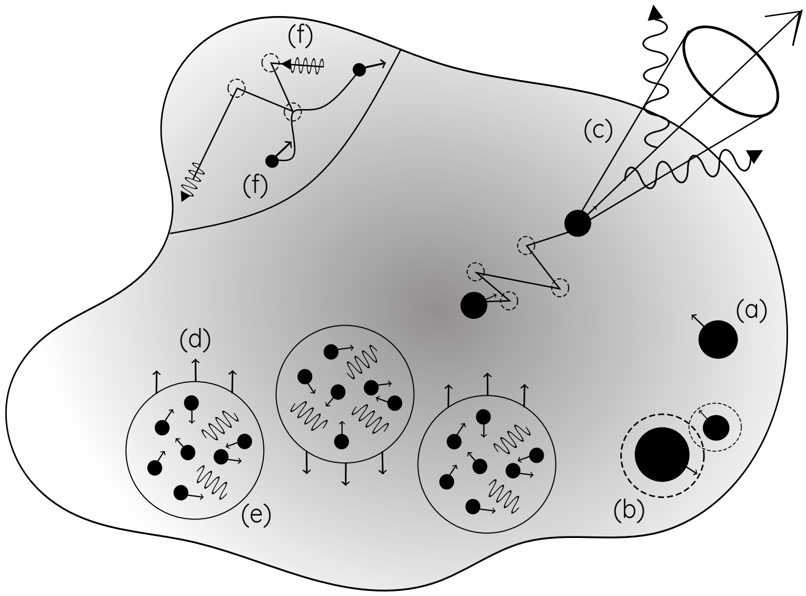

Figure 1.1: A landscape of different effective field theories. (a): Heavy fermions ($m \gg T$), e.g muons in the EPP or charm quarks in the QGP case, can be treated with non-relativistic (NR) effective field theories of QED and QCD [11–13]. (b): Heavy quarkonium, i.e bound states composed of a quark and an antiquark, can be studied within potential NRQCD (pNRQCD) [14]. (c): Highly energetic jets in the QGP or EPP admit a description based on the soft collinear effective theory SCET [15]. (d): At the soft scales, i.e gT, many-body oscillations occur. There is a well suited effective field theory to characterize the collective modes, the so called hard thermal loop (HTL) effective field theory [16–18]. (e): Plasma constituents with $E \sim T$ admit a description based on the OSEFT. (f): The propagation of quanta with $E \gtrsim T$ can be studied with semi-classical transport equations, which can also be derived from the OSEFT.

this thesis, we used a particular class of EFT, the so called on-shell effective field theories (OSEFT) [9, 10]. The excitations of the OSEFT fields are *quasiparticles* of finite size $\sim 1/E$, where E is their energy. In the context of the QGP or EPP, the OSEFT can successfully characterize the effective degrees of freedom that operate at the hard scale. Specifically, plasma constituents whose momentum is comparable to the plasma temperature can be treated as quasiparticles of finite size $\lambda_T \sim 1/T$, so that they admit an OSEFT description (assuming $E \sim T$). In addition, the OSEFT can also be used to study the propagation of quanta with momenta that is greater or of similar order than the hard scale with semi-classical transport equations. In fact, the OSEFT was first formulated with the aim to derive quantum corrections to classical transport equations, in the context of chiral kinetic theory (CKT) [9]. Moreover, it is nowadays understood that the effective degrees of freedom at each energy scale have to be treated differently. For instance, plasma constituents (hard) and collective modes (soft) can be treated as quasiparticles and classical background fields respectively. A specific case can be found in [10], where the authors showed that incorporating background electromagnetic fields to the OSEFT for fermions one can derive the HTL polarization tensor and systematically compute their power corrections.

Apart from EFT methods, in the works presented in this thesis we required the techniques of thermal field theory (TFT) [19–22] because of the following physical reasons:

1. A high temperature and/or very dense plasma is naturally a relativistic system, in the sense that the temperature (and/or chemical potential) is greater than most of the plasma constituents masses i.e $T \gg m$ (and/or $\mu \gg m$).

2. Due to the large ensemble of particles present in those systems, accounting for their thermodynamic properties is essential.

3. Since the mean inter-particle distance, given by $n^{-1/3}$ where n is the particle density, is comparable to the typical size of the quasiparticles (λ_T), the effective degrees of freedom operating at the hard scale have quantum statistical properties.

TFT can be seen as a generalization of quantum field theory in vacuum, through the incorporation of the medium. Nowadays, there are two formulations of TFT, the *real* and *imaginary time* formalism. In this thesis, we have used the real time formalism, with the physical motivation that it can be generalized to the non-equilibrium scenario. What this means is that with the real time formalism one can study non-equilibrium thermodynamic properties of plasmas and is not limited to the equilibrium case, as in the imaginary time formalism. Notably, non-equilibrium quantities are also difficult to obtain on the lattice, which gives even more value to the real time formulation.

2 Overview of thesis works

In the high temperature regime of a QGP or an EPP, a widespread assumption in the perturbative computations found in the literature is that the fermionic plasma constituents, i.e quarks/antiquarks in the QGP and electrons/positrons in the EPP, are massless. That is indeed a good assumption for extremely hot plasmas in which all the plasma constituent masses strictly obey $m \ll T$. Considering temperatures above $T_c \sim 155$ MeV and in the context of a QGP, ignoring the masses of the up ($m_u \sim 2$ MeV) and down ($m_d \sim 5$ MeV) quarks is justified, but neglecting the mass of the strange quark ($m_s \sim 100$ MeV) might not be such a good approximation. On the other hand, for an EPP neglecting the electron mass ($m_e \sim 0.5$ MeV) is also a good approximation in most cases, but for moderate temperature plasmas, e.g in supernovae plasma with $T \sim (1-10)$ MeV, it might be not. Hence, accounting for small plasma constituent mass effects could be relevant to accurately determine the properties of QGP and EPP. A necessary first step in this direction was done in our first work [23]. There, we computed small mass ($m \ll T$) corrections to the HTL photon polarization tensor, a key ingredient in the evaluation of many EPP properties. The diagrammatic computation was carried employing the OSEFT for fermions[1] and the real time formalism of TFT. Additionally, we also evaluated the mass corrections using classical kinetic theory, reaching to the same result. Remarkably, the mass corrections to the HTL gluon polarization tensor have exactly the same form except for some color factors, so the result is also valid for the QGP case.

Once the mass corrections to the photon/gluon polarization tensor were properly evaluated, we wanted to check their effect on a given physical quantity. This was done in our second work [25], in which we evaluated the impact of the mass corrections in the collisional energy loss. The idea is that when a heavy and highly energetic $E, M \gg T$ fermion transverses a QGP or an EPP, it loses energy as it interacts with the plasma constituents. In the particular regime where $E \ll M^2/T$ holds, the dominant contribution to the total energy loss is the collisional energy loss. Let us remark that although we performed the computation for an EPP plasma, our results were generalized to the QGP case.

[1] Generalized in the presence of a small mass and background electromagnetic fields in [24].

At the end of this first stage of the thesis, we had seen that the OSEFT for fermions provides a powerful framework to characterize the effective fermionic degrees of freedom operating at the hard scales of a weakly interacting QGP or EPP. However, one also expects hard gluons and photons to operate at those scales, which are of bosonic nature. Although one can study their effects from the full theories of QCD and QED respectively, it is also desirable to have an EFT approach to address them. This was the motivation for our third work [26], where we developed the OSEFT for abelian gauge fields. Once the EFT was formulated and their basic symmetries understood, we developed some applications, so as to confirm the validity of our approach (see Chap.3).

The OSEFT for photons describes the so called eikonal or semi-classical optical limit, allowing for corrections organized in a systematic expansion on inverse powers of the photon energy. Thus, this new EFT provides a well suited framework to study photon transport properties beyond the eikonal limit, an approximation that is also commonly used in astrophysics and cosmology settings. This was the motivation for our last work [27], where we developed a quantum kinetic theory for photons in the presence of the axion background, an hypothetical field which was proposed a while ago as a solution to the strong CP problem [28] and is nowadays also considered a possible dark matter candidate. As a first approach to the subject, we constructed a quantum kinetic theory for photons in the presence of an axion background from the *full* QED theory. We also obtained the same results by generalizing the OSEFT for photons in the presence of the axion background, but we decided to present in our work the derivation from the full theory. This is mainly due to two reasons; first, we have only considered the classical limit of the kinetic equations and in this case it is easier to construct them from the full theory, and second, we wanted to reach the dark matter community, which may be not so familiarized with the EFT methods.

3 Thermal field theory

Thermal field theory mixes three important branches of physics: quantum mechanics, thermodynamics and special relativity. Excellent introductions to the subject can be found in the books of Kapusta and Gale [19], Le Bellac [20] or Laine and

Vuorinen [21]. For a recent review, see [22]. In this section, we will briefly review some of the theoretical challenges that one encounters in perturbative computations at finite temperature, which are relevant for the works presented in this thesis. Mainly, we will cover how real time Green functions at finite temperature can be defined, the appearance of thermal effective masses, the breakdown of perturbation theory and the necessity of the HTL resummation technique.

3.1 Real time Green functions at finite temperature

Contrary to most situations encountered in vacuum, in medium quantum physics one is generally dealing with a large ensemble of quanta, characterized by a non-trivial density matrix ρ. Then, if O denotes an arbitrary operator, instead of its vacuum expectation value one is usually interested in its quantum statistic expectation value or thermal average

$$\langle O \rangle = \mathrm{Tr}\,\{\rho\, O\} \ , \tag{1.1}$$

where we use the notation $\mathrm{Tr}\{\ldots\}$ for the trace. Let us consider the canonical ensemble, in which the number of particles N and the (equilibrium) temperature $T = \beta^{-1}$ of the system are fixed. Then, the density matrix is given by

$$\rho = \frac{e^{-\beta H}}{Z} \ , \quad \text{with} \quad Z = \mathrm{Tr}\{e^{-\beta H}\} \ . \tag{1.2}$$

Above, H the full Hamiltonian operator of the system and Z its partition function. We could as well extend the discussion in the presence of a chemical potential μ, by just replacing $H \to H - \mu N$, being N the number operator. To introduce the main features of the formalism, we consider the following theory

$$\mathcal{L} = \frac{1}{2}(\partial^\mu \phi)(\partial_\mu \phi) - V(\phi) \ , \tag{1.3}$$

where $\phi(x)$ is a real scalar field and $V(\phi)$ is a self-interaction potential. A fundamental ingredient in the real time formalism of TFT are the Green functions. Those can be defined as the thermal average of time ordered products of fields in the operator formalism or by functional differentiation of a generating functional in the path integral formalism. Here we employ the operator formalism. The 2-point

Green function may be written as

$$\Delta(x,y) = \langle \mathcal{T}\phi(x)\phi(y)\rangle = \frac{1}{Z}\mathrm{Tr}\{e^{-\beta H}\mathcal{T}\phi(x)\phi(y)\}\ , \tag{1.4}$$

where $\mathcal{T}$ denotes time ordering[2]. However, there is a fundamental problem in loop computations with this naive formulation of the real time propagator, that is the appearance of the so called pinch singularities. Those can be easily identified after evaluating Eq.(1.4). Introducing both a complete set of eigenstates of the free Hamiltonian[3], i.e $H_0 |n\rangle_0 = \mathcal{E}_n |n\rangle_0$ with $\mathcal{E}_n$ the energy of the $|n\rangle_0$ state, and a Fourier modes decomposition of $\phi(x)$ in terms of creation and annihilation operators, the propagator can be written as [20, 29]

$$\Delta(x,y) = \int \frac{d^4q}{(2\pi)^4}\left[\frac{i}{q^2+i0^+} + 2\pi n_B(q_0)\delta(q^2)\right] e^{-iq\cdot(x-y)}\ , \tag{1.5}$$

where $n_B(q_0) = 1/(e^{\beta|q_0|}-1)$ is the Bose-Einstein distribution function. Then, note that in loop diagrams involving two or more propagators one encounters ill-defined products of distribution functions, e.g $\Delta^2(q) \sim \delta^2(q^2)$. This technical issue is related to the peculiar analytic properties of the real time Green functions. In order to discuss them, let us introduce the so called greater ($>$) and lesser ($<$) components of the propagator

$$\Delta^>(x,y) = \langle\phi(x)\phi(y)\rangle\ , \quad \Delta^<(x,y) = \langle\phi(y)\phi(x)\rangle\ , \tag{1.6}$$

as well as the advanced (A) and retarded (R) propagators

$$\Delta_A(x,y) = -i\theta(y_0-x_0)\left[\Delta^>(x,y)-\Delta^<(x,y)\right]\ , \tag{1.7a}$$

$$\Delta_R(x,y) = i\theta(x_0-y_0)\left[\Delta^>(x,y)-\Delta^<(x,y)\right]\ . \tag{1.7b}$$

Both the greater and lesser components of the Green function satisfy a remarkable identity

$$\Delta^>(x_0, y_0+i\beta) = \Delta^>(y_0,x_0)\ , \quad \Delta^<(x_0,y_0+i\beta) = \Delta^<(y_0,x_0)\ , \tag{1.8}$$

---

[2]Given by $\mathcal{T}\phi(x)\phi(y) = \theta(x^0-y^0)\phi(x)\phi(y) + \theta(y^0-x^0)\phi(y)\phi(x)$ where $\theta(x)$ is the Heavisde step function.

[3]Recall that in perturbation theory, one typically assumes the decomposition $H = H_0 + H_I$ with $H_0 \gg H_I$, being H_0 and H_I the free and the interaction Hamiltonian respectively.

where we neglected the spatial arguments for simplicity. The above properties are known as the Kubo-Martin-Schwinger (KMS) relations. Introducing now a complete set of eigenstates of the full Hamiltonian operator H in Eq.(1.4) one may re-evaluate the greater component as[4]

$$\Delta^{>}(x_0, y_0) = \frac{1}{Z}\sum_{n,m} e^{-\beta E_n} e^{i\Delta_{mn}\Delta t} |\, \langle n|\phi_0|m\rangle \,|^2 \ , \tag{1.9}$$

where $\Delta t = x_0 - y_0$ and $\Delta_{nm} = E_n - E_m$, being E_n the energy of the $|n\rangle$ state ($H\,|n\rangle = E_n\,|n\rangle$). Assuming that the convergence of the sum is governed by the exponential factors, one sees that the sum converges in the interval $-\beta < \Im(\Delta t) < 0$, where $\Im$ denotes the imaginary part, and for the lesser component one finds $0 < \Im(\Delta t) < \beta$. Thus, the lesser and greater component are analytic in their respective domains and convergence requires an imaginary part on the time coordinate. At this point, one may take one of the two possible options: use the *imaginary time formalism* or introduce *contour Green functions*. The first option involves technical mathematical techniques, such as Wick rotation, analytic continuation, frequency or Matsubara sums... that we will not cover here. We will use the second option, with the physical motivation being that it can be generalized to the non-equilibrium scenario, while the imaginary time formalism is restricted to the thermal equilibrium case. Using the KMS relation, the propagator can be written in the useful form

$$\Delta(x,y) = \int \frac{d^4q}{(2\pi)^4}[\theta(x^0 - y^0) + f(q_0)]\rho(q)e^{-iq\cdot(x-y)} \ , \tag{1.10}$$

where $f(q_0) = (e^{\beta q_0} - 1)^{-1}$ is the Bose-Einstein occupation number and we introduced the spectral density as $\rho(q) = \Delta^{>}(q) - \Delta^{<}(q)$. Contour Green functions can be defined generalizing Eq.(1.10) to complex time variables and introducing a time contour C, as the one depicted in Fig.(1.2). For more details on this technical step of the formulation, we refer the interested reader to [20, 30, 31]. The point is that the contour Green function, say $\Delta_C(x,y)$ with $x_0, y_0 \in$ C, can be related with four real time components by restricting the complex time variables to lie in one

[4] We set $x^\mu = (x^0, \mathbf{0})$ and $y^\mu = (y^0, \mathbf{0})$ in Eq.(1.9), and employ the notation $\phi_0 \equiv \phi(0, \mathbf{0})$.

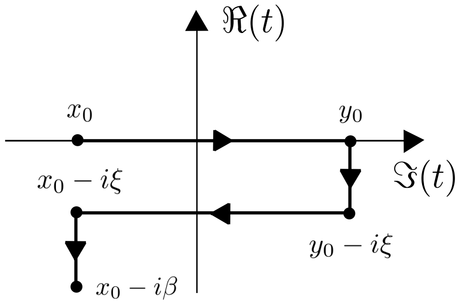

Figure 1.2: Our choice for the time contour C. If $\xi \to 0^+$ one has $C = C^+ + C^- + C^0$, where C^+ goes from x_0 to y_0, C^- from $y_0 - i\xi$ to $x_0 - i\xi$ and C^0 from $x_0 - i\xi$ to $x_0 - i\beta$.

specific branch of the contour. Explicitly

$$\Delta_{11}(x,y) = \langle \mathcal{T}_C\, \phi(x)\phi(y)\rangle = \Delta_C(x,y)\,, \text{ if } \quad x_0, y_0 \in C^+\,, \tag{1.11a}$$

$$\Delta_{12}(x,y) = \langle \phi(y)\phi(x)\rangle = \Delta_C(x,y)\,, \text{ if } \quad x_0 \in C^+\,,\, y_0 \in C^-\,, \tag{1.11b}$$

$$\Delta_{21}(x,y) = \langle \phi(x)\phi(y)\rangle = \Delta_C(x,y)\,, \text{ if } \quad x_0 \in C^-\,,\, y_0 \in C^+\,, \tag{1.11c}$$

$$\Delta_{22}(x,y) = \langle \widetilde{\mathcal{T}}_C\, \phi(x)\phi(y)\rangle = \Delta_C(x,y)\,, \text{ if } \quad x_0, y_0 \in C^-\,. \tag{1.11d}$$

Above, $\mathcal{T}_C$ is the usual time ordered product while $\widetilde{\mathcal{T}}_C$ denotes anti-time ordering[5]. Note that Δ_{12} and Δ_{21} are the lesser and greater component introduced in Eq.(1.6). Then, one can directly get a momentum space representation for the propagators by substituting in Eq.(1.10) the specific temporal components. In perturbative computations, one needs the expression for the free propagators, achieved by specializing the spectral density to the non-interacting case[6]. After some manipulation, the propagator components in momentum space read

$$\Delta_{11}(q) = \frac{i}{q^2 + i0^+} + 2\pi n_B(q_0)\delta(q^2) = \Delta^*_{22}(q)\ , \tag{1.12a}$$

$$\Delta_{12}(q) = 2\pi\delta(q^2)[n_B(q_0) + \theta(-q_0)]\ , \tag{1.12b}$$

$$\Delta_{21}(q) = 2\pi\delta(q^2)[n_B(q_0) + \theta(q_0)]\ , \tag{1.12c}$$

which is often called the 1-2 representation in the literature. Analogous definitions and derivations can be done for fermionic and gauge fields, which can be found in the articles of this thesis or in the references. Let us give an example of cancellation

[5] Given by $\widetilde{\mathcal{T}}_C\phi(x)\phi(y) = \theta(y^0 - x^0)\phi(x)\phi(y) + \theta(x^0 - y^0)\phi(y)\phi(x)$.
[6] That is $\rho_0(q) = 2\pi\text{sgn}(q_0)\delta(q^2)$, with $\text{sgn}(x)$ the sign function (see [20]).

of pinch singularities in this representation. For that, we need an explicit form of the potential, that we choose $V(\phi) = \frac{1}{4!}\lambda\phi^4$ with $\lambda \ll 1$ for this discussion, and Feynman rules for the evaluation of diagrams:

(i) Propagators: $\Delta_{ij}(q)$, where the indices $i, j = 1, 2$ label the matrix components in Eqs.(1.12a-1.12c).

(ii) Vertices: The general vertex in the theory may be written as V_{ijkl} where $i, j, k, l = 1, 2$ label the four legs arriving at the vertex. In practice, since fields defined in C^+ can not mix with those defined in C^- in a vertex, one only has two type of vertices $V_{1111} = -i\lambda$ and $V_{2222} = i\lambda$. The V_{2222} vertex contains an additional minus sign coming from the anti-time ordering in C^-.

The rest of Feynman rules, e.g symmetry factors, are the same as in vacuum. Using naive perturbation theory, the first order correction to the propagator would be the one-loop diagram of Fig.(1.3).(a). In the real time formalism however, self-energies also have different components, e.g Π_{ij} for $i, j = 1, 2$, so that the diagram is split into the two diagrams of Fig.(1.3).(b). Note that $\Pi_{12}^{\text{one-loop}} = \Pi_{21}^{\text{one-loop}} = 0$, because all the indices in the vertex must be equal. Using the above Feynman rules, one may evaluate the temperature dependent[7] part of the one-loop self-energy [20]

$$\Pi_{11}^{\text{one-loop}} = i\frac{(-i\lambda)}{2}\int \frac{d^4q}{(2\pi)^4}\Delta_{11}(q) = \frac{\lambda}{2}\int \frac{d^3\boldsymbol{q}}{(2\pi)^3}\frac{1+2n_B(\boldsymbol{q})}{2|\boldsymbol{q}|} \overset{T\geq 0}{=} \frac{\lambda T^2}{24}\ . \tag{1.13}$$

The other diagram gives the same contribution $\Pi_{22}^{\text{one-loop}} = -\Pi_{11}^{\text{one-loop}}$, except for a minus sign. Here we can already see one of the effects of the medium; particles gain effective masses $\sim \lambda T^2$. Now we consider the first correction to the effective mass. At second order in naive perturbation theory, there are many topologically distinct diagrams that contribute, for instance, the two-loop diagram of Fig.(1.3).(c). One encounters in the lower loop the product of two propagators $\sim \Delta^2(q)$, which gives rise to the aforementioned pinch singularities. However, in the real time formalism, the diagram is split into the four contributions of Eq.(1.3).(d). Each diagram contains pinch singularities that contribute with different signs, so all of them cancel when the diagrams are added. As an example, let us consider the sum of the first and the last diagram. Factoring out a one-loop self-energy, their sum is

[7] The $T = 0$ part is UV divergent and needs to be renormalized as in the vacuum case. Also note the symmetry factor of $1/2$ in Eq.(1.13).

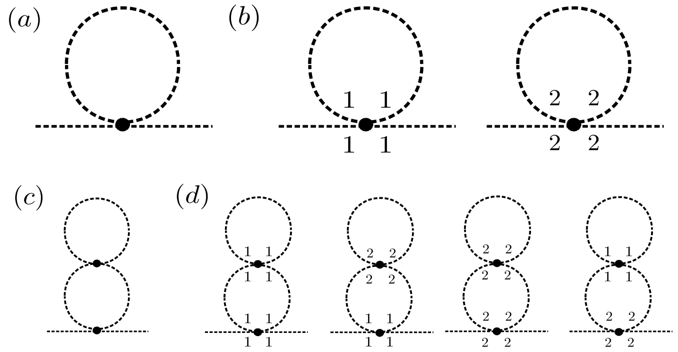

Figure 1.3: (a) and (c) are the naive one-loop and two-loop diagram respectively. The corresponding ones in the RTF are given by (b) and (d).

proportional to

$$\Pi_{11}^{\text{two-loop}} + \Pi_{22}^{\text{two-loop}} \sim \Pi_{11}^{\text{one-loop}}(-i\lambda) \int \frac{d^4q}{(2\pi)^4} \left[\Delta_{11}^2(q) - \Delta_{21}(q)\Delta_{12}(q)\right] =$$
$$= \Pi_{11}^{\text{one-loop}}(-i\lambda) \int \frac{d^4q}{(2\pi)^4} \left[\Delta_0^2 + n_B(q_0)(\Delta_0^2 - \Delta_0^{*2})\right] , \quad (1.14)$$

where we used the notation $\Delta_0 = i/(q^2 + i0^+)$ in the last step. Above, there is no presence of pinch singularities, as we wanted to show here.

In practice, the 1-2 representation is not very well suited for computations, a more useful one can be achieved exploiting the fact that not all the propagator and self-energy components are independent, but satisfy the constraints

$$\Delta_{11} + \Delta_{22} - \Delta_{12} - \Delta_{21} = 0 , \quad (1.15a)$$
$$\Pi_{11} + \Pi_{22} + \Pi_{12} + \Pi_{21} = 0 , \quad (1.15b)$$

respectively. That is, one defines advanced (A), retarded (R) and symmetric (S) propagators and self-energies as

$$\Delta_A = \Delta_{11} - \Delta_{21} , \quad \Delta_R = \Delta_{11} - \Delta_{21} , \quad \Delta_S = \Delta_{11} + \Delta_{22} , \quad (1.16a)$$
$$\Pi_A = \Pi_{11} + \Pi_{21}, \quad \Pi_R = \Pi_{11} + \Pi_{12} , \quad \Pi_S = \Pi_{11} + \Pi_{22} , \quad (1.16b)$$

which is often called the Keldysh or physical representation. For completeness, we also write down the inverse relations for the propagators

$$\Delta_{11} = \frac{1}{2}(\Delta_S + \Delta_R + \Delta_A) , \quad \Delta_{12} = \frac{1}{2}(\Delta_S - \Delta_R + \Delta_A) , \quad (1.17)$$

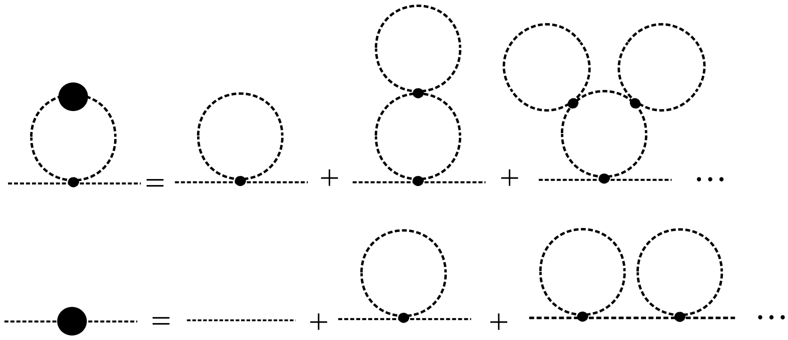

Figure 1.4: Examples of ressumations in $\lambda\phi^4$ theory.

$$\Delta_{21} = \frac{1}{2}(\Delta_S + \Delta_R - \Delta_A) \ , \quad \Delta_{22} = \frac{1}{2}(\Delta_S - \Delta_R - \Delta_A) \ . \tag{1.18}$$

From Eqs.(1.12a-1.12c) one can find a momentum space representation of the Keldysh propagators

$$\Delta_{A,R}(q) = \frac{i}{q^2 \mp i\mathrm{sgn}(q_0)0^+} \ , \tag{1.19a}$$

$$\Delta_S(q) = 2\pi\delta(q^2)[1 + 2n_B(q_0)] \ . \tag{1.19b}$$

The corresponding real time propagators can be obtained after inverse Fourier transform [20]. Note that $\Pi^{\text{one-loop}}_{A,R} = \Pi^{\text{one-loop}}_{11}$ and $\Pi^{\text{one-loop}}_{S} = 0$ in this representation. Even if there are no pinch singularities, the evaluation of the two-loop diagram has another problem: it contains an IR logarithmic divergence $\sim \lambda^2 \int d^4q/q^4$ whose appearance can be interpreted as the absence of screening for long-wavelengths. One can solve this problem by resummation of infinite series of diagrams. For instance, consider the self-energy diagram in Fig.(1.4).(a), where the bare propagator in the loop is substituted by a resummed one. Dressed or resummed propagators can be constructed through Dyson-Schwigner equations, for instance $\overline{\Delta} = 1/(\Delta^{-1} - \Pi)$ (see Fig.(1.4).(b)). All the machinery of the real time formalism can also be applied to the resummed propagators, in particular, one can also define advanced, retarded and symmetric components. For our discussion, it is sufficient to assume $\Pi \approx \Pi^{\text{one-loop}}_R = \lambda T^2/24$, then the advanced/retarded ($\overline{\Delta}_{A,R}$) and symmetric ($\overline{\Delta}_S$) resummed propagators are given by Eqs.(1.19a-1.19b) respectively, after simply replacing $q^2 \to q^2 - \Pi$. The retarded component of the dressed self-energy is given by $\overline{\Pi}_R = \overline{\Pi}_{11} + \overline{\Pi}_{12}$ and we set $\overline{\Pi}_{12} = 0$, as it starts to contribute at order λ^2. Then, the expression for $\overline{\Pi}_R$ is the same as Π_{11} in Eq.(1.13), but replacing

$|\boldsymbol{q}| \to E_{\boldsymbol{q}} = \sqrt{\boldsymbol{q}^2 + \Pi}$ in the integrand. Precisely

$$\overline{\Pi}_R = \frac{\lambda}{2} \int \frac{d^3\boldsymbol{q}}{(2\pi)^3} \frac{1 + 2n_B(E_{\boldsymbol{q}})}{2E_{\boldsymbol{q}}} \ . \tag{1.20}$$

Note that if the momenta obeys $q \gg \lambda^{1/2}T$, e.g when it is hard $q \sim T$, the integral gives[8] $\lambda T^2/24$, because the resummed propagators reduce to the bare ones in that limit. However, if the momentum is soft $q \sim \lambda^{1/2}T$, the contribution from Π can no longer be ignored. In the soft regime, one further notes that the vacuum contribution to $\overline{\Pi}_R$ is of order $\lambda^2 T^2$, hence it is subleading compared to the medium contribution, which, after expansion for small λ, gives [20]

$$\overline{\Pi}_R^{T>0} = \frac{\lambda T^2}{24} \left(1 - \sqrt{\frac{3\lambda}{8\pi^2}} + \mathcal{O}(\lambda \ln \lambda) \right) \ . \tag{1.21}$$

Remarkably, the coupling dependence of the first order correction to the effective mass is not of order λ^2 as one would naively expect but $\lambda^{3/2}$, it is a non-perturbative correction. It emanates from the soft momentum space region $q \sim \lambda^{1/2}T$ so it is capturing the long distance physics in the system. This is an example of the so called breakdown of the perturbative expansion at finite temperature.
So far, we have used $\lambda\phi^4$ theory to discuss some of the issues that one encounters in perturbative computations at finite temperature. However, the underlying quantum field theories in the works presented in this thesis are QED and QCD. Most of the issues discussed in this section are shared by gauge theories in general, for instance, pinch singularities and the breakdown of perturbation theory. However, in gauge theories, self-energies have a richer structure, although one can recover the behavior λT^2 under certain approximations, as we will see in the next section.

3.2 Hard thermal loops

In the early developments of thermal field theory and in the context of perturbative computations in gauge theories, infrared divergent and gauge dependent results were encountered in the computation of physical quantities. A well-known case is the gluon damping rate in the QGP, which turned out to depend on the gauge choice. Another example that we have worked on in this thesis is the collisional

[8] After renormalizing the vacuum ($T = 0$) contribution.

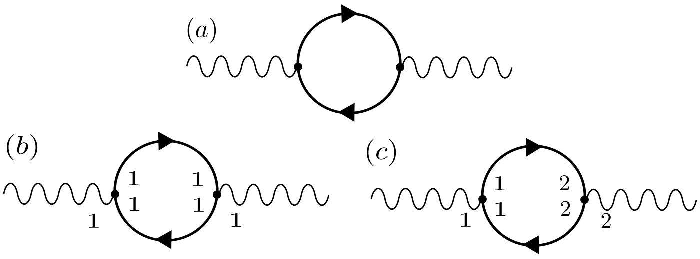

Figure 1.5: (a) Photon polarization tensor in QED. (b) Polarization tensor in the real time-formalism. The HTL self-energy is introduced considering that the external momentum is soft $L \sim gT$ and the internal momentum is hard $Q \sim T$.

energy loss experienced by a heavy fermion that traverses a QGP or EPP, that is infrared divergent when evaluated using the bare theory. Braaten and Pisarski found a general solution to these problems [32–34], which is usually referred to as the hard thermal loop (HTL) resummation technique. The main idea is to use effective vertices and propagators instead of the bare ones, obtained after resumming certain HTL diagrams. Let us elaborate on how this effectively works. The first step is to introduce HTL self-energies, for instance, consider the QED polarization tensor in Fig.(1.5).(a). Using QED Feynman rules, one can write[9]

$$\Pi^{\mu\nu}(L) = -ie^2 \int \frac{d^4Q}{(2\pi)^4} \mathrm{Tr}\{\gamma^\mu S(Q)\gamma^\nu S(Q-L)\} \ ,$$

where $S(Q)$ is the usual vacuum fermion propagator, e the electron-photon coupling and γ^μ are the gamma matrices. Now, we assume a high temperature plasma, such that one can ignore the masses of the fermionic particles ($m \ll T$). In the real time formalism, the components of the fermion propagator in the 1-2 basis are then given by $S_{ij}(Q) = \not{Q}\Delta_{ij}(Q)$ for $i, j = 1, 2$, where $\Delta_{ij}(Q)$ are the same as Eqs.(1.12a-1.12c) but replacing $n_B(Q_0) \to -n_F(Q_0)$ where $n_F(Q_0) = 1/(e^{\beta|Q_0|}+1)$ is the Fermi-Dirac distribution function. The polarization tensor is then split into the diagrams of Fig.(1.5)(b), so that the retarded component is given by

$$\begin{aligned}\Pi^{\mu\nu}_R(L) &= \Pi^{\mu\nu}_{11}(L) + \Pi^{\mu\nu}_{12}(L) = \\ &= -ie^2 \int \frac{d^4Q}{(2\pi)^4} \left[\mathrm{Tr}\{\gamma^\mu S_{11}(Q)\gamma^\nu S_{11}(K)\} - \mathrm{Tr}\{\gamma^\mu S_{21}(Q)\gamma^\nu S_{12}(K)\} \right] \ , \end{aligned} \tag{1.22}$$

[9]Here we follow the sign conventions of [29].

with $K = Q - L$. Moving to the Keldysh representation and after some manipulation (see for instance [20, 29]) the retarded photon self-energy can be written as

$$\Pi_R^{\mu\nu}(L) = -8\pi e^2 \int \frac{d^4Q}{(2\pi)^4} \frac{K^\mu Q^\nu + K^\nu Q^\mu - g^{\mu\nu}(K\cdot Q)}{K^2 - i\mathrm{sgn}(K_0)0^+}[1-2n_F(Q_0)]\delta(Q^2) \ . \quad (1.23)$$

In the medium, Lorentz invariance is broken but the Ward–Takahashi identity still holds, i.e $L_\nu \Pi_R^{\mu\nu} = 0$, due to gauge invariance. These leaves two independent scalar functions for the polarization tensor [19] which are appropriately called longitudinal and transverse component. Precisely, using the notation $L^\mu = (\ell_0, \boldsymbol{\ell})$ for the external photon momenta, one has

$$\Pi_R^L(L) = \Pi_R^{00}(L) \ , \quad \Pi_R^T(L) = \frac{1}{2}\left(\delta_{ij} - \frac{\ell_i \ell_j}{|\boldsymbol{\ell}|^2}\right)\Pi_R^{ij}(L) \ , \quad i,j = 1,2,3 \ . \quad (1.24)$$

Contrary to the scalar field theory case discussed in the previous section, in gauge theories self energies have a non-trivial dependence on the external momenta, impeding their analytical evaluation[10]. However, since the coupling is small, i.e $e \ll 1$, one expects a well defined hierarchy of scales in the plasma. In particular, one assumes a momentum separation into *hard* ($\sim T$) and *soft* ($\sim eT$) scales. HTL self-energies are then introduced assuming that the external momentum is soft ($L \sim eT$) and the momentum circulating in the loop is hard ($Q \sim T$). Under this approximation, one can expand Eq.(1.23) for $Q \gg L$ and analytically evaluate the loop integrals. The medium contribution to the longitudinal and transverse component give [20, 29]

$$\Pi_R^{L,\mathrm{htl}}(\ell_0, \boldsymbol{\ell}) = -m_D^2\left[1 - \frac{\ell_0}{2|\boldsymbol{\ell}|}\ln\left(\frac{\ell_0 + |\boldsymbol{\ell}|}{\ell_0 - |\boldsymbol{\ell}|}\right)\right] \ , \quad (1.25a)$$

$$\Pi_R^{T,\mathrm{htl}}(\ell_0, \boldsymbol{\ell}) = \frac{m_D^2}{2}\frac{\ell_0^2}{\boldsymbol{\ell}^2}\left[1 - \left(1 - \frac{\boldsymbol{\ell}^2}{\ell_0^2}\right)\frac{\ell_0}{2|\boldsymbol{\ell}|}\ln\left(\frac{\ell_0 + |\boldsymbol{\ell}|}{\ell_0 - |\boldsymbol{\ell}|}\right)\right] \ , \quad (1.25b)$$

where $m_D = eT/\sqrt{3}$ is the Debye mass and $\ell_0 \to \ell_0 + i0^+$ for retarded boundary conditions. One notes that the above self-energy is of order e^2T^2, which justifies ignoring[11] the vacuum contribution at leading order in the HTL approximation. The symmetric self-energy can also be determined under this approximation [20,

[10] In particular, they can not be analytically determined for $L \sim T$ and $Q \sim T$.

[11] However, the vacuum contribution, which is of order e^4T^2, must be kept at next to leading order in the HTL approximation, in the so called power corrections [35]

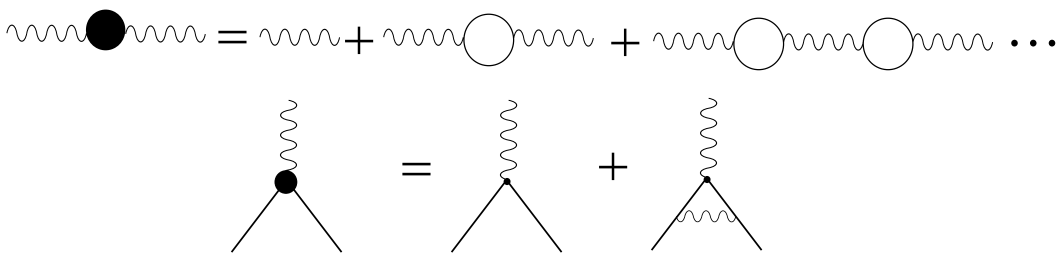

Figure 1.6: HTL ressumed propagator or simply dressed propagator (top). Effective HTL vertex (bottom).

29], notably, it is of lower order (eT^2) but purely imaginary. Once HTL self-energies are determined, one is ready to construct effective propagators and vertices. Before doing so, let us illustrate the need for resummation of HTL self-energies with the following example: consider the series of diagrams in Fig.(1.6) where each empty blob represents a (retarded) self-energy. Within the HTL approximation, each photon propagator contributes as $1/e^2T^2$ while each HTL self-energy gives a factor of e^2T^2, so that all diagrams in the series are of the same order, and have to be resummed. In addition, since in gauge theories corrections to the bare vertices are related to self-energies through Ward identities [6], one also has to use effective HTL vertices if all the momenta arriving at a vertex are soft (see Fig.(1.6).(b)). Similarly to the polarization tensor, the dressed photon propagator can also be split into longitudinal and transverse components. Resummed propagators can then be introduced as in the scalar case, through the corresponding Dyson-Schwinger equations. In the Coulomb gauge, those can be written as

$$\overline{D}^L_R(\ell_0, \boldsymbol{\ell}) = \frac{1}{\boldsymbol{\ell}^2 - \Pi^L_R(\ell_0, \boldsymbol{\ell})} \ , \quad \overline{D}^T_R(\ell_0, \boldsymbol{\ell}) = \frac{1}{L^2 - \Pi^T_R(\ell_0, \boldsymbol{\ell})} \ . \tag{1.26}$$

Hence, if the photon momenta obeys $L \sim eT$, one has to use Eqs.(1.25a-1.25b) for the self-energies. Let us summarize the main features of the HTL resummed propagators:

1. The denominators in Eq.(1.26) determine the HTL dispersion relations that characterize the soft collective modes in the plasma. The longitudinal dispersion relation yields to the so called plasmon mode $\omega_L^{\rm htl}(\boldsymbol{\ell})$, absent in the vacuum case, while the transverse dispersion relation describes a (degenerate) transverse mode $\omega_T^{\rm htl}(\boldsymbol{\ell})$. The exact solutions for $\omega_{L,T}^{\rm htl}(\boldsymbol{\ell})$ can

only be determined numerically (see Fig.(1.7)), but in certain limits they can be analytically determined [20].

2. For $\ell_0^2 < \boldsymbol{\ell}^2$ (below the light cone) the logarithms in Eqs.(1.25a-1.25b) develop an imaginary part

$$\ln\left(\frac{\ell_0 + i0^+ + |\boldsymbol{\ell}|}{\ell_0 + i0^+ - |\boldsymbol{\ell}|}\right) = \ln\left|\frac{\ell_0 + |\boldsymbol{\ell}|}{\ell_0 - |\boldsymbol{\ell}|}\right| - i\pi\theta(\boldsymbol{\ell}^2 - \ell_0^2) \ , \tag{1.27}$$

called Landau damping. It is interpreted as momentum transfer between the collective modes and the plasma constituents. However, since $\omega_{L,T}^{\rm htl}(\boldsymbol{\ell}) > |\boldsymbol{\ell}|$ the collective modes are undamped, hence, they propagate through the medium and characterize the physics at the soft scale.

3. In the static limit, one has

$$\overline{D}_L^{\rm htl}(\ell_0 \to 0, \boldsymbol{\ell}) = \frac{1}{\boldsymbol{\ell}^2 + m_D^2} \ , \quad \overline{D}_T^{\rm htl}(\ell_0 \to 0, \boldsymbol{\ell}) = -\frac{1}{\boldsymbol{\ell}^2} \ , \tag{1.28}$$

so that that the presence of the medium leads to the screening of electric fields while magnetic fields are not.

Using HTL propagators and vertices an improved perturbation theory is achieved, which has given, for instance, success in the determination of many QGP and EPP properties [19, 20]. As we mentioned, in this thesis we have worked on the topic of the collisional energy loss [25] where the use of the HTL resummation technique is mandatory for its correct evaluation.

3.3 The Schwigner-Keldysh formalism

Perhaps the most general framework to study the many-body physics of quantum systems is the Schwigner-Keldysh (SK) formalism [36, 37]. The SK formalism allows to consider a wide variety of interesting physical scenarios, for instance, it can be successfully applied to both perturbative and non-perturbative phenomena, at equilibrium and non-equilibrium settings. In this section we will introduce the Kadanoff-Baym equations [38] and the so called *gradient expansion*, which are relevant concepts for the works [26, 27] of this thesis. We will employ the scalar

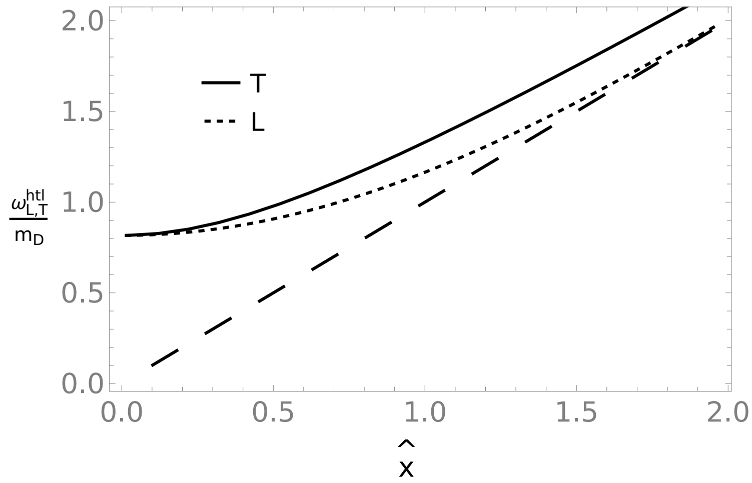

Figure 1.7: The longitudinal (thick line) and transverse (dot-dashed) HTL dispersion relations over the Debye mass $\omega^{\rm htl}_{L,T}/m_D$, plotted as a function of the dimensionless variable $\hat{x} = |\boldsymbol{\ell}|/m_D$. The dashed-line is a free dispersion relation ($\ell_0 = |\boldsymbol{\ell}|$).

theory of Eq.(1.3) for that purpose. A more rigorous introduction can be found, for instance, in the excellent references [20, 30, 31].

The SK formalism is obtained after generalizing the contour Green functions introduced in Sec.(3.1), which are only valid for the thermal equilibrium case. The technicalities associated to the introduction of the complex contour can be found in [30]. The equation of motion obeyed by the mean field, defined as $\Phi(x) = \langle \phi(x) \rangle$, in the presence of an external source $j(x)$ is

$$-\partial^2 \Phi(x) - \left\langle \frac{\delta V}{\delta \phi}(x) \right\rangle = j(x) \ . \tag{1.29}$$

Then, the general equation of motion obeyed by the contour Green function can be obtained by functional differentiation with respect to the external source. One then finds

$$-\partial_x^2 \Delta(x,y) - i \int_C d^4z \, \Pi(x,z) \Delta(x,z) = i \delta_C(x,y) \ , \tag{1.30}$$

where in the above equation it should be understood that the temporal components generally take complex values and we introduced the quantities

$$\Delta(x,y) = -i \frac{\delta \Phi(x)}{\delta j(y)} \ , \quad \Pi(x,y) = -i \frac{\delta}{\delta \Phi(y)} \left\langle \frac{\delta V}{\delta \phi}(x) \right\rangle \ , \quad \delta_C(x,y) = \frac{\delta j(x)}{\delta j(y)} \ . \tag{1.31}$$

The solution of Eq.(1.30) in the absence of interactions ($\Pi = 0$) and in the thermal equilibrium case is given by Eq.(1.10). Then, by restricting the temporal components in Eq.(1.30) to lie in a specific branch of the complex contour, one can write the equations of motion obeyed by each propagator component. The Kadanoff-Baym equations are then obtained by deforming the contour of Fig.(1.2) to include the whole real time axis. In particular, one sets $x_0 \to -\infty$ and assumes that the external sources are turned off adiabatically at the remote past, where the system is supposed to be at thermal equilibrium. Under these assumptions, one can write the equations of motion obeyed by the lesser and greater components as [30]

$$(\partial_x^2 + \Pi^t)\, \Delta^<(x,y) = -i \int d^4z \, \{\Pi_R(x,z)\Delta^<(z,y) + \Pi^<(x,z)\Delta_A(z,y)\} \;\; , \quad (1.32a)$$

$$(\partial_x^2 + \Pi^t)\, \Delta^>(x,y) = -i \int d^4z \, \{\Pi_A(x,z)\Delta^>(z,y) + \Pi^>(x,z)\Delta_R(z,y)\} \;\; , \quad (1.32b)$$

where Π^t is a possible tadpole contribution. The above equations are known as Kadanoff-Baym equations [38] and they describe the general non-equilibrium evolution of the many-body system. Generally, these equations are difficult to solve for obvious reasons and approximations have to be used. In the works [26, 27] presented in this thesis, we resorted to some commonly used assumptions to simplify the Kadanoff-Baym equations, that we summarize below:

1. The particle ensemble is initially ($x_0 \to -\infty$) at thermal equilibrium, so most of the particles have energy of the plasma temperature. Then, since Green functions at thermal equilibrium solely depend on $s = x - y$, one has $s \sim 1/T$. Thus, the (equilibrium) Green functions vary over a characteristic length of $\lambda_T \sim 1/T$.

2. A long-wavelength, slowly varying perturbation disturbs the system from its initial thermal equilibrium state. Then, the system acquires an inhomogeneity on a typical scale $\lambda \gg \lambda_T$. Now Green functions can not solely depend on s, however, one expects that their dependence on s is close to that in thermal equilibrium. Thus, one also assumes that $s \sim \lambda_T$ is small compared to $X = (x+y)/2 \sim \lambda \gg \lambda_T$ or, in terms of the derivatives, $\partial_s \gg \partial_X$. This is the so called *gradient expansion.*

With the use of this approximations, the Kadanoff-Baym equations are reduced to kinetic equations, which are easier to solve. Notably, in the kinetic equations derived in this thesis we have worked in the absence of interactions ($\Pi = 0$). This is of course not a realistic approximation in most practical applications, but it is a good starting point for the consideration of more general and complicated scenarios.

Chapter 2

Publications

In this thesis we present four works [23, 25–27], that we attach in this chapter. All of them have been published in Physical Review D (PRD).

1 Mass corrections to the hard thermal or dense loops

In this section one can find the publication [23].

Mass corrections to the hard thermal or dense loops

Marc Comadran* and Cristina Manuel†

Instituto de Ciencias del Espacio (ICE, CSIC), C. Can Magrans s.n., 08193 Cerdanyola del Vallès, Catalonia, Spain and Institut d'Estudis Espacials de Catalunya (IEEC), C. Gran Capità 2-4, Ed. Nexus, 08034 Barcelona, Spain

(Received 28 June 2021; accepted 14 September 2021; published 7 October 2021)

We compute corrections to the hard thermal (or dense) loop photon polarization tensor associated to a small mass m of the fermions of an electromagnetic plasma at high temperature T (or chemical potential μ). To this aim we use the on-shell effective field theory, amended with mass corrections. We also carry out the computation using transport theory, reaching to the same result. Intermediate steps in the computations reveal the presence of potential infrared divergencies. We use dimensional regularization, as it is respectful with the gauge symmetry, and then show that all infrared divergencies cancel in the final result. We compare the mass corrections with both the power and two-loop corrections, and claim that they are equally important if the mass is soft, that is, of order eT (or $e\mu$), where e is the gauge coupling constant, but are dominant if the mass obeys $eT < m \ll T$ (or $e\mu < m \ll \mu$).

DOI: 10.1103/PhysRevD.104.076006

I. INTRODUCTION

Relativistic QED and QCD plasmas have attracted the interest of the physics community for their wide range of applications in both cosmological, astrophysical and also heavy-ion physics. In their weak coupling regime perturbative computations of different physical observables require the resummation of Feynman diagrams [1,2], the so called hard thermal loops (HTL), to attain a result valid at a certain order in the gauge coupling expansion (see [3] for a review and complete set of basic references). This makes the studies of relativistic plasmas particularly cumbersome.

For very large values of the temperature T (or of the chemical potential μ), a well-defined hierarchy of energy scales appears in these relativistic plasmas, that allows for effective field theory descriptions, very similar to those applied for nonthermal physics. In a series of papers [4–9], the on-shell effective field theory (OSEFT) has been developed in order to describe the physics of the hard scales, or scales of order T (or μ), which are on-shell degrees of freedom. This effective field theory was initially developed to obtain quantum corrections to classical transport equations. Then it was realized that it could be used to improve the description of the hard scales of the plasma, and as by-product, also the soft scales of order eT (or $e\mu$), where e is the gauge coupling constant.

The rationale and technical tools used by OSEFT are the same as that of other effective field theories, such as high density field theory (HDET) [10], or soft collinear effective field theory (SCET) [11,12], for example. After fixing the value of the high energy scale, in this case the energy of the (quasi) massless fermion, which is of order $\sim T$ for thermal plasmas, one defines some small fluctuations around that scale. Integrating out the high energy modes, one is left with an effective theory for the lower scales or quantum fluctuations. The resulting Lagrangian is organized as an expansion of operators of increasing dimension over powers of the high energy scale.

In this manuscript we focus our attention to thermal corrections to the HTL photon polarization tensor associated to the fact that fermions on the plasma might not be strictly massless, but have indeed a small mass m much less than the temperature, $m \ll T$. This is a realistic assumption, as only in the cosmological epoch before the electroweak phase transition all elementary particles were strictly massless. While the power corrections to the HTL photon polarization tensor have been computed with OSEFT in Ref. [5], here we will use the OSEFT for the computation of the leading fermion mass corrections. We also check that the same result is obtained if derived from transport theory. Intermediate steps in the computations reveal the presence of potential infrared divergencies. A regularization of the momentum integrals is needed. We use dimensional regularization, as it is respectful with the gauge symmetry, and then show that all infrared divergencies cancel in the final result. We also

*marc.comadranc@e-campus.uab.cat
†cmanuel@ice.csic.es

explain why our results remain valid in the presence of a chemical potential, even for high values of μ and $T = 0$.

This paper is structured as follows. In Sec. II we review the OSEFT Lagrangian including small mass corrections. We present the computation of the Feynman diagrams in OSEFT that provide mass corrections to the photon polarization tensor in Sec. III. The same result is obtained if computed from transport theory, as shown in Sec. IV. We then compare our results with both the power and two-loop corrections to the HTL in Sec. V, and discuss when the mass corrections are the dominant correction to the HTL polarization tensor. We denote with boldface letters 3 dimensional vectors. Natural units $\hbar = k_B = 1$ are used throughout this manuscript.

II. SMALL MASS CORRECTIONS TO THE OSEFT

In this section we derive the OSEFT Lagrangian including mass corrections to the third order in the energy expansion. Let us briefly discuss how this is achieved.

In the spirit of the OSEFT we split the momentum of the energetic fermion as

$$q^\mu = p v^\mu + k^\mu, \tag{1}$$

where v^μ is a lightlike vector, p is the high scale, while k^μ is the so called residual momentum, associated to the quantum fluctuation, and is such that $k^\mu \ll p$. For the antifermion we will write

$$q^\mu = -p\tilde{v}^\mu + k^\mu, \tag{2}$$

where $\tilde{v}^\mu$ is also a lightlike vector. We will impose that

$$u^\mu = \frac{v^\mu + \tilde{v}^\mu}{2}, \tag{3}$$

where u^μ is a frame vector, such that $u^2 = 1$, thus, it is timelike.

The OSEFT Lagrangian including small mass corrections has been derived in Ref. [9], and in an arbitrary frame it reads

$$\begin{aligned}\mathcal{L}_{p,v} = {} & \bar{\chi}_v(x)\left(iv\cdot D + i\not{D}_\perp \frac{1}{2p + i\tilde{v}\cdot D} i\not{D}_\perp - m^2 \frac{1}{2p + i\tilde{v}\cdot D}\right)\frac{\tilde{\not{v}}}{2}\chi_v(x) \\ & - \bar{\chi}_v(x)\left(m\left[\frac{1}{2p + i\tilde{v}\cdot D}, i\not{D}_\perp\right]\right)\frac{\tilde{\not{v}}}{2}\chi_v(x),\end{aligned} \tag{4}$$

for the particle field χ_v, where $\not{D}_\perp = P_\perp^{\mu\nu}\gamma_\mu D_\nu$, and the transverse projector is defined as $P_\perp^{\mu\nu} = g^{\mu\nu} - \frac{1}{2}(v^\mu\tilde{v}^\nu + v^\nu\tilde{v}^\mu)$. For antiparticles, the Lagrangian can be obtained after replacing $p \leftrightarrow -p$ and $v^\mu \leftrightarrow \tilde{v}^\mu$. The Lagrangian has the same structure of that of SCET amended with small mass corrections [13,14]. Note that OSEFT and SCET are different theories, as the power counting is not the same (see [7] for a discussion on this point).

In writing the above Lagrangian, one assumes that the covariant derivatives, defined as $iD_\mu = i\partial_\mu + eA_\mu$, are *soft*, meaning that they are much less than the high energy scale, which here it is p. Equally, one assumes that the mass is such that $m \ll p$. The Lagrangian can then be now expanded using that p is the hard scale of the problem.

For applications of plasma physics in thermal field theory, it is convenient to use the frame at rest with the plasma, thus $u^\mu = (1, \mathbf{0})$. Then one can replace $\frac{\tilde{\not{v}}}{2}$ by $\not{u} = \gamma_0$ (recall that $\not{v}\chi_v = 0$). Expanding the Lagrangian on the high energy scale, one gets easily the first two terms in the energy expansion, which respect chirality

$$\mathcal{L}^{(0)}_{p,v} = \bar{\chi}_v(iv\cdot D)\gamma^0\chi_v, \tag{5}$$

$$\mathcal{L}^{(1)}_{p,v} = -\frac{1}{2p}\bar{\chi}_v\left(D_\perp^2 + m^2 - \frac{e}{2}\sigma_\perp^{\mu\nu}F_{\mu\nu}\right)\gamma^0\chi_v. \tag{6}$$

It is convenient to introduce local field redefinitions to eliminate the temporal derivative appearing at second order, as in Ref. [5]. These simplify the computations at higher orders. Thus, after the field redefinition

$$\chi_v \to \chi'_v = \left(1 + \frac{\not{D}_\perp^2 + m^2}{8p^2}\right)\chi_v, \tag{7}$$

the Lagrangian at second order reads

$$\begin{aligned}\mathcal{L}^{(2)}_{p,v} = \bar{\chi}'_v \frac{1}{8p^2}\big(& [\not{D}_\perp, [i\tilde{v}\cdot D, \not{D}_\perp]] \\ & - \{\not{D}_\perp^2 + m^2, iv\cdot D - i\tilde{v}\cdot D\} \\ & + 2iem\,\tilde{v}^\mu F_{\mu\alpha}\gamma_\perp^\alpha\big)\gamma^0\chi'_v.\end{aligned} \tag{8}$$

Note that the term linear in the mass describes a breaking of chirality.

We will also need the Lagrangian up to third order. To eliminate temporal derivatives at that order, we perform the local field redefinition

$$\chi_v \to \chi''_v = \left(1 - \frac{i}{8p^3}\not{P}_\perp[\tilde{v}\cdot D, \not{P}_\perp] + \frac{i}{16p^3}(\not{P}_\perp^2 + m^2)(v\cdot D - \tilde{v}\cdot D) - \frac{i}{16p^3}(\not{P}_\perp^2 + m^2)\tilde{v}\cdot D + \frac{m}{8p^3}[i\tilde{v}\cdot D, i\not{P}_\perp]\right)\chi'_v, \tag{9}$$

so that the final Lagrangian reads

$$\mathcal{L}^{(3)}_{p,v} = \frac{1}{8p^3}\bar{\chi}''_v((\not{P}_\perp^2 + m^2)^2 + [i\tilde{v}\cdot D, \not{P}_\perp]^2 - (iv\cdot D - i\tilde{v}\cdot D)(\not{P}_\perp^2 + m^2)(iv\cdot D - i\tilde{v}\cdot D) + (iv\cdot D - i\tilde{v}\cdot D)\not{P}_\perp[i\tilde{v}\cdot D, \not{P}_\perp] - [i\tilde{v}\cdot D, \not{P}_\perp]\not{P}_\perp(iv\cdot D - i\tilde{v}\cdot D) + m\{iv\cdot D - i\tilde{v}\cdot D, [i\tilde{v}\cdot D, i\not{P}_\perp]\})\gamma^0\chi''_v. \tag{10}$$

Please note that in the limit $m = 0$ we recover the same Lagrangians derived in Ref. [5]. The pieces which are quadratic in the mass can be recovered from those of Ref. [5] simply by replacing $\not{P}_\perp^2 \to \not{P}_\perp^2 + m^2$. The linear terms in m, originating from the expansion of the last term in Eq. (4), describe the breaking of the chiral symmetry induced by the fermion mass.

We present here how the OSEFT fermion propagators are modified in the presence of a small mass. The particle/antiparticle projectors in the frame at rest with the plasma are defined as $P_v = \frac{1}{2}\not{v}\gamma_0$ and $P_{\tilde{v}} = \frac{1}{2}\not{\tilde{v}}\gamma_0$, respectively. We introduce chirality projectors

$$P_\chi = \frac{1+\chi\gamma_5}{2}, \qquad \chi = \pm. \tag{11}$$

The propagators for a fermion of chirality χ in the Keldysh formulation of the real time formalism of thermal field theory Ref. [15] read

$$S^{R/A}_\chi(k) = \frac{P_\chi P_v \gamma_0}{k_0 \pm i\epsilon - f(\mathbf{k}, m)}, \tag{12}$$

$$S^S_\chi(k) = P_\chi P_v\gamma_0(-2\pi i\delta(k_0 - f(\mathbf{k}, m)) \times (1 - 2n_F(p + k_0))), \tag{13}$$

where $n_F(x) = 1/(\exp|x|/T + 1)$ is the Fermi-Dirac equilibrium distribution function. The function $f(\mathbf{k}, m)$ determines the dispersion law, and it is expanded also, we denote as $f^{(n)}(\mathbf{k}, m)$ the n order term in the $1/p$ expansion. At lowest order

$$f^{(0)}(\mathbf{k}, m) = k_\parallel, \tag{14}$$

and we have defined $k_\parallel = \mathbf{k}\cdot\mathbf{v}$, while

$$f^{(1)}(\mathbf{k}, m) = k_\parallel + \frac{\mathbf{k}_\perp^2 + m^2}{2p},$$
$$f^{(2)}(\mathbf{k}, m) = k_\parallel + \frac{\mathbf{k}_\perp^2 + m^2}{2p} - \frac{k_\parallel(\mathbf{k}_\perp^2 + m^2)}{2p^2}, \tag{15}$$

as follows from Eqs. (6) and (8), respectively. The propagators for the antiparticle quantum fluctuations can be also easily deduced. They read

$$\tilde{S}^{R/A}_\chi(k) = \frac{P_\chi P_{\tilde{v}}\gamma_0}{k_0 \pm i\epsilon - \tilde{f}(\mathbf{k}, m)}, \tag{16}$$

$$\tilde{S}^S_\chi(k) = -P_\chi P_{\tilde{v}}\gamma_0(-2\pi i\delta(k_0 - \tilde{f}(\mathbf{k}, m))(1 - 2n_F(-p + k_0))), \tag{17}$$

where the function $\tilde{f}(\mathbf{k}, m)$ can be obtained from $f(\mathbf{k}, m)$, with the replacements $\mathbf{v} \to -\mathbf{v}$ and $p \to -p$. Note the extra minus sign in the symmetric antiparticle propagator, absent in its particle counterpart.

In summary, the OSEFT fermion propagators in this case can be deduced from those of the massless case simply by replacing $\mathbf{k}_\perp^2 \to \mathbf{k}_\perp^2 + m^2$ in the function that determines the dispersion relation at every order in the energy expansion.

Note that, for convenience, we keep the propagators above unexpanded in this section, as done in Ref. [5], but in the explicit computation of the different diagrams they are to be expanded in a $1/p$ series.

III. DIAGRAMMATIC COMPUTATION OF THE MASS CORRECTION TO THE RETARDED PHOTON POLARIZATION TENSOR

In this section we compute the mass corrections to the retarded photon polarization tensor computed in OSEFT. Recall that there are two possible different topological diagrams that contribute to the computation, the bubble and the tadpole diagrams, see Fig. 1. The tadpole diagrams,

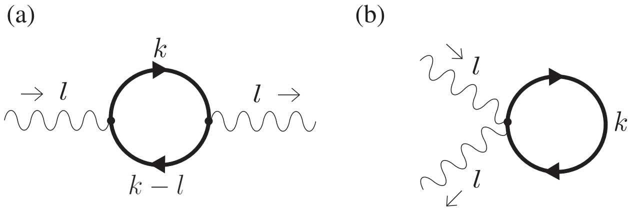

FIG. 1. (a) Bubble diagram (b) Tadpole diagram.

absent in QED, take into account particle-photon interactions mediated by an off-shell antiparticle (and viceversa for antiparticle-photon interactions), and are needed to respect the Ward identity obeyed by the polarization tensor, as we will explicitly check in this manuscript.

In the Keldysh representation the particle contribution to the bubble diagram of the retarded polarization tensor has the structure[1]

$$\Pi^{\mu\nu}_{b,\chi}(l) = \frac{i}{2}\sum_{p,\mathbf{v}}\int \frac{d^4k}{(2\pi)^4}\{\mathrm{Tr}[V^\mu S^\chi_S(k-l)V^\nu S^\chi_R(k)] + \mathrm{Tr}[V^\mu S^\chi_A(k-l)V^\nu S^\chi_S(k)]\}, \tag{18}$$

while the particle contribution to the tadpole diagram can be expressed as

$$\Pi^{\mu\nu}_{t,\chi}(l) = -\frac{i}{2}\sum_{p,\mathbf{v}}\int \frac{d^4k}{(2\pi)^4}\mathrm{Tr}\,[W^{\mu\nu}S^\chi_S(k)], \tag{19}$$

where the momentum dependence of the vertex functions V^μ and $W^{\mu\nu}$ are understood. Similar expressions can be written for the antiparticle contributions to the polarization tensor.

Using the explicit expressions of the fermion propagators, one can carry out the integral in k_0 to arrive to the general expressions

$$\Pi^{\mu\nu}_{b,\chi}(l) = -\sum_{p,\mathbf{v}}\int \frac{d^3\mathbf{k}}{(2\pi)^3}\mathrm{Tr}[V^\mu P_\chi P_v\gamma^0 V^\nu P_v\gamma^0] \times \frac{n_F(p+f(\mathbf{k}-\boldsymbol{l},m)) - n_F(p+f(\mathbf{k},m))}{l_0 + i0^+ + f(\mathbf{k}-\boldsymbol{l},m) - f(\mathbf{k},m)}, \tag{20}$$

and

$$\Pi^{\mu\nu}_{t,\chi}(l) = -\frac{1}{2}\sum_{p,\mathbf{v}}\int \frac{d^3\mathbf{k}}{(2\pi)^3}\mathrm{Tr}\,[W^{\mu\nu}P_\chi P_v\gamma^0] \times (1 - 2n_F(p+f(\mathbf{k},m))), \tag{21}$$

for the bubble and tadpole diagrams, respectively.

[1] We have changed the sign conventions of the definition of the polarization tensor as with respect to those used in Ref. [5].

The Feynman rules needed for the computation of the photon polarization tensor were given in Ref. [5] (see Tables I and II of that reference). In the presence of a mass in the OSEFT Lagrangian, new vertices appear proportional to the mass squared, which are given by

$$V^\mu_{(2),m^2} = -\frac{em^2}{2p^2}\gamma_0\,\delta^{\mu i}v^i, \tag{22}$$

$$W^{\mu\nu}_{(3),m^2} = -\frac{m^2e^2\gamma^0}{2p^3}\left[P^{\mu\nu}_\perp + \frac{(v^\mu - \tilde{v}^\mu)(v^\nu - \tilde{v}^\nu)}{2}\right]. \tag{23}$$

There are also new vertices proportional to the mass, which imply a change in the fermion chirality. At the order we will compute the mass corrections, $n = 3$ in the energy expansion, these will not be needed, although they would be required at fourth order in the energy expansion. Note that at least two of these vertices would be needed in a computation of the photon polarization tensor to preserve the fermion chirality inside the loop.

We now evaluate the polarization tensor at different orders, noting that we either consider the energy expansion in the vertex functions, or in the fermion propagators, which can be used at the desired order of accuracy.

The first nonvanishing contribution to the photon polarization tensor occurs at $n = 1$, but it does not carry any mass dependence. This was computed in Ref. [5], and it reproduces the HTL contribution. Let us recall the main results here. Adding the bubble and the tadpole diagrams at order $n = 1$ gives

$$\Pi^{\mu\nu}(l) = -e^2\sum_{\chi=\pm}\sum_{p,\mathbf{v}}\int \frac{d^3\mathbf{k}}{(2\pi)^3}\frac{dn_F}{dp}\left(\frac{P^{\mu\nu}_\perp}{2} + v^\mu v^\nu - l_0\frac{v^\mu v^\nu}{v\cdot l}\right). \tag{24}$$

where the retarded prescription $l_0 \to l_0 + i0^+$ is understood.

It is now important to return to the original momentum variable q^μ. Using the identity [5]

$$\sum_{p,\mathbf{v}}\int \frac{d^3\mathbf{k}}{(2\pi)^3} \equiv \int \frac{d^3\mathbf{q}}{(2\pi)^3} \tag{25}$$

and the relations [5]

$$p = q - k_{\parallel,\hat{\mathbf{q}}} + \frac{\mathbf{k}^2_{\perp,\hat{\mathbf{q}}}}{2q} + \mathcal{O}\left(\frac{1}{q^2}\right), \tag{26}$$

$$\mathbf{v} = \hat{\mathbf{q}} - \frac{\mathbf{k}_{\perp,\hat{\mathbf{q}}}}{q} - \frac{\hat{\mathbf{q}}\mathbf{k}^2_{\perp,\hat{\mathbf{q}}} + 2k_{\parallel,\hat{\mathbf{q}}}\mathbf{k}_{\perp,\hat{\mathbf{q}}}}{2q^2} + \mathcal{O}\left(\frac{1}{q^3}\right), \tag{27}$$

$$n_F(p) = n_F(q) + \frac{dn_f}{dq}\left(-k_{\parallel,\hat{\mathbf{q}}} + \frac{\mathbf{k}^2_{\perp,\hat{\mathbf{q}}}}{2q}\right) + \frac{1}{2}\frac{d^2 n_F}{dq^2} k^2_{\parallel,\hat{\mathbf{q}}} + \mathcal{O}\left(\frac{1}{q^3}\right), \tag{28}$$

where now the symbols $\mathbf{k}_{\parallel,\hat{\mathbf{q}}}$ and $\mathbf{k}_{\perp,\hat{\mathbf{q}}}$ denote the components of $\mathbf{k}$ parallel and perpendicular to $\hat{\mathbf{q}} \equiv \mathbf{q}/q$ with $q = |\mathbf{q}|$, respectively. We also define the vectors

$$v^\mu_{\hat{\mathbf{q}}} \equiv (1, \hat{\mathbf{q}}), \qquad \tilde{v}^\mu_{\hat{\mathbf{q}}} \equiv (1, -\hat{\mathbf{q}}). \tag{29}$$

After adding both the particle and antiparticle contributions to the photon polarization tensor one arrives to the well-known HTL expression

$$\Pi^{\mu\nu}_{\rm htl}(l) = -4e^2 \int \frac{d^3\mathbf{q}}{(2\pi)^3}\frac{dn_F}{dq}\left(\delta^\mu_0\delta^\nu_0 - l_0\frac{v^\mu_{\hat{\mathbf{q}}} v^\nu_{\hat{\mathbf{q}}}}{v_{\hat{\mathbf{q}}}\cdot l}\right). \tag{30}$$

At second order in the energy expansion, and in the absence of chiral misbalance, the Bose-Einstein statistics and the crossing symmetry demands that the polarization tensor $\Pi^{\mu\nu}(l)$ be symmetric under the simultaneous exchange of $\mu \leftrightarrow \nu$ and $l \leftrightarrow -l$ [16]. These symmetries explain the absence of linear terms in the photon momenta in the polarization tensor, which ultimately explain why there are not $n = 2$ corrections in the polarization tensor in OSEFT. This was explicitly checked in Refs. [5,17]. This reasoning applies actually to all the even orders of the energy expansion, $n = 4, 6, 8, \ldots$. We do not expect thus mass corrections at even orders, neither, and we actually have checked that there are none at $n = 2$.

The first mass corrections to the photon polarization tensor occur at third order in the energy expansion, the same as the power corrections to the HTL computed in Refs. [5,17].

The mass dependent terms that arise in the bubble diagram are

$$\Pi^{\mu\nu}_b(l) = -m^2 e^2 \sum_{\chi=\pm}\sum_{p,\mathbf{v}} \int \frac{d^3\mathbf{k}}{(2\pi)^3}\left\{-\frac{l_\parallel}{2p}\left[\left(\frac{d^2 n_F}{dp^2} - \frac{1}{p}\frac{dn_F}{dp}\right)\frac{v^\mu v^\nu}{v\cdot l} - \frac{l_\parallel}{p}\frac{dn_F}{dp}\frac{v^\mu v^\nu}{(v\cdot l)^2} - \frac{1}{2p}\frac{dn_F}{dp}\frac{v^\mu(v^\nu - \tilde{v}^\nu) + v^\nu(v^\mu - \tilde{v}^\mu)}{v\cdot l}\right]\right\}, \tag{31}$$

while in the tadpole one gets

$$\Pi^{\mu\nu}_t(l) = -m^2 e^2 \sum_{\chi=\pm}\sum_{p,\mathbf{v}} \int \frac{d^3\mathbf{k}}{(2\pi)^3}\left\{\frac{n_F}{2p^3}\left[P^{\mu\nu}_\perp + \frac{(v^\mu - \tilde{v}^\mu)(v^\nu - \tilde{v}^\nu)}{2}\right] - \frac{P^{\mu\nu}_\perp}{2p^2}\frac{dn_F}{dp}\right\}. \tag{32}$$

We add the two pieces, and go back to the full momentum variables. The final result, after adding also the antiparticle contributions, yields

$$\Pi^{\mu\nu}_{\rm m}(l) = -4m^2 e^2 \int \frac{d^3\mathbf{q}}{(2\pi)^3}\left\{\frac{n_F}{2q^3}\left[P^{\mu\nu}_{\perp,\hat{\mathbf{q}}} + \frac{(v^\mu_{\hat{\mathbf{q}}} - \tilde{v}^\mu_{\hat{\mathbf{q}}})(v^\nu_{\hat{\mathbf{q}}} - \tilde{v}^\nu_{\hat{\mathbf{q}}})}{2}\right] + \frac{1}{q^2}\frac{dn_F}{dq}\left[-\frac{P^{\mu\nu}_{\perp,\hat{\mathbf{q}}}}{2} + l_{\parallel,\hat{\mathbf{q}}}\left(\frac{v^\mu_{\hat{\mathbf{q}}} v^\nu_{\hat{\mathbf{q}}}}{v_{\hat{\mathbf{q}}}\cdot l} + \frac{l_{\parallel,\hat{\mathbf{q}}}}{2}\frac{v^\mu_{\hat{\mathbf{q}}} v^\nu_{\hat{\mathbf{q}}}}{(v_{\hat{\mathbf{q}}}\cdot l)^2} + \frac{1}{4}\frac{v^\mu_{\hat{\mathbf{q}}}(v^\nu_{\hat{\mathbf{q}}} - \tilde{v}^\nu_{\hat{\mathbf{q}}}) + v^\nu_{\hat{\mathbf{q}}}(v^\mu_{\hat{\mathbf{q}}} - \tilde{v}^\mu_{\hat{\mathbf{q}}})}{v_{\hat{\mathbf{q}}}\cdot l}\right)\right]\right\}. \tag{33}$$

We note that the first two terms of the second line of Eq. (33) can be written as the HTL contribution, but with a coefficient proportional to $e^2 m^2$ rather than the Debye mass squared $m_D^2 = e^2T^2/3$. Note also that in the tadpole diagram the pieces that are proportional to $n_F(q)/q^3$ are in principle infrared divergent. These terms have to be evaluated using a regularization. We use dimensional regularization (DR), by assuming that the system is in $d = 3 + 2\epsilon$ dimensions. In this case the momentum integrals become

$$\int \frac{d^d q}{(2\pi)^d} \to \frac{4}{(4\pi)^{2+\epsilon}\Gamma(1+\epsilon)}\int_0^\infty dq\, q^{2+2\epsilon} \times \int_{-1}^{1} d\cos\theta\,(1 + \epsilon\ln(\sin^2\theta)), \tag{34}$$

where θ parametrizes an angle with respect to an external vector, and $\Gamma(z)$ stands for the Gamma function. Furthermore, in d dimensions one has to change the coupling constant as $e^2 \to e^2\nu^{3-d}$, where ν is a renormalization scale.

The relevant infrared radial integral is

$$\nu^{-2\epsilon}\int_0^\infty dq q^{-1+2\epsilon} n_F(q) = \frac{1}{4\epsilon} + \frac{1}{2}\ln\left(\frac{\pi T e^{-\gamma_E}}{2\nu}\right) + \mathcal{O}(\epsilon), \tag{35}$$

where γ_E is Euler's constant. However, when carrying out the angular integrals in $d = 3 + 2\epsilon$ dimensions, the pole term and logarithm exactly cancel, as the angular integral turns out to be proportional to ϵ (that is, it would cancel if $d = 3$). If $d\Omega_d$ is the solid angle element in d dimensions, and $S_d = 2\pi^d/\Gamma(d/2)$ is the area of a d-dimensional unit sphere, one can check

$$S_{3+2\epsilon}^{-1}\int d\Omega_{3+2\epsilon}(-\delta^{ij} + 3\hat{\mathbf{q}}^i\hat{\mathbf{q}}^j) = -\frac{2}{3}\epsilon + \mathcal{O}(\epsilon^2). \tag{36}$$

Thus, combing the two results one gets

$$-4m^2 e^2 \nu^{-2\epsilon}\int \frac{d^d q}{(2\pi)^d}\frac{n_F}{2q^3}\left[P^{\mu\nu}_{\perp,\hat{\mathbf{q}}} + \frac{(v^\mu_{\hat{\mathbf{q}}} - \tilde{v}^\mu_{\hat{\mathbf{q}}})(v^\nu_{\hat{\mathbf{q}}} - \tilde{v}^\nu_{\hat{\mathbf{q}}})}{2}\right] = \frac{m^2 e^2}{6\pi^2}\delta^{ij} + \mathcal{O}(\epsilon), \tag{37}$$

and there is no infrared divergence, but only a finite term. This finite term is ultimately needed to preserve the Ward identity obeyed by the polarization tensor, as can be checked after computing

$$l_\mu \Pi^{\mu\nu}_{\mathrm{m}}(l) = 4m^2 e^2 \int \frac{d^3\mathbf{q}}{(2\pi)^3}\frac{1}{q^2}\frac{dn_F}{dq}\left[\frac{l^2_{\parallel,\hat{\mathbf{q}}}}{2}\frac{v^\nu_{\hat{\mathbf{q}}}}{v_{\hat{\mathbf{q}}}\cdot l} - \frac{2l^2_{\parallel,\hat{\mathbf{q}}}}{4}\frac{v^\nu_{\hat{\mathbf{q}}}}{v_{\hat{\mathbf{q}}}\cdot l} + \frac{l_{\parallel,\hat{\mathbf{q}}}}{4}(v^\nu_{\hat{\mathbf{q}}} - \tilde{v}^\nu_{\hat{\mathbf{q}}})\right] - \frac{m^2 e^2}{6\pi^2} l^j \delta^{\nu j} = 0. \tag{38}$$

Note that if we had used a cutoff regularization of the integrals, the IR divergent terms would also vanish, but the above integral would not yield the finite contribution, the last term of Eq. (38), needed to respect the gauge invariance of the computation.

We define the longitudinal and transverse parts of the photon polarization tensor in d dimensions by

$$\Pi^L(l_0, \boldsymbol{l}) \equiv \Pi^{00}(l_0, \boldsymbol{l}),$$
$$\Pi^T(l_0, \boldsymbol{l}) \equiv \frac{1}{d-1}\left(\delta^{ij} - \frac{l^i l^j}{\boldsymbol{l}^2}\right)\Pi^{ij}(l_0, \boldsymbol{l}). \tag{39}$$

We then find the following mass corrections to the longitudinal and transverse parts of the polarization tensor

$$\Pi^{\mathrm{L}}_{\mathrm{m}}(l_0, \boldsymbol{l}) = \frac{e^2 m^2}{2\pi^2}\frac{\boldsymbol{l}^2}{l_0^2 - \boldsymbol{l}^2}, \tag{40}$$

$$\Pi^{\mathrm{T}}_{\mathrm{m}}(l_0, \boldsymbol{l}) = \frac{e^2 m^2}{2\pi^2}\frac{l_0}{2|\boldsymbol{l}|}\ln\left(\frac{l_0 + |\boldsymbol{l}|}{l_0 - |\boldsymbol{l}|}\right). \tag{41}$$

Let us finally stress that Eqs. (40)–(41) remain also valid in the presence of a finite chemical potential μ. In the presence of a chemical potential the particle and antiparticle contributions differ, but the final result can be recovered from Eq. (33), simply by replacing in Eq. (33)

$$n_F(q) \to \frac{1}{2}[n_F(q-\mu) + n_F(q+\mu)]. \tag{42}$$

After an explicit evaluation of the corresponding integrals, one reaches to the same mass corrections to the polarization tensor which are valid at high temperature. In particular, our results still hold if we take $T = 0$ and keep the chemical potential μ as the high scale of the problem.

IV. COMPUTATION OF THE PHOTON POLARIZATION TENSOR FROM KINETIC THEORY

We compute in this section the mass corrections to the photon polarization tensor as computed from kinetic theory. We use the transport approach derived from OSEFT, and focus on the vectorial component of the Wigner function. From Ref. [9], the transport equation associated to a fermion with chirality χ up to second order in the energy expansion reads

$$\left[v^\mu_\chi - \frac{e}{2E_q^2}S^{\mu\nu}_\chi F_{\nu\rho}(X)(2u^\rho - v^\rho_\chi)\right] \times (\partial^X_\mu - eF_{\mu\rho}(X)\partial^\rho_q)G^\chi(X, q) = 0, \tag{43}$$

where $v^\mu_\chi = q^\mu/E_q$, and we take the frame vector that defines the system as $u^\mu = (1, \mathbf{0})$. Furthermore

$$G^\chi(X, q) = 2\pi\delta(Q^\chi_m)n^\chi(X, q), \tag{44}$$

where $n^\chi(X, q)$ is the distribution function, and the delta gives the on-shell constraint, Q^χ_m being a function of the momentum and the mass. The particle contribution to the electromagnetic current is expressed, at $n = 2$ order as

$$j^\mu(X) = e\sum_{\chi=\pm}\int \frac{d^4q}{(2\pi)^4}\left[v^\mu_\chi - \frac{S^{\mu\nu}_\chi \Delta_\nu}{E_q} - \frac{e}{2}\frac{S^{\mu\nu}_\chi}{E_q^2}F_{\nu\rho}(X)(2u^\rho - v^\rho_\chi)\right]2G^\chi(X,q) + \mathcal{O}\left(\frac{1}{E_q^3}\right). \tag{45}$$

We ignore in this manuscript the possible effect of the spin coherence function discussed in Ref. [9], which represent coherent quantum states of mixed chiralities. We also will ignore the terms in the transport equation, on-shell constraint, and in the vector current proportional to the spin tensor $S^{\mu\nu}_\chi$, as they are irrelevant if the chiral chemical potential is zero, as the contribution of the two fermion chiralities makes these pieces to cancel in the macroscopic current. Those terms are relevant, though, to derive the chiral magnetic effect, which is not our goal here (see appendix of Ref. [7] for that derivation). We thus write the on-shell constraint to the considered order of accuracy

$$q_0 = E_q = q + \frac{m^2}{2q}. \tag{46}$$

Where $q = |\mathbf{q}|$. We now assume to be close to thermal equilibrium, such that

$$G^\chi = G^\chi_{(0)} + \delta G^\chi + \cdots \tag{47}$$

where $G^\chi_{(0)}$ is the Wigner function in thermal equilibrium. Using the transport equation, we find

$$v^\chi \cdot \partial_X \delta G^\chi = e v^\chi_\mu F^{\mu\nu}\frac{\partial G^\chi_{(0)}}{\partial q^\nu}, \tag{48}$$

and after computing

$$\delta j^\mu(X) = e\sum_{\chi=\pm}\int \frac{d^4q}{(2\pi)^4} v^\mu_\chi \delta G^\chi(X,q), \tag{49}$$

one derives the polarization tensor as

$$\Pi^{\mu\nu} = \frac{\delta j^\mu}{\delta A_\nu}. \tag{50}$$

It is not difficult to find the particle contribution to the polarization tensor, which reads

$$\Pi^{\mu\nu}(l) = e^2\sum_{\chi=\pm}\int \frac{d^3\mathbf{q}}{(2\pi)^3}\left(g^{\mu\nu} - \frac{l^\mu v^\nu_m + v^\mu_m l^\nu}{l\cdot v_m} + L^2\frac{v^\mu_m v^\nu_m}{(l\cdot v_m)^2}\right) \times \frac{n_F(q_0 = E_q)}{E_q}, \tag{51}$$

where $L^2 = l_0^2 - \boldsymbol{l}^2$, and

$$v^\mu_m = v^\mu_{\hat{\mathbf{q}}} - \delta^{\mu i} v^i_{\hat{\mathbf{q}}}\frac{m^2}{2q^2}, \tag{52}$$

for the particles. A similar expression holds for the antiparticles.

We compute all the pieces up to $\mathcal{O}(m^2)$, by noting that

$$\frac{1}{E_q} = \frac{1}{q} - \frac{m^2}{2q^3} + \cdots \tag{53}$$

$$\frac{1}{l\cdot v_m} = \frac{1}{l\cdot v_{\hat{\mathbf{q}}}} - \frac{\boldsymbol{l}\cdot \mathbf{v}_{\hat{\mathbf{q}}}}{(l\cdot v_{\hat{\mathbf{q}}})^2}\frac{m^2}{2q^2} + \cdots \tag{54}$$

$$n_F(E_q) = n_F(q) + \frac{m^2}{2q}\frac{dn_F}{dq} + \cdots \tag{55}$$

We thus find that the polarization tensor can be written as

$$\Pi^{\mu\nu}(l) = \Pi^{\mu\nu}_{\rm htl}(l) + \Pi^{\mu\nu}_{\rm m}(l). \tag{56}$$

The HTL part, as arising from particles and antiparticles of the two possible chiralities, reads

$$\Pi^{\mu\nu}_{\rm htl}(l) = 4e^2\int \frac{d^3\mathbf{q}}{(2\pi)^3}\left(g^{\mu\nu} - \frac{l^\mu v^\nu_{\hat{\mathbf{q}}} + v^\mu_{\hat{\mathbf{q}}} l^\nu}{l\cdot v_{\hat{\mathbf{q}}}} + L^2\frac{v^\mu_{\hat{\mathbf{q}}} v^\nu_{\hat{\mathbf{q}}}}{(l\cdot v_{\hat{\mathbf{q}}})^2}\right) \times \frac{n_F(q)}{q}. \tag{57}$$

While the leading mass correction is

$$\begin{aligned}\Pi^{\mu\nu}_{\rm m}(l) &= 4e^2m^2\int \frac{d^3\mathbf{q}}{(2\pi)^3}\left(g^{\mu\nu} - \frac{l^\mu v^\nu_{\hat{\mathbf{q}}} + v^\mu_{\hat{\mathbf{q}}} l^\nu}{l\cdot v_{\hat{\mathbf{q}}}} + L^2\frac{v^\mu_{\hat{\mathbf{q}}} v^\nu_{\hat{\mathbf{q}}}}{(l\cdot v_{\hat{\mathbf{q}}})^2}\right)\left(\frac{1}{2q^2}\frac{dn_F(q)}{dq}\right)\\ &+ 4e^2m^2\int \frac{d^3\mathbf{q}}{(2\pi)^3}\left(g^{\mu\nu} - l_0\frac{l^\mu v^\nu_{\hat{\mathbf{q}}} + v^\mu_{\hat{\mathbf{q}}} l^\nu}{(l\cdot v_{\hat{\mathbf{q}}})^2} - L^2\frac{v^\mu_{\hat{\mathbf{q}}} v^\nu_{\hat{\mathbf{q}}}}{(l\cdot v_{\hat{\mathbf{q}}})^2} + 2L^2 l_0\frac{v^\mu_{\hat{\mathbf{q}}} v^\nu_{\hat{\mathbf{q}}}}{(l\cdot v_{\hat{\mathbf{q}}})^3}\right.\\ &\left. - \frac{\delta^{\mu i} v^i_{\hat{\mathbf{q}}} l^\nu + \delta^{\nu i} v^i_{\hat{\mathbf{q}}} l^\mu}{l\cdot v_{\hat{\mathbf{q}}}} + L^2\frac{\delta^{\mu i} v^i_{\hat{\mathbf{q}}} v^\nu_{\hat{\mathbf{q}}} + \delta^{\nu i} v^i_{\hat{\mathbf{q}}} v^\mu_{\hat{\mathbf{q}}}}{(l\cdot v_{\hat{\mathbf{q}}})^2}\right)\left(-\frac{n_F(q)}{2q^3}\right).\end{aligned} \tag{58}$$

One can check that

$$l_\mu \Pi_{\rm m}^{\mu\nu}(l) = 0, \tag{59}$$

so that the Ward identity is respected for the mass dependent pieces of the polarization tensor at this order. Note that the first integral of Eq. (58) has the same structure than the HTL contribution, but it is proportional to the fermion mass squared. This contribution was also found out in the diagrammatic computation of Sec. III. The second integral contains IR divergencies, but are of a quite different structure as those appearing in the diagrammatic computation, see Eq. (37). The apparent IR divergencies here are clearly nonlocal. We evaluate these integrals using DR.

Note that we only need to evaluate the integral

$$\begin{aligned} I_1 \equiv& \int_{-1}^{1} d\cos\theta (1-\cos^2\theta)^\epsilon \frac{1}{l_0 - |\boldsymbol{l}|\cos\theta} \\ =& \frac{1}{|\boldsymbol{l}|}\left\{ \ln\left(\frac{l_0+|\boldsymbol{l}|}{l_0-|\boldsymbol{l}|}\right) + \epsilon\left[\ln(4)\ln\left(\frac{l_0+|\boldsymbol{l}|}{l_0-|\boldsymbol{l}|}\right)\right.\right. \\ &\left.\left. + \mathrm{Li}_2\left(-\frac{2|\boldsymbol{l}|}{l_0-|\boldsymbol{l}|}\right) - \mathrm{Li}_2\left(\frac{2|\boldsymbol{l}|}{l_0+|\boldsymbol{l}|}\right)\right]\right\} + \mathcal{O}(\epsilon^2), \end{aligned} \tag{60}$$

where Li_2 stands for the Euler polylogarithmic function of order 2. All the remaining non-local integrals can be deduced from this one, after simple manipulations.

An explicit computation shows that after angular integration in $d = 3 + 2\epsilon$ dimensions the IR divergencies exactly cancel, but there are remaining finite pieces, which in this case turn out to be non-local, and that allows one to reproduce the same value of the photon polarization tensor that we found in Sec. III.

V. DISCUSSION

We used OSEFT to assess how a small fermion mass would affect the retarded photon polarization tensor at soft scales in a ultrarelativistic electromagnetic plasma. While it could be obvious that such corrections would be of order m^2/T^2, the effective field theory techniques we used allowed us their proper evaluation.

Our results could have also been derived from the expression of the full QED polarization tensor, by assuming that both the external momentum and the fermion mass are small in front of the hard loop momentum, expanding the corresponding expressions. As this expansion produces infrared divergencies, it is important to use a regularization of all the involved integrals before the expansion. We have emphasized in the whole manuscript the relevance of using a regulator that respects the gauge symmetry, as dimensional regularization, to obtain physical results. OSEFT ultimately yields the same results of this expansion, up to possible local terms. We have presented an alternative computation from transport theory so as to be sure of the absence of possible extra pieces.

Our results should be compared to both the power and two-loop corrections to the HTL tensor that have been computed in Refs. [5,17], and [18], respectively. More precisely, we will write

$$\Pi_I = \Pi_I^{\rm htl} + \Pi_I^m + \Pi_I^{\rm pow\cdot corr} + \Pi_I^{2\,\rm loop}, \qquad I = L, T, \tag{61}$$

where Π_I^m were displayed in Eqs. (40), (41) and

$$\begin{aligned} \Pi_L^{\rm htl}(l_0,\boldsymbol{l}) &= \frac{e^2T^2}{3}\left(1 - \frac{l_0}{2|\boldsymbol{l}|}\ln\left(\frac{l_0+|\boldsymbol{l}|}{l_0-|\boldsymbol{l}|}\right)\right), \\ \Pi_L^{\rm pow\cdot corr}(l_0,\boldsymbol{l}) &= -\frac{e^2}{4\pi^2}\left(\boldsymbol{l}^2 - \frac{l_0^2}{3}\right)\left(1 - \frac{l_0}{2|\boldsymbol{l}|}\ln\left(\frac{l_0+|\boldsymbol{l}|}{l_0-|\boldsymbol{l}|}\right)\right), \\ \Pi_L^{\rm 2loop}(l_0,\boldsymbol{l}) &= \frac{e^4T^2L^2}{8\pi^2\boldsymbol{l}^2}, \\ \Pi_T^{\rm htl}(l_0,\boldsymbol{l}) &= \frac{e^2T^2}{3}\frac{l_0}{4\boldsymbol{l}^3}\left(2|\boldsymbol{l}|l_0 - L^2\ln\left(\frac{l_0+|\boldsymbol{l}|}{l_0-|\boldsymbol{l}|}\right)\right), \\ \Pi_T^{\rm pow\cdot corr}(l_0,\boldsymbol{l}) &= \frac{e^2}{4\pi^2}\left(\frac{l_0^2}{2} + \frac{l_0^4}{6\boldsymbol{l}^2} - \frac{2\boldsymbol{l}^2}{3} - \frac{l_0^3}{12\boldsymbol{l}^3}\left(2\boldsymbol{l}^2 + l_0^2 - \frac{3\boldsymbol{l}^4}{l_0^2}\right)\ln\left(\frac{l_0+|\boldsymbol{l}|}{l_0-|\boldsymbol{l}|}\right)\right), \\ \Pi_T^{\rm 2loop}(l_0,\boldsymbol{l}) &= -\frac{e^4T^2}{16\pi^2}\frac{l_0}{|\boldsymbol{l}|}\ln\left(\frac{l_0+|\boldsymbol{l}|}{l_0-|\boldsymbol{l}|}\right). \end{aligned} \tag{62}$$

For simplicity, $\Pi_I^{\rm pow\cdot corr}$ above is taken at the value of the renormalization scale $\nu = Te^{-\gamma_E/2-1}\sqrt{\pi}/2$ in the MS scheme. This fixes the scale of $e^2 = e^2(\nu)$ in $\Pi_I^{\rm htl}$.

Let us recall the meaning of every term in Eq. (61). While the HTL contribution is proportional to e^2T^2, the results computed in this manuscript, even if they do not depend on the temperature, should be viewed as a a correction of order m^2/T^2 to the HTL. Similarly, the power corrections are of order l^2/T^2 respect to the HTL, while the two-loop results are corrections of order e^2. These three corrections are of the same order if $m, l \sim eT$, and should be equally considered. However, if the mass is such that $eT < m \ll T$, then the mass corrections are dominant at soft scales, $l \sim eT$.

For example, let us take the value of the photon screening mass, defined as $-m_S^2 = \Pi_L(l^0 = 0, \boldsymbol{l}^2 = -m_S^2)$. Calculated from the value of the longitudinal part of the polarization tensor, as given in Eq. (61), results in

$$m_S^2 = \frac{e^2T^2}{3}\left(1 - \frac{e^2}{8\pi^2} - \frac{1}{2\pi^2}\frac{m^2}{T^2}\right). \tag{63}$$

Note that for values $m^2/T^2 > \pi\alpha$, where α is the electromagnetic fine structure constant $\sim 1/137$, the mass effects give the most important corrections.

Let us finally remind the reader here that while we focused our discussion on thermal plasmas, our results and also the power corrections of Refs. [5,17] remain valid in the presence of a chemical potential, or even for high μ and $T = 0$. Our results can also be easily generalized to QCD, for the mass corrections to the HTL gluon polarization tensor, after taking into account some color factors, and replacing e^2 by $g^2/2$ for fermions in the fundamental representation, where g is the QCD coupling constant.

Our results might be useful to obtain a better evaluation of different physical observables whenever the fermions in the plasma are not strictly massless, which is a realistic condition for most of the physical scenarios where the HTL resummation techniques have been applied so far.

ACKNOWLEDGMENTS

We thank J. M. Torres-Rincon for discussions on extensive parts of this project, and S. Carignano and J. Soto for a critical reading of the manuscript. We have been supported by the Ministerio de Ciencia e Innovación (Spain) under the project No. PID2019–110165GB-I00 (MCI/AEI/FEDER, UE), as well as by the project No. 2017-SGR-247 (Catalonia). This work was also supported by the COST Action No. CA15213 THOR.

[1] R. D. Pisarski, Phys. Rev. Lett. **63**, 1129 (1989).
[2] E. Braaten and R. D. Pisarski, Nucl. Phys. **B337**, 569 (1990).
[3] J. Ghiglieri, A. Kurkela, M. Strickland, and A. Vuorinen, Phys. Rep. **880**, 1 (2020).
[4] C. Manuel and J. M. Torres-Rincon, Phys. Rev. D **90**, 076007 (2014).
[5] C. Manuel, J. Soto, and S. Stetina, Phys. Rev. D **94**, 025017 (2016); **96**, 129901(E) (2017).
[6] C. Manuel, J. Soto, and S. Stetina, EPJ Web Conf. **137**, 07014 (2017).
[7] S. Carignano, C. Manuel, and J. M. Torres-Rincon, Phys. Rev. D **98**, 076005 (2018).
[8] S. Carignano, C. Manuel, and J. M. Torres-Rincon, Phys. Rev. D **102**, 016003 (2020).
[9] C. Manuel and J. M. Torres-Rincon, Phys. Rev. D **103**, 096022 (2021).
[10] D. K. Hong, Phys. Lett. B **473**, 118 (2000).
[11] C. W. Bauer, S. Fleming, and M. E. Luke, Phys. Rev. D **63**, 014006 (2000).
[12] C. W. Bauer, S. Fleming, D. Pirjol, and I. W. Stewart, Phys. Rev. D **63**, 114020 (2001).
[13] J. Chay, C. Kim, and A. K. Leibovich, Phys. Rev. D **72**, 014010 (2005).
[14] A. K. Leibovich, Z. Ligeti, and M. B. Wise, Phys. Lett. B **564**, 231 (2003).
[15] K. C. Chou, Z. B. Su, B. L. Hao, and L. Yu, Phys. Rep. **118**, 1 (1985).
[16] J. F. Nieves and P. B. Pal, Phys. Rev. D **39**, 652 (1989); **40**, 2148(E) (1989).
[17] S. Carignano, C. Manuel, and J. Soto, Phys. Lett. B **780**, 308 (2018).
[18] S. Carignano, M. E. Carrington, and J. Soto, Phys. Lett. B **801**, 135193 (2020).

2 Accounting for plasma constituent mass effects in heavy fermion energy loss calculations in hot QED and QCD

In this section one can find the publication [25].

Accounting for plasma constituent mass effects in heavy fermion energy loss calculations in hot QED and QCD

Marc Comadran,[1,2,3,*] Cristina Manuel,[1,2,†] and Stefano Carignano[4,‡]

[1] *Instituto de Ciencias del Espacio (ICE, CSIC), C. Can Magrans s.n., 08193 Cerdanyola del Vallès, Spain*
[2] *Institut d'Estudis Espacials de Catalunya (IEEC), C. Gran Capità 2-4, Ed. Nexus, 08034 Barcelona, Spain*
[3] *Departament de Física Quàntica i Astrofísica and Institut de Ciències del Cosmos, Universitat de Barcelona (IEEC-UB), Martí i Franqués 1, 08028 Barcelona, Spain*
[4] *Barcelona Supercomputing Center (BSC), 08034 Barcelona, Spain*

(Received 5 May 2023; accepted 24 May 2023; published 21 June 2023)

We evaluate the collisional energy loss of a energetic fermion with mass M propagating through a hot QED plasma with temperature T, including mass corrections, that is, keeping the mass m of the fermion constituents of the plasma, assuming $m \ll T \ll M$. We use the bare theory to compute the contribution of hard momentum transfer collisions, and the Braaten-Pisarski resummed theory, amended with small mass corrections, for the contribution of low momentum transfer collisions, and compute the mass corrections at leading logarithmic accuracy in the regime where the energy of the heavy fermion obeys $E \ll M^2/T$. We use dimensional regularization to regulate all possible divergences in the computation. If the fermion mass is of order of the soft scale eT, where e is the gauge coupling constant, the mass corrections are of the same order as pure perturbative corrections, while they can be substantial for larger values of m. We also evaluate the impact of this correction for a QCD plasma.

DOI: 10.1103/PhysRevD.107.116016

I. INTRODUCTION

Jet energy loss is a prominent probe for characterizing the properties of matter in heavy-ion collision experiments. Theoretical predictions for the energy loss of an energetic parton produced in the early stages of the collision, which subsequently interacts with the constituents of the produced quark-gluon plasma, can provide invaluable guidance for extracting properties of the system from experimental data (for recent reviews see, e.g., [1–4]).

The first estimate of the collisional energy loss of a heavy fermion in a quark-gluon plasma was made by Bjorken more than 40 years ago [5]. A naive computation of this quantity is affected by logarithmic infrared (IR) divergences associated to collisions with low momentum transfer. A good estimate could be done by choosing physical reasonable cutoffs for the momentum transfer. A much more detailed full computation was then carried out by Braaten and Thoma (BT), first for QED [6] and then also for QCD [7]. These authors showed how to deal with these divergences consistently, by separating the energy loss computation into two parts, one that would consider high values (or hard) of momentum transfer, or the order of the temperature T, and the other with low values (or soft) of momentum transfer, of order eT, where e is the gauge coupling constant. The last should be treated using the hard thermal loop resummed photon propagators, according to the Braaten-Pisarski resummation program [8,9]. In the original BT treatment, these two contributions were computed by including an artificial cutoff in momentum transfer to split the two momentum transfer regions, such that when the two contributions are added, the cutoff dependence disappears. The computation by Braaten and Thoma was later on reviewed by Peigne and Peshier [10], correcting the computation for ultrarelativistic fermions, and further discussing the QCD energy loss in [11]. These authors stressed that the cutoff separating the two different regions should be implemented differently than in Ref. [6].

Even if the relevant computations of collisional energy loss are more than 30 years old, there have not been attempts so far to evaluate how they are perturbatively corrected, see [12] for the status of perturbation theory for QCD plasmas, for example. Only recently for QED the perturbative correction to the hard thermal loops (HTL) associated to the photon degrees of freedom has been computed. The perturbative correction arises from both the so called power corrections of the HTL [13–15], and also

*mcomadca60@alumnes.ub.edu
†cmanuel@ice.csic.es
‡stefano.carignano@bsc.es

from two-loop diagrams [16–18]. It has also been noted that the HTLs might be also corrected by effects associated to the (small) mass of the fermions in the plasma [19]. If the mass is of order $\sim eT$, then these mass corrections should be equally important as the genuine perturbative corrections [19].

In this article we evaluate how the collisional energy loss is modified by a small fermion mass of the QED plasma constituents at leading logarithmic accuracy. We will thus concentrate only in the t-channel photon exchange diagram, as the s and u-channel diagrams (Compton scattering) are subleading in the regime we are considering. We will assume that there is a good separation of scales, such that $eT \ll m \ll T$, as if $m \sim eT$ our results should be corrected by including genuine perturbative corrections. We will also comment on how the computation should be carried if the fermion mass gets close to T. While we provide all the ingredients for such a computation, we will not address such a case here, as it requires a more detailed analysis.

We will use dimensional regularization (DR) to separate the high (or hard) and low (or soft) momentum transfers parts of the computation. DR is a regularization respectful with gauge invariance. With its use we avoid the ambiguities of how a cutoff is implemented. DR was used in Ref. [20] to recover the leading logarithmic behavior of Ref. [6]. In this paper we also show that the finite term can be recovered using DR, reproducing the same result than the original one in Ref. [6].

As we will see, the inclusion of a small fermion mass is nontrivial, as new infrared divergences arise in intermediate steps in the computation. Those divergences can only be treated consistently with the use of dimensional regularization. This was already apparent in the computation of the small mass corrections to the HTL, see Ref. [19], as if the IR is regulated with a cutoff one generates a correction to the photon polarization tensor that violates gauge invariance. Even if IR divergences arise in the intermediate steps of the mass corrections to the HTL, the final result is finite, as there is a subtle cancellation of divergences [19]. We witness a similar cancellation of the IR divergences associated to the small mass expansion in the hard part of collisional energy loss. After this regularization, only the IR divergence associated to the low momentum transfer remains, which is canceled with the ultraviolet (UV) divergence to the soft part, yielding a finite result.

We have organized this paper in a way very similar to Ref. [6], where the computation was carried out with the use a cutoff, emphasizing the points where our treatment is different, and including the corresponding mass corrections. The hard contribution to the collisional energy loss is given in Sec. II. We provide two different computations of the soft contribution, the first in Sec. III, which is based on writing the collisional energy loss as a function of the heavy fermion damping rate, the second one in Sec. IV, based on writing the scattering rate of the collision, using resummed propagators. We present our final results in Sec. V, where we evaluate the relevance of the mass corrections in the QED collisional energy loss, and comment on the same effect for the QCD plasma. We show in Appendix A some details of the computation of the hard sector, and in Appendix B, the integral needed for the computation of soft momentum transfer. We provide in Appendix C the form of the polarization tensor that would be needed for the computation for a generic fermion mass m.

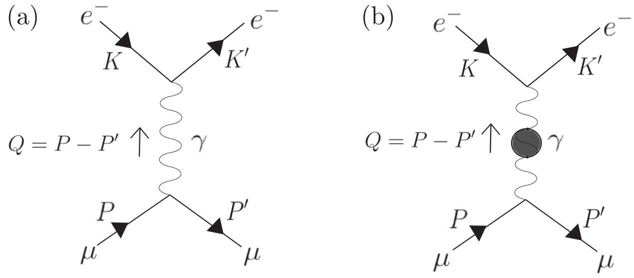

FIG. 1. A highly energetic and massive fermion (μ) scatters with the electrons/positrons (e^-/e^+) of the medium by the exchange of a virtual photon (γ). The diagrams with positrons e^+ should also be considered (reversing the electron line). (a) Hard contribution. (b) Soft contribution, with the blob representing the resummed propagator.

We denote four momenta with capital letters, $K^\mu = (k, \boldsymbol{k})$, and denote with boldface letters 3 dimensional vectors. Natural units $\hbar = k_B = c = 1$ and metric conventions $g^{\mu\nu} = \mathrm{diag}(+1, -1, -1, -1)$ are used throughout this manuscript.

II. HARD CONTRIBUTION TO THE COLLISIONAL ENERGY LOSS

The hard contribution to the energy loss from the process $e^-\mu \to e^-\mu$ is depicted diagrammatically in Fig. 1(a). The diagram with positrons gives exactly the same result, which accounts for a global factor of 2. We use the following notation for the kinematic variables. The four momentum of the heavy fermion of mass M is $P^\mu = (E, \boldsymbol{p})$, and $K^\mu = (E_k, \boldsymbol{k})$ is the four momentum of the plasma constituents, with mass m. We denote with $Q = P - P' = (\omega, \boldsymbol{q}) = (E - E', \boldsymbol{p} - \boldsymbol{p}')$ the momentum of the virtual photon, where we use primed variables for the outgoing particles in the collision.

Our starting expression for the computation of the hard contribution to the energy loss in d spatial dimensions is

$$-\frac{dE}{dx}\bigg| = \frac{1}{E}\int \frac{d^dp'}{(2\pi)^d 2E'}\int \frac{d^dk}{(2\pi)^d 2E_k} n_F(E_k)\int \frac{d^dk'}{(2\pi)^d 2E'_k}[1-n_F(E'_k)] \\ \times (2\pi)^{d+1}\delta^{d+1}(P+K-P'-K')\frac{E-E'}{v}\frac{1}{2}\sum_{\text{spins}}|\mathcal{M}|^2, \tag{1}$$

where $\mathcal{M}$ is the matrix element associated to the tree-level Feynman diagram. The matrix element is averaged over the spin of the incoming heavy fermion (μ), and the sum runs over the spins of the involved particles in the process. In Feynman gauge, squaring the amplitude and performing the sum over spins gives

$$\frac{1}{2}\sum_{\text{spins}}|\mathcal{M}|^2 = \frac{16e^4\nu^{6-2d}}{t^2}E^2\left\{2(E_k-\boldsymbol{v}\cdot\boldsymbol{k})(E'_k-\boldsymbol{v}\cdot\boldsymbol{k}') + \frac{d-1}{2}\frac{t^2}{4E^2} + \frac{m^2+M^2}{2E^2}t\right\}, \tag{2}$$

where $\boldsymbol{v} = \boldsymbol{p}/E$ is the velocity of the heavy fermion and $t = Q^2$. Here ν is the renormalization scale that naturally enters in the computation, as in changing the spatial dimensions from 3 to d the gauge coupling constant is modified from e^2 to $e^2\nu^{3-d}$. Let us stress that no approximation has been used in order to derive the last expression, and we can recover the result for the amplitude squared given in Ref. [10] taking the ultrarelativistic limit for the electrons/positrons of the plasma. Using the delta function in Eq. (1) we can integrate over $\boldsymbol{p}'$, which yields

$$-\frac{dE}{dx}\bigg|^{\text{hard}} = \frac{8\pi e^4\nu^{6-2d}}{v}\int\frac{d^dk}{(2\pi)^d}n_F(E_k)\int\frac{d^dk'}{(2\pi)^d}[1-n_F(E'_k)]\frac{1}{2E'}\delta(\omega+E_k-E'_k) \\ \times\frac{E}{E_kE'_k}\frac{\omega}{t^2}\left\{2(E_k-\boldsymbol{v}\cdot\boldsymbol{k})(E'_k-\boldsymbol{v}\cdot\boldsymbol{k}') + \frac{d-1}{2}\frac{t^2}{4E^2} + \frac{m^2+M^2}{2E^2}t\right\}. \tag{3}$$

It is convenient to rewrite the remaining delta function of energy conservation in terms of the energy and momentum of the virtual photon

$$\frac{1}{2E'}\delta(\omega+E_k-E'_k) = \frac{1}{2E}\delta(\omega-\boldsymbol{v}\cdot\boldsymbol{q}-t/(2E)). \tag{4}$$

As discussed in Refs. [9,10], in the Pauli-blocking factor $1-n_F(E'_k)$ of Eq. (3), $n_F(E'_k)$ can be dropped if the energy of the plasma constituents is assumed to be of the order of the temperature, i.e., $E'_k \sim T$. Indeed, in this regime $t/(2E) \sim T^2/E$ is suppressed inside the delta function of Eq. (4) and then the corresponding term in the integrand is odd under the interchange of $\boldsymbol{k}$ and $\boldsymbol{k}'$, while the measure is even, hence it integrates to zero. Introducing a mass m for the constituents of the plasma does not change any of these assumptions, as long as we do not allow the mass to be higher than the temperature.

Introducing the following identity

$$1 = \int d^dq\,\delta^d(\boldsymbol{q}+\boldsymbol{k}-\boldsymbol{k}')\int d\omega\,\delta(\omega+E_k-E'_k), \tag{5}$$

in Eq. (3) we can perform the integration over $\boldsymbol{k}'$ using the delta function. The remaining delta function of energy conservation in Eq. (5) can also be written in terms of ω and q using the relation

$$\frac{1}{2E_{k+q}}\delta(\omega+E_k-E_{k+q}) = \delta(t+2\omega E_k-2\boldsymbol{k}\cdot\boldsymbol{q}). \tag{6}$$

Applying all these changes we can cast the hard contribution to the energy loss in terms of the energy and momentum transfer variables

$$-\frac{dE}{dx}\bigg|^{\text{hard}} = \frac{8\pi e^4\nu^{6-2d}}{v}\int\frac{d^dk}{(2\pi)^d}\frac{n_F(E_k)}{E_k}\int\frac{d^dq}{(2\pi)^d}\int d\omega\,\delta(t+2\omega E_k-2\boldsymbol{k}\cdot\boldsymbol{q})\delta(\omega-\boldsymbol{v}\cdot\boldsymbol{q}-t/(2E)) \\ \times\frac{\omega}{t^2}\left\{2(E_k-\boldsymbol{v}\cdot\boldsymbol{k})(E_{k+q}-\boldsymbol{v}\cdot\boldsymbol{k}-\omega) + (E_k-\boldsymbol{v}\cdot\boldsymbol{k})\frac{t}{E} + \frac{d-1}{2}\frac{t^2}{4E^2} + \frac{m^2+M^2}{2E^2}t\right\}. \tag{7}$$

If the plasma is macroscopically isotropic, the energy loss should not depend on the particular direction of the velocity of the heavy fermion. Thus, it is common to average [6] the last expression over the directions of $\boldsymbol{v}$. The required formulas in d spatial dimensions are

$$\frac{1}{S_d}\int d\Omega_d \delta(\tilde{\omega}-\boldsymbol{v}\cdot\boldsymbol{q}) = \frac{1}{L_d}\left(1-\frac{\tilde{\omega}^2}{v^2q^2}\right)^{(d-3)/2}\frac{1}{vq}\Theta(v^2q^2-\tilde{\omega}^2), \tag{8a}$$

$$\frac{1}{S_d}\int d\Omega_d v^i \delta(\tilde{\omega}-\boldsymbol{v}\cdot\boldsymbol{q}) = \frac{1}{L_d}\left(1-\frac{\tilde{\omega}^2}{v^2q^2}\right)^{(d-3)/2}\frac{1}{vq}\Theta(v^2q^2-\tilde{\omega}^2)\frac{\tilde{\omega}}{q}\hat{q}^i, \tag{8b}$$

$$\frac{1}{S_d}\int d\Omega_d v^i v^j \delta(\tilde{\omega}-\boldsymbol{v}\cdot\boldsymbol{q}) = \frac{1}{L_d}\left(1-\frac{\tilde{\omega}^2}{v^2q^2}\right)^{(d-3)/2}\frac{1}{vq}\Theta(v^2q^2-\tilde{\omega}^2)\left(\frac{v^2q^2-\tilde{\omega}^2}{(d-1)q^2}\delta^{ij}+\frac{d\tilde{\omega}^2-v^2q^2}{(d-1)q^2}\hat{q}^i\hat{q}^j\right), \tag{8c}$$

where $\Theta(x)$ is the Heaviside step function, we define $\tilde{\omega}=\omega-t/(2E)$ and use the notation $S_d=\int d\Omega_d = 2\pi^{d/2}/\Gamma(d/2)$ for the surface of a d-sphere and $L_d=\Gamma(\frac{d-1}{2})\sqrt{\pi}/\Gamma(\frac{d}{2})$.

After the average over the directions of $\boldsymbol{v}$, we can further simplify Eq. (7) introducing the explicit form of the measures in d dimensions and using the remaining delta function to perform the integration over the angle $\theta_{\boldsymbol{k},\boldsymbol{q}}\equiv\theta$. The result may be written as

$$\begin{aligned}&\int_{-1}^{1} d(\cos\theta)(\sin\theta)^{d-3}\delta(t+2\omega E_k-2kq\cos\theta)\\&=\frac{1}{2kq}\Theta\left(\sqrt{(q-k)^2+m^2}\le|\omega+E_k|\le\sqrt{(q+k)^2+m^2}\right)\left(1-\left[\frac{t}{2kq}+\frac{\omega E_k}{kq}\right]^2\right)^{(d-3)/2}.\end{aligned} \tag{9}$$

Performing these changes, the hard contribution to the energy loss reads

$$\begin{aligned}-\frac{dE}{dx}\bigg|^{\text{hard}} &= \frac{2e^4\nu^{6-2d}}{v^2}C_d\int_0^\infty dk k^{d-2}\frac{n_F(E_k)}{E_k}\int_0^\infty dq q^{d-5}\\&\times\int d\omega\omega\Theta\left(\sqrt{(q-k)^2+m^2}\le|\omega+E_k|\le\sqrt{(q+k)^2+m^2}\right)\Theta(v^2q^2-\tilde{\omega}^2)\\&\times\frac{q^2}{t^2}\left\{2E_k^2-2\frac{E_k\tilde{\omega}}{q^2}(t+2\omega E_k)+\frac{2}{d-1}\left[\frac{v^2q^2-\tilde{\omega}^2}{q^2}k^2+\frac{d\tilde{\omega}^2-v^2q^2}{4q^4}(t+2\omega E_k)^2\right]\right.\\&\left.+\left(E_k-\tilde{\omega}\frac{t+2\omega E_k}{2q^2}\right)\frac{t}{E}+\frac{d-1}{2}\frac{t^2}{4E^2}+\frac{m^2+M^2}{2E^2}t\right\}\times\mathcal{K}_d(\omega,q,k).\end{aligned} \tag{10}$$

Here we collected the numerical factors and functions arising from the d dimensional integration measures in

$$C_d=\frac{2^{3-d}}{\Gamma\left(\frac{d-1}{2}\right)^2(2\pi)^d}, \tag{11}$$

and

$$\mathcal{K}_d(\omega,q,k)=\left(1-\frac{\tilde{\omega}^2}{v^2q^2}\right)^{\frac{(d-3)}{2}}\times\left(1-\left[\frac{t}{2kq}+\frac{\omega E_k}{kq}\right]^2\right)^{\frac{(d-3)}{2}}, \tag{12}$$

respectively. The theta functions in Eq. (10) affect the integration boundaries of the energy and momentum transfer integrals. Let us discuss how introducing a mass m for the plasma constituents modifies the boundaries given in Ref. [10]. From the theta function $\Theta(v^2q^2-\tilde{\omega}^2)$ we get the boundaries for the energy transfer $\omega_\pm(q)=E-\sqrt{E^2+q^2\mp 2Evq}$, then taking into account $-q\le\omega_-(q)\le\omega_+(q)\le q$ it can be shown that

$$\Theta\left(\sqrt{(q-k)^2+m^2}\le|\omega+E_k|\le\sqrt{(q+k)^2+m^2}\right)\Theta(\omega_-\le\omega\le\omega_+)$$
$$=\Theta(0\le q\le q_{\mathrm{in}})\Theta(\omega_-\le\omega\le\omega_+)+\Theta(q_{\mathrm{in}}\le q\le q_{\mathrm{max}})\Theta(\omega_{\mathrm{min}}\le\omega\le\omega_+). \quad (13)$$

Being $\omega_{\mathrm{min}}(q)=-E_k+\sqrt{(q-k)^2+m^2}$. In addition, the limits of integration for the momentum transfer q_{in} and q_{max} are obtained solving the equations

$$|\omega_-(q_{\mathrm{in}})+E_k|=\sqrt{(q_{\mathrm{in}}-k)^2+m^2}\quad\text{and}\quad|\omega_+(q_{\mathrm{max}})+E_k|=\sqrt{(q_{\mathrm{max}}-k)^2+m^2}, \quad (14)$$

which gives

$$q_{\mathrm{in}}=\frac{2E^2(k-vE_k)+2EE_k(k-vE_k)}{E^2(1-v^2)+2E(E_k-vk)+m^2}\quad\text{and}\quad q_{\mathrm{max}}=\frac{2E^2(k+vE_k)-2EE_k(k-vE_k)}{E^2(1-v^2)+2E(E_k+vk)+m^2}, \quad (15)$$

respectively. Thus, according to Eq. (13), the integration over energy and momentum transfer is separated into two regions

$$\int_0^\infty dq\int_{\omega_-(q)}^{\omega_+(q)}d\omega\Theta\left(\sqrt{(q-k)^2+m^2}\le|\omega+E_k|\le\sqrt{(q+k)^2+m^2}\right)$$
$$\to\int_0^{q_{\mathrm{in}}}dq\int_{\omega_-(q)}^{\omega_+(q)}d\omega+\int_{q_{\mathrm{in}}}^{q_{\mathrm{max}}}dq\int_{\omega_{\mathrm{min}}(q)}^{\omega_+(q)}d\omega. \quad (16)$$

Now we re-express $\tilde{\omega}=\omega-t/(2E)$ in Eq. (10) and organize all terms in inverse powers of E. Then the hard contribution to the energy loss may be written as

$$-\frac{dE}{dx}\bigg|^{\mathrm{hard}}=\frac{2e^4\nu^{6-2d}}{v^2}C_d\int_0^\infty dkk^{d-2}\frac{n_F(E_k)}{E_k}\left\{\int_0^{q_{\mathrm{in}}}dqq^{d-5}\int_{\omega_-(q)}^{\omega_+(q)}d\omega\omega+\int_{q_{\mathrm{in}}}^{q_{\mathrm{max}}}dqq^{d-5}\int_{\omega_{\mathrm{min}}(q)}^{\omega_+(q)}d\omega\omega\right\}$$
$$\times\left\{\frac{3\omega^2-v^2q^2}{4q^2}+\frac{3E_k(E_k+\omega)}{q^2}+\left[\frac{m^2q^2}{t^2}+\frac{E_k(E_k+\omega)}{t}+\frac{q^2}{2t}\right](1-v^2)+\frac{m^2}{t}\right.$$
$$-\frac{\omega[12E_k(E_k+\omega)+3\omega^2-q^2]}{4q^2E}-\frac{\omega m^2}{tE}+\frac{4E_k(E_k+\omega)(3\omega^2-q^2)+3(\omega^4+q^4)-2\omega^2q^2}{16q^2E^2}+\frac{m^2}{4}\frac{\omega^2+q^2}{tE^2}$$
$$\left.-\frac{d-3}{2}\left[\frac{1}{4}+\frac{m^2q^2}{t^2}+\frac{E_k(E_k+\omega)}{t}\right]\left(\frac{\omega^2-v^2q^2}{q^2}+\frac{t^2}{4q^2E^2}-\frac{\omega t}{q^2E}\right)+\frac{d-3}{2}\frac{q^2}{4E^2}\right\}\times\mathcal{K}_d(\omega,q,k). \quad (17)$$

We expanded the terms inside the curly brackets of Eq. (10) for $d\to3$, keeping only pieces proportional to $d-3$, as they are needed for the computation of the finite pieces of the energy loss. Let us recall which assumptions are necessary to extract the leading order pieces to the energy loss, which are of order $\sim e^4T^2$, for a detailed discussion see Ref. [10]. In thermal equilibrium, the energy of most plasma constituents is of the order of temperature, i.e., $E_k\sim T$. In addition, we assume that the energy of the incoming heavy fermion is much larger than the temperature. This gives the hierarchy $E_k\sim T\ll E$. Furthermore, the integration boundaries for the momentum transfer can be simplified in the limit $E\ll M^2/T$ as

$$q_{\mathrm{in}}\approx2\frac{k-vE_k}{1-v^2},\quad\text{and}\quad q_{\mathrm{max}}\approx2\frac{k+vE_k}{1-v^2}. \quad (18)$$

Consequently, the momentum transfer is much smaller than the energy of the heavy fermion $q\sim E^2/(M^2/T)\ll E$, so we can assume that it is of the order of the temperature $q\sim T\ll E$. In addition, in the region $0\le q\le q_{\mathrm{in}}$ the integration boundaries for the energy transfer can be approximated as $\omega_\pm(q)\approx\pm vq$, so we conclude that the energy transfer is also of the order of the temperature $\omega\sim T$. Now it can be easily seen that the terms which are not suppressed by powers of E in Eq. (17) are of order e^4T^2 while all other terms are of order e^4T^3/E and e^4T^4/E^2 so they can be ignored in the regime $T \ll E$. Taking this into account and moving to the dimensionless variable $x = \omega/q$, we reach to

$$-\frac{dE}{dx}\bigg|^{\mathrm{hard}} = \frac{2e^4\nu^{6-2d}}{v^2} C_d \int_0^\infty dk k^{d-2} \frac{n_F(E_k)}{E_k} \left\{ \int_0^{2\frac{k-vE_k}{1-v^2}} dq q^{d-5} \int_{-v}^{v} dx x + \int_{2\frac{k-vE_k}{1-v^2}}^{q_{\max}} dq q^{d-5} \int_{x_{\min}(q)}^{x_+(q)} dx x \right\}$$
$$\times \left\{ (E_k^2 + qxE_k)\left(3 + \frac{1-v^2}{x^2-1}\right) + m^2 \frac{x^2-v^2}{(x^2-1)^2} + q^2\left(\frac{3x^2-v^2}{4} + \frac{1-v^2}{2(x^2-1)}\right) \right.$$
$$\left. - \frac{d-3}{2}\left[(E_k^2 + qxE_k)\frac{x^2-v^2}{x^2-1} + m^2\frac{x^2-v^2}{(x^2-1)^2} + \frac{q^2}{4}(x^2-v^2) \right] \right\} \times \mathcal{K}_d(x,q,k). \tag{19}$$

The momentum transfer integrals in the integration region $0 \le q \le q_{\mathrm{in}}$ contain an IR divergence, while in the region $q_{\mathrm{in}} \le q \le q_{\max}$ the momentum transfer integrals are finite. We focus now on the dominant IR divergent region, and use DR to regularize possible divergences. The terms $\sim q^{d-4}$ in the integrand of Eq. (19) yield the relevant IR divergent integral in momentum transfer, which we evaluate (see Appendix A)

$$\nu^{3-d} \int_0^{2\frac{k-vE_k}{1-v^2}} dq q^{d-4} \left(1 - \left[\frac{q(x^2-1)}{2k} + \frac{xE_k}{k}\right]^2\right)^{\frac{(d-3)}{2}} = \frac{1}{d-3}\left(2\frac{k-vE_k}{(1-v^2)\nu}\right)^{d-3}\left(1 - \frac{x^2E_k^2}{k^2}\right)^{\frac{(d-3)}{2}} + \mathcal{O}(d-3). \tag{20}$$

The momentum transfer integral for the terms $\sim q^{d-5}$ in Eq. (19) is free of divergences, but is necessary to reproduce the finite pieces of Ref. [6] as well as the mass corrections to the pole computed in this manuscript. The required momentum transfer integral is

$$\nu^{3-d} \int_0^{2\frac{k-vE_k}{1-v^2}} dq q^{d-5} \left(1 - \left[\frac{q(x^2-1)}{2k} + \frac{xE_k}{k}\right]^2\right)^{\frac{(d-3)}{2}}$$
$$= \left(1 - \frac{x^2E_k^2}{k^2}\right)^{\frac{(d-3)}{2}} \left(2\frac{k-vE_k}{(1-v^2)\nu}\right)^{d-3} \left\{ \frac{1}{d-4}\left(2\frac{k-vE_k}{1-v^2}\right) + x\frac{E_k}{2k^2}\frac{1-x^2}{1-x^2E_k^2/k^2} + \mathcal{O}(d-3) \right\}. \tag{21}$$

Then, the first term inside the curly brackets above does not contribute to the pole, as it would vanish due to antisymmetry in x, while the second term does not and thus must be taken into account.[1] The remaining terms, those $\sim q^{d-3}$ of Eq. (19) are not necessary for the evaluation of the hard contribution in the region $0 < q < q_{\mathrm{in}}$. We give more details on this last statement and the computation of the momentum transfer integrals in Appendix A. Using Eqs. (20) and (21) we may write the hard contribution to the energy loss as

$$-\frac{dE}{dx}\bigg|^{\mathrm{hard}} \approx \frac{2e^4\nu^{3-d}}{v^2} C_d \int_0^\infty dk k^{d-2} n_F(E_k) \int_{-v}^{v} dx (1 - x^2/v^2)^{(d-3)/2}(1 - x^2E_k^2/k^2)^{(d-3)/2}$$
$$\times \frac{1}{d-3}\left(2\frac{k-vE_k}{(1-v^2)\nu}\right)^{d-3} \left\{ 3x^2 + \frac{x^2(1-v^2)}{x^2-1} + \frac{d-3}{2}\left[\frac{E_k^2}{k^2}\frac{1-x^2}{1-x^2E_k^2/k^2}\left(3x^2 + \frac{x^2(1-v^2)}{x^2-1}\right)\right.\right.$$
$$\left.\left. + \frac{m^2}{k^2}\frac{1-x^2}{1-x^2E_k^2/k^2}\frac{x^2(x^2-v^2)}{(x^2-1)^2} - \frac{x^2(x^2-v^2)}{x^2-1}\right] + \mathcal{O}[(d-3)^2] \right\}. \tag{22}$$

Let us recall that we have not yet made any assumption for the mass m of the constituents of the plasma. Hence, the above expression may be valid for arbitrary mass m as long as it does not surpass the plasma temperature. Though, in this work we assume that the mass of the plasma constituents is smaller than the temperature of the thermal bath $m \ll T$, which allows us to expand Eq. (22) for small m. Performing such expansion produces new pieces, some of them potentially divergent for $k \to 0$. This is the reason why we kept explicit $\mathcal{O}(d-3)$ pieces in the integrand of Eq. (22), since those pieces, after expanding for small mass m produce IR divergent terms, i.e., $\sim 1/(d-3)$, thus giving a contribution to the pole. Note however, that if we computed the k integrals in Eq. (22) for a generic mass m, all $\mathcal{O}(d-3)$ pieces would yield only finite contributions, because in this scenario the k integrals are free of divergences (the mass m acts as a lower cut-off). That

[1]Notice that as $d \to 3$ the measure of (19) is symmetric in x in the region $0 < q < q_{\mathrm{in}}$.

generic case could be considered if the Braaten-Pisarski resummation program is generalized for generic values of the fermion mass. We comment on how this should be done in the remaining part of the paper.

Setting $m = 0$ in Eq. (22) gives the leading order pieces of the hard contribution to the energy loss

$$-\frac{dE}{dx}\bigg|_{m=0}^{\mathrm{hard}} \approx \frac{2e^4\nu^{3-d}}{v^2} C_d \int_0^\infty dk k^{d-2} n_F(k) \int_{-v}^{v} dx (1-x^2/v^2)^{(d-3)/2} (1-x^2)^{(d-3)/2} \times \frac{1}{d-3}\left(\frac{2k}{(1+v)\nu}\right)^{d-3} \left\{3x^2 + \frac{x^2(1-v^2)}{x^2-1} + (d-3)x^2\right\}. \tag{23}$$

All remaining integrals are finite and can be computed analytically, they are given in Appendix A. Using the expressions derived there we find

$$-\frac{dE}{dx}\bigg|_{m=0}^{\mathrm{hard}} \approx \frac{e^2 m_{D,3+2\epsilon}^2}{16\pi}\left\{\left(\frac{1}{\epsilon} + \ln\frac{4T^2}{(1+v)^2\bar{\nu}^2}\right)\left(\frac{1}{v} - \frac{1-v^2}{2v^2}\ln\frac{1+v}{1-v}\right) + \frac{2v}{3} + \frac{P(v)}{v^2}\right\} + \frac{e^2 m_{D,3+2\epsilon}^2}{8\pi}\left(\frac{1}{v} - \frac{1-v^2}{2v^2}\ln\frac{1+v}{1-v}\right)\left\{1 - \gamma_E + \frac{\zeta'(2)}{\zeta(2)} + \ln 2\right\}, \tag{24}$$

where we defined the Debye mass in d dimensions

$$m_{D,d}^2 \equiv 16 e^2 \nu^{3-d} F_d \int_0^\infty dk\, k^{d-2} n_F(k), \tag{25}$$

also $\bar{\nu}^2 = 4\pi e^{-\gamma_E}\nu^2$, being γ_E the Euler-Mascheroni constant and $\zeta(x)$ is the Riemann zeta function. Furthermore, we conveniently defined the quantity

$$P(v) = \int_{-v}^{v} dx\, x^2 \left(1 + \frac{1}{2}\frac{x^2 - v^2}{x^2 - 1}\right) \ln[(1-x^2)(1-x^2/v^2)]. \tag{26}$$

Remarkably, regularizing the momentum transfer integrals with DR instead of a cutoff, as was done in Refs. [6,10], produces the same logarithmic dependence in $\bar{\nu}$ that the one found out with a cutoff q^*, but it generates extra finite pieces that we have partially absorbed in our definition of $m_{D,3+2\epsilon}^2$, the function $P(v)$ and the term $2v/3$. However, the very same extra pieces with opposite sign are generated in the soft contribution to the energy loss, and ultimately they cancel when both contributions are added.

For completeness, we should also include in Eq. (24) the finite pieces generated in the momentum transfer region $q_{\mathrm{in}} < q < q_{\mathrm{max}}$. Since the q integrals are finite in that region, there is no need of regularization and we can compute them in $d = 3$, reaching the same result of Ref. [6].

We turn now our attention in computing small mass, i.e., $m \ll T$ corrections to Eq. (24). The scale of the IR divergence in momentum transfer of Eq. (22) should be approximated as

$$\left(2\frac{k - vE_k}{(1-v^2)\nu}\right)^{d-3} \approx \left(\frac{2k}{(1+v)\nu}\right)^{d-3}, \tag{27}$$

as we concentrate in the IR divergent term in momentum transfer. Using the following small m expansions

$$n_F(E_k) = n_F(k) + \frac{m^2}{2k}\frac{dn_F}{dk} + \mathcal{O}(m^4), \tag{28a}$$

$$\frac{E_k^2}{k^2}\frac{1-x^2}{1-x^2E_k^2/k^2} = 1 + \frac{m^2}{k^2}\frac{1}{1-x^2} + \mathcal{O}(m^4), \tag{28b}$$

$$(1 - x^2E_k^2/k^2)^{(d-3)/2} = (1-x^2)^{(d-3)/2}\left(1 - \frac{d-3}{2}\frac{m^2}{k^2}\frac{x^2}{1-x^2}\right) + \mathcal{O}(m^4), \tag{28c}$$

and keeping only terms up to $\mathcal{O}(m^2)$ in Eq. (22) we find

$$-\frac{dE}{dx}\bigg|_{m^2}^{\mathrm{hard}} \approx \frac{2e^4 m^2 \nu^{3-d}}{v^2} C_d \int_0^\infty dk k^{d-3} \int_{-v}^{v} dx (1-x^2/v^2)^{(d-3)/2}(1-x^2)^{(d-3)/2} \frac{1}{d-3}\left(\frac{2k}{(1+v)\nu}\right)^{d-3} \times\left\{\frac{1}{2}\frac{dn_F}{dk}\left(3x^2 + \frac{x^2(1-v^2)}{x^2-1}\right) + \frac{d-3}{2}\frac{n_F(k)}{k}\left(3x^2 + \frac{x^2(1-v^2)}{x^2-1} + \frac{x^2(x^2-v^2)}{(x^2-1)^2}\right) + \mathcal{O}[(d-3)^2]\right\}. \tag{29}$$

The momentum integral $\sim n_F(k)/k$ of the above expression contains an extra IR divergence for low k, which appears because of the small m expansion. These are the same sort of IR divergences that appear in the computation of the small m corrections to the HTL, which however cancel after performing the angular integrals, see Ref. [19]. A similar situation happens now here. After the complete computation, only the IR divergence associated to the low momentum transfer integral survives. We discuss this issue in detail in Appendix A, where we derive the relevant IR energy integral

$$e^4 m^2 \nu^{3-d} C_d \int_0^\infty dk\, k^{d-4} \left(\frac{2k}{(1+v)\nu}\right)^{d-3} n_F(k) = \frac{e^2}{16\pi}\frac{e^2 m^2}{2\pi^2}\left\{\frac{1}{\epsilon} + \left(-2\gamma_E + 2\ln\pi + \ln\frac{T^2}{\bar{\nu}^2} + \ln\frac{4T^2}{(1+v)^2\bar{\nu}^2}\right) + \mathcal{O}(\epsilon)\right\}. \quad (30)$$

The logarithm $\ln(T^2/\bar{\nu}^2)$ above is canceled when the soft contribution is added (see Sec. IV). Also, we can ignore the finite pieces inside the parenthesis of the second line, since we are just interested in extracting the leading logarithmic behavior. Then, plugging the results Eqs. (A8) and (30) into Eq. (29), we note that the pole of the k-integral in Eq. (30) vanishes. In addition, we see that the remaining necessary integral in energy transfer is

$$\int_{-v}^{v} dx(1-x^2/v^2)^{(d-3)/2}(1-x^2)^{(d-3)/2}\frac{x^2(x^2-v^2)}{(x^2-1)^2} = v^2\left\{\left(\frac{3}{v} - \frac{v^2-3}{2v^2}\ln\frac{1+v}{1-v}\right) + \mathcal{O}(\epsilon)\right\}. \quad (31)$$

Collecting these results we can write down the leading mass correction to the hard contribution

$$-\frac{dE}{dx}\bigg|_{m^2}^{\mathrm{hard}} \approx \frac{e^2}{16\pi}\frac{e^2 m^2}{2\pi^2}\left(\frac{1}{\epsilon} + \ln\frac{4T^2}{(1+v)^2\bar{\nu}^2}\right)\left(\frac{3}{v} - \frac{v^2-3}{2v^2}\ln\frac{1+v}{1-v}\right). \quad (32)$$

We recall here that in this manuscript we computed leading order mass corrections to the energy loss at logarithmic accuracy, and we have not included the computation of all finite pieces, which would require a more involved analysis. For instance, we would need to consider the explicit $\mathcal{O}[(d-3)^2]$ pieces that we have ignored in Eq. (29) together with the finite pieces generated in the region $q_{\mathrm{in}} \le q \le q_{\mathrm{max}}$.

III. SOFT CONTRIBUTION TO THE COLLISIONAL ENERGY LOSS

In this section we will compute the soft contribution to the energy loss. We will derive the soft contribution trough the computation of the damping rate of the heavy fermion traversing the QED plasma. This requires to compute the imaginary part of the heavy fermion self-energy, see Fig. 2 and relate the collisional energy-loss to this damping rate, see for example Ref. [6]. Generalizations in d dimensions of the energy loss formula for the soft contribution can be found in Ref. [20]. The final formula appears in terms of the resummed photon propagators. The mass corrections we are aiming to compute only enter in the resummed photon propagators. Our starting expression is in Coulomb gauge (see Appendix A of Ref. [20])

$$\begin{aligned}-\frac{dE}{dx}\bigg|^{\mathrm{soft}} &= \frac{e^2\nu^{3-d}}{v^2}F_d\int_0^\infty dq q^{d-1} \\ &\times \int_{-v}^{v} dx(1-x^2/v^2)^{(d-3)/2}[1+n_B(qx)] \\ &\times (qx)(\rho_L^d(qx,q) + (v^2-x^2)\rho_T^d(qx,q)). \quad (33)\end{aligned}$$

Here $\rho^d_{L/T}(qx,q)$ stand for the longitudinal/transverse HTL photon spectral functions in d dimensions, respectively, $F_d = 2^{1-d}\pi^{-(d+1)/2}/\Gamma(\frac{d-1}{2})$ is the constant that arises from the momentum transfer measure in d dimensions and we used the dimensionless variable $x = q_0/q$. The longitudinal and transverse spectral functions can be obtained using their relation with the imaginary part of the (resummed) longitudinal and transverse retarded propagators, i.e. $\rho^d_{L/T}(q_0,q) = 2\mathrm{Im}\Delta^d_{L/T}(q_0+i0^+,q)$ [21]. Note that this definition of the spectral function differs by a factor (-2π) to the one used in Ref. [6]. In terms of the longitudinal/transverse retarded polarization tensors $\Pi_d^{L/R}$ in d dimensions one can write

$$\rho_d^L(q_0,q) = -\frac{2\mathrm{Im}\Pi_d^L(q_0,q)}{[q^2-\mathrm{Re}\Pi_d^L(q_0,q)]^2 + [\mathrm{Im}\Pi_d^L(q_0,q)]^2}, \quad (34a)$$

$$\rho_d^T(q_0,q) = -\frac{2\mathrm{Im}\Pi_d^T(q_0,q)}{[q_0^2-q^2-\mathrm{Re}\Pi_d^T(q_0,q)]^2+[\mathrm{Im}\Pi_d^T(q_0,q)]^2}. \tag{34b}$$

To be able to compute mass corrections to the soft contribution of the energy loss, we will need the mass corrections to the HTL polarization tensor, which were computed in Ref. [19]. In the presence of a small mass $m \ll T$, the longitudinal and transverse components of the retarded polarization read

$$\Pi^L_{3+2\epsilon}(q_0,q) = -m^2_{D,3+2\epsilon}\left(1-\frac{x}{2}\ln\frac{x+1}{x-1}\right) - \frac{m^2e^2}{2\pi^2}\frac{1}{x^2-1} + \mathcal{O}(\epsilon), \tag{35a}$$

$$\Pi^T_{3+2\epsilon}(q_0,q) = m^2_{D,3+2\epsilon}\frac{x^2}{2}\left(1-\left(1-\frac{1}{x^2}\right)\frac{x}{2}\ln\frac{x+1}{x-1}\right) - \frac{m^2e^2}{2\pi^2}\frac{x}{2}\ln\frac{x+1}{x-1} + \mathcal{O}(\epsilon), \tag{35b}$$

where $x = (q_0 + i0^+)/q$, and $m^2_{D,3+2\epsilon}$ is the Debye mass in $d = 3+2\epsilon$ dimensions defined in Eq. (25). As discussed in Ref. [19], when the mass of the fermionic particles obeys $eT \ll m \ll T$ the mass corrections are dominant in comparison to the perturbative corrections. Then, the longitudinal and transverse spectral function including mass corrections read

$$\rho^L_{3+2\epsilon}(qx,q) = 2\pi\frac{(1+\epsilon)m^2_{D,3+2\epsilon}x\,\Theta(1-x^2)(1-x^2)^\epsilon}{2\left(q^2+m_D^2Q_1(x)-\frac{m^2e^2}{2\pi^2}\frac{1}{1-x^2}\right)^2+\frac{\pi^2x^2}{2}m_D^4} + \mathcal{O}(\epsilon), \tag{36}$$

and

$$\rho^T_{3+2\epsilon}(qx,q) = \frac{2\pi}{1-x^2}\frac{\left(m^2_{D,3+2\epsilon}-\frac{m^2e^2}{\pi^2}\frac{1}{1-x^2}\right)x\,\Theta(1-x^2)(1-x^2)^\epsilon}{\left(2q^2+m_D^2Q_2(x)-\frac{m^2e^2}{2\pi^2}Q_3(x)\right)^2+\frac{\pi^2x^2}{4}\left(m_D^2-\frac{m^2e^2}{\pi^2}\frac{1}{1-x^2}\right)^2} + \mathcal{O}(\epsilon). \tag{37}$$

respectively. We kept the Debye mass in $d = 3+2\epsilon$ dimensions of the numerators unexpanded for small ϵ in the spectral functions for convenience. Furthermore, we did not include $\mathcal{O}(\epsilon)$ pieces arising from the denominator, since those pieces do not generate UV divergences when expanded for small ϵ, and thus vanish in the limit $\epsilon \to 0$. Lastly, we also did not include $\mathcal{O}(\epsilon)$ pieces coming from the mass corrections to the HTL, although they would be needed in order to determine the mass correction to the soft contribution of the energy loss beyond logarithmic accuracy. We also introduced, to shorten the notation, the functions

$$Q_1(x) = 1-\frac{x}{2}\ln\left|\frac{x+1}{x-1}\right|, \qquad Q_2(x) = \frac{1}{1-x^2} - Q_1(x), \qquad Q_3(x) = \frac{x}{x^2-1}\ln\left|\frac{x+1}{x-1}\right|. \tag{38}$$

Due to the symmetries of the integrand, we can replace $1+n_B(qx)$ in Eq. (33) by its even part, which is just $1/2$. The spectral functions should also be expanded for small mass m, however, the pieces generated are subleading corrections, so we can ignore them. Taking these remarks into account, we plug the spectral functions of Eqs. (36) and (37) in Eq. (33) reaching to

$$\begin{aligned}-\frac{dE}{dx}\bigg|^{\mathrm{soft}} &= \frac{\pi e^2\nu^{-2\epsilon}}{v^2}F_{3+2\epsilon}\int_0^\infty dq\,q^{3+2\epsilon}\int_{-v}^{v}dx\,x^2(1-x^2/v^2)^\epsilon(1-x^2)^\epsilon \\ &\quad\times\left\{\frac{(1+\epsilon)m^2_{D,3+2\epsilon}}{2(q^2+m_D^2Q_1(x))^2+\pi^2x^2m_D^4/2} + \frac{v^2-x^2}{1-x^2}\frac{(m^2_{D,3+2\epsilon}-(e^2m^2/\pi^2)/(1-x^2))}{(2q^2+m_D^2Q_2(x))^2+\pi^2x^2m_D^4/4} + \mathcal{O}(\epsilon)\right\}.\end{aligned} \tag{39}$$

The theta function $\Theta(1-x^2)$ in the spectral functions does not affect the limits of integration for the energy transfer, since $v < 1$. Furthermore, the momentum transfer integral contains an UV divergence for $q \gg eT$, which we regularize using DR. All remaining integrals are finite and can be computed analytically, they are given in Appendix B. Hence, the leading order term of the soft contribution is

$$-\frac{dE}{dx}\bigg|_{m=0}^{\mathrm{soft}} = \frac{e^2 m_{D,3+2\epsilon}^2}{16\pi}\left\{\left(-\frac{1}{\epsilon}+\ln\frac{\bar{\nu}^2}{m_D^2}\right)\left(\frac{1}{v}-\frac{1-v^2}{2v^2}\ln\frac{1+v}{1-v}\right)-\frac{2v}{3}-\frac{1}{v^2}(P(v)+A_{\mathrm{soft}}(v))\right\}. \tag{40}$$

The extra finite pieces coming from the Debye mass in $d=3+2\epsilon$ dimensions, the function $P(v)$ given in Eq. (26) and the term $-2v/3$ cancel exactly with those computed in the hard contribution. The function $A_{\mathrm{soft}}(v)$ reads

$$A_{\mathrm{soft}}(v) = \int_{-v}^{v} dx\, x^2 \left\{\frac{1}{2}\ln\left(Q_1(x)^2+\frac{\pi^2 x^2}{4}\right)+\frac{1}{4}\frac{v^2-x^2}{1-x^2}\ln\left(\frac{Q_2(x)^2}{4}+\frac{\pi^2x^2}{16}\right)\right.$$
$$\left. +\frac{2Q_1(x)}{\pi x}\arccos\left(\frac{Q_1(x)}{\sqrt{Q_1(x)^2+\pi^2x^2/4}}\right)+\frac{v^2-x^2}{1-x^2}\frac{Q_2(x)}{\pi x}\arccos\left(\frac{Q_2(x)}{\sqrt{Q_2(x)^2+\pi^2x^2/4}}\right)\right\}. \tag{41}$$

Focusing now on the mass dependent part of Eq. (39) and computing the relevant integral in energy transfer [see Eq. (31)] we arrive to the final result for the mass correction to the soft contribution of the energy loss

$$-\frac{dE}{dx}\bigg|_{m^2}^{\mathrm{soft}} \approx \frac{e^2}{16\pi}\frac{e^2m^2}{2\pi^2}\left(-\frac{1}{\epsilon}+\ln\frac{\bar{\nu}^2}{m_D^2}\right)\left(\frac{3}{v}-\frac{v^2-3}{2v^2}\ln\frac{1+v}{1-v}\right). \tag{42}$$

IV. ALTERNATIVE COMPUTATION OF THE SOFT CONTRIBUTION

In this section we will provide an alternative way of computing the soft contribution to the energy loss. We will perform the computation starting from the general expression of the energy loss, given in Eq. (1), but using the amplitude of diagram Fig. 1(b). The amplitude can be constructed following QED Feynman rules but replacing bare propagators by HTL resummed propagators in Coulomb gauge. Then, squaring the amplitude and performing the sum over spins of the involved particles in the process we find

$$\frac{1}{2}\sum_{\mathrm{spins}}|\mathcal{M}|^2 = 8e^4\nu^{6-2d}E^2\Big\{|\Delta_L^d(Q)|^2(E'/E+\boldsymbol{v}'\cdot\boldsymbol{v}+M^2/E^2)(E'_kE_k+\boldsymbol{k}'\cdot\boldsymbol{k}+m^2)$$
$$+2\mathrm{Re}[\Delta_L^d(Q)\Delta_T^d(Q)^*][(\boldsymbol{v}'\cdot\boldsymbol{k}'_{\perp,\hat{q}})E_k+(\boldsymbol{v}'\cdot\boldsymbol{k}_{\perp,\hat{q}})E'_k+(\boldsymbol{v}\cdot\boldsymbol{k}'_{\perp,\hat{q}})E_k+(\boldsymbol{v}\cdot\boldsymbol{k}_{\perp,\hat{q}})E'_k]$$
$$+2|\Delta_T^d(Q)|^2\Big[(\boldsymbol{v}'\cdot\boldsymbol{k}'_{\perp,\hat{q}})(\boldsymbol{v}\cdot\boldsymbol{k}_{\perp,\hat{q}})+(\boldsymbol{v}'\cdot\boldsymbol{k}_{\perp,\hat{q}})(\boldsymbol{v}\cdot\boldsymbol{k}'_{\perp,\hat{q}})+(\boldsymbol{v}'_{\perp,\hat{q}}\cdot\boldsymbol{v}_{\perp,\hat{q}})(E'_kE_k-\boldsymbol{k}'\cdot\boldsymbol{k}-m^2)$$
$$-\frac{d-1}{2}(E'/E-\boldsymbol{v}'\cdot\boldsymbol{v}-M^2/E^2)(E'_kE_k-\boldsymbol{k}'\cdot\boldsymbol{k}-m^2)+(\boldsymbol{k}'_{\perp,\hat{q}}\cdot\boldsymbol{k}_{\perp,\hat{q}})(E'/E-\boldsymbol{v}'\cdot\boldsymbol{v}-M^2/E^2)\Big]\Big\}, \tag{43}$$

where $\boldsymbol{v}=\boldsymbol{p}/E$ is the velocity of the heavy fermion and we also defined $\boldsymbol{k}_{\perp,\hat{q}}=-P^{ij}_{\perp,\hat{q}}k^i$ and $\boldsymbol{v}_{\perp,\hat{q}}=-P^{ij}_{\perp,\hat{q}}v^i$, being $P^{ij}_{\perp,\hat{q}}=-(\delta^{ij}-\hat{q}^i\hat{q}^j)$ minus the transverse projector to $\hat{\boldsymbol{q}}=\boldsymbol{q}/q$. We used primed variables for the outgoing particles. In the above expression, $\Delta^d_{L/T}(Q)$ denote the longitudinal and transverse components of HTL resumed propagators in d dimensions respectively, assuming that the fermions in the plasma have mass m. In order to simplify the expression for the amplitude we make use of the exact kinematic relation

$$\frac{M^2}{E^2}=\frac{E'}{E}-\boldsymbol{v}'\cdot\boldsymbol{v}+\frac{m^2}{E^2}-\frac{E'_kE_k-\boldsymbol{k}'\cdot\boldsymbol{k}}{E^2}. \tag{44}$$

Since the amplitude squared in Eq. (43) is invariant under the interchange of $\boldsymbol{k}\leftrightarrow\boldsymbol{k}'$, we can antisymmetrize the thermal distribution functions [9], i.e., replacing $n_F(E_k)[1-n_F(E'_k)]$ by $[n_F(E_k)-n_F(E'_k)]/2$. Then we move to the transfer momentum variables, as we did in Sec. II for the hard contribution. Eventually, we reach the following expression for the soft contribution to the energy loss

$$-\frac{dE}{dx}\bigg|^{\text{soft}} = \frac{4\pi e^4 \nu^{6-2d}}{v}\int\frac{d^dk}{(2\pi)^d}\int\frac{d^dq}{(2\pi)^d}\int d\omega\omega\frac{n_F(E_k)-n_F(E_k+\omega)}{E_k}\delta(t+2\omega E_k-2\boldsymbol{k}\cdot\boldsymbol{q})\delta(\omega-\boldsymbol{v}\cdot\boldsymbol{q}-t/(2E))$$
$$\times\left\{|\Delta_L^d(Q)|^2\left(1-\frac{\omega}{E}-\frac{\omega E_k-\boldsymbol{k}\cdot\boldsymbol{q}}{2E^2}\right)(2E_k^2+\omega E_k+\boldsymbol{k}\cdot\boldsymbol{q})+2\mathrm{Re}[\Delta_L^d(Q)\Delta_T^d(Q)^*](\boldsymbol{v}\cdot\boldsymbol{k}_{\perp,\hat{q}})(2E_k+\omega)\right.$$
$$\left.+|\Delta_T^d(Q)|^2\left[2(\boldsymbol{v}\cdot\boldsymbol{k}_{\perp,\hat{q}})^2+\boldsymbol{v}_{\perp,\hat{q}}^2(\omega E_k-\boldsymbol{k}\cdot\boldsymbol{q})+\left(\frac{\omega E_k-\boldsymbol{k}\cdot\boldsymbol{q}}{E^2}\right)\left(\boldsymbol{k}_{\perp,\hat{q}}^2-\frac{d-1}{2}(\omega E_k-\boldsymbol{k}\cdot\boldsymbol{q})\right)\right]\right\}. \tag{45}$$

Now we introduce the average over velocities $\boldsymbol{v}$ in d dimensions using Eqs. (8a)–(8c). We note that the piece that mixes the longitudinal and transverse component of the propagator vanishes in this process because it is transverse to $\boldsymbol{q}$. In addition, we eliminate all suppressed pieces in E since we will work in the regime $T \ll E$. The integral over the angle $\theta \equiv \theta_{\boldsymbol{k},\boldsymbol{q}}$ is the same as that of the hard contribution, given in Eq. (9). Then, moving to the dimensionless variable $x = \omega/q$ we can cast the soft contribution as

$$-\frac{dE}{dx}\bigg|^{\text{soft}} = \frac{2e^4\nu^{6-2d}}{v^2}C_d\int_0^\infty dkk^{d-2}\int_0^\infty dqq^{d-1}\int dxx\frac{n_F(E_k)-n_F(E_k+qx)}{E_k}$$
$$\times\Theta\left(1-\left[\frac{q(x^2-1)}{2k}+\frac{xE_k}{k}\right]^2\right)\Theta(v^2-x^2)\left\{|\Delta_L^d(qx,q)|^2\left(E_k^2+qxE_k+\frac{q^2}{4}(x^2-1)\right)\right.$$
$$\left.+|\Delta_T^d(qx,q)|^2\frac{1}{d-1}(v^2-x^2)\left(k^2-x^2E_k(qx+E_k)+qxE_k+\frac{q^2}{4}(x^2-1)(3-x^2)\right)\right\}\times\mathcal{K}_d(x,q,k). \tag{46}$$

In the above expression, the momentum transfer is soft $q \sim eT$ and the momentum of the plasma constituents is hard $k \sim T$, which allows us to perform several approximations. The thermal distribution function can be expanded for $q \ll E_k$

$$n_F(E_k+qx) = n_F(E_k)+qx\frac{dn_F(E_k)}{dE_k}+\mathcal{O}(q^2). \tag{47}$$

In addition, the theta function in the second line can be simplified

$$\Theta\left(1-\left[\frac{q(x^2-1)}{2k}+\frac{xE_k}{k}\right]^2\right)\approx\Theta\left(1-\frac{x^2E_k^2}{k^2}\right). \tag{48}$$

Moreover, the function $\mathcal{K}_d(x,q,k)$ must be expanded for $q \ll E_k$ in order to be consistent with the HTL approximation

$$\mathcal{K}_d(x,q,k) = (1-x^2/v^2)^{(d-3)/2}(1-x^2E_k^2/k^2)^{(d-3)/2}\left\{1+\frac{d-3}{2}\frac{xE_k}{k^2}\frac{1-x^2}{1-x^2E_k^2/k^2}q+\mathcal{O}(q^2)\right\}. \tag{49}$$

Finally, we note that the terms $\sim q^n|\Delta_{L/T}^d(qx,q)|^2$ for $n > 3$ can be ignored, as they would contribute at higher order in the coupling constant. Thus, the leading order pieces of the soft contribution to the energy loss are

$$-\frac{dE}{dx}\bigg|^{\text{soft}} = \frac{2e^4\nu^{6-2d}}{v^2}C_d\int_0^\infty dkk^{d-2}\left(-\frac{1}{E_k}\frac{dn_F(E_k)}{dE_k}\right)\int_0^\infty dqq^d\int dxx^2(1-x^2/v^2)^{(d-3)/2}(1-x^2E_k^2/k^2)^{(d-3)/2}$$
$$\times\Theta(1-x^2E_k^2/k^2)\Theta(v^2-x^2)\left\{|\Delta_L^d(qx,q)|^2E_k^2+|\Delta_T^d(qx,q)|^2\frac{v^2-x^2}{d-1}(k^2-x^2E_k^2)\right\}. \tag{50}$$

Explicit expressions for $\Delta_{L/T}^d$ are known for $m = 0$. In Appendix C we comment how the polarization tensors needed to build these propagators should be computed for a generic value of the fermion mass. However, for a small fermion mass, and at the order of accuracy we are going to compute, we will only need the resummed propagators at $m = 0$.

Let us remark that the above expression may be valid for a generic mass m, as long as it does not surpass the plasma temperature. From Eq. (50) we can reconstruct exactly Eq. (39) in a very few steps. Setting $m = 0$ and integrating by parts the distribution function, we easily arrive to

$$
-\frac{dE}{dx}\bigg|_{m=0}^{\mathrm{soft}} = \frac{\pi e^2\nu^{3-d}}{v^2} m_{D,d}^2 F_d \int_0^\infty dq q^d \int_{-v}^{v} dx x^2 (1-x^2/v^2)^{(d-3)/2}(1-x^2)^{(d-3)/2} \times \left\{\frac{1}{2}|\Delta_L^d(qx,q)|^2 \frac{d-1}{2} + \frac{1}{4}|\Delta_T^d(qx,q)|^2 (v^2-x^2)(1-x^2)\right\}, \tag{51}
$$

where we used the relation between the numerical constants defined through this manuscript $C_d = 2\pi F_d^2$ and $m_{D,d}^2$ denotes the Debye mass squared in d dimensions defined in Eq. (25). What remains to be done is to insert the definition of the thermal HTL resummed propagators in $d = 3+2\epsilon$ dimensions. They may be written as

$$
|\Delta_L^{3+2\epsilon}(qx,q)|^2 = \frac{1}{(q^2+m_D^2 Q_1(x))^2 + \pi^2 m_D^4 x^2/2} + \mathcal{O}(\epsilon), \tag{52a}
$$

$$
|\Delta_T^{3+2\epsilon}(qx,q)|^2 = \frac{1}{(x^2-1)^2}\frac{1}{(q^2+m_D^2 Q_2(x)/2)^2 + \pi^2 m_D^4 x^2/16} + \mathcal{O}(\epsilon). \tag{52b}
$$

When writing the longitudinal and transverse components of the propagators above, we did not include $\mathcal{O}(\epsilon)$ pieces, since they do not give rise to new UV divergences, and thus vanish in the limit $\epsilon \to 0$. We also did not include small mass corrections to the propagators, for the same reasons that we discarded the mass corrections in the denominators of the spectral functions [Eqs. (36) and (37)]. Setting $d = 3+2\epsilon$ everywhere and inserting the expression for the propagators of Eqs. (52a) and (52b) in Eq. (51) we get exactly Eq. (39) for $m = 0$.

Now we show how to reproduce the remaining $\sim m^2$ term in Eq. (39) from the more general expression Eq. (50). In the regime $m \ll T \ll M$, the energy transferred to the plasma constituents is determined by $\Theta(x^2-v^2)$ rather than $\Theta(1-x^2k^2/E_k^2)$, as in this scenario the velocity of the heavy fermion is always smaller compared to the velocity of the fermionic particles in the plasma. Then, expanding Eq. (50) for small m and keeping only pieces of $\mathcal{O}(m^2)$, we note that many pieces vanish after integrating by parts the thermal distribution functions, and the only nonvanishing piece is

$$
-\frac{dE}{dx}\bigg|_{m^2}^{\mathrm{soft}} = -\frac{4\pi e^4 m^2 \nu^{6-2d}}{v^2} F_d^2 \int_0^\infty dk k^{d-3}\left(-\frac{dn_F}{dk}\right) \times \int_0^\infty dq q^d \int_{-v}^{v} dx x^2 (1-x^2/v^2)^{(d-3)/2}(1-x^2)^{(d-3)/2} \frac{1}{d-1}|\Delta_T^d(x,q)|^2 (v^2-x^2). \tag{53}
$$

Now the k integral can be evaluated, yielding to

$$
16 e^2 m^2 \nu^{3-d} \frac{F_d}{d-1}\int_0^\infty dk k^{d-3}\left(-\frac{dn_F}{dk}\right) = \frac{e^2 m^2}{\pi^2}\left(1 + \left(-1 - 2\gamma_E - 2\ln 2 + 2\ln\pi + \ln\frac{T^2}{\bar{\nu}^2}\right)\epsilon + \mathcal{O}(\epsilon^2)\right) \tag{54}
$$

The finite pieces $\sim\epsilon$ in the second line can be ignored at the order we are working and, as we pointed below Eq. (30), the logarithms $\ln(T^2/\bar{\nu}^2)$ cancel when the hard and soft contribution are added. Thus, we may write Eq. (53) as

$$
-\frac{dE}{dx}\bigg|_{m^2}^{\mathrm{soft}} = \frac{\pi e^2 \nu^{-2\epsilon}}{v^2} F_{3+2\epsilon} \int_0^\infty dq q^{3+2\epsilon} \int_{-v}^{v} dx x^2 (1-x^2/v^2)^{\epsilon}(1-x^2)^{\epsilon}\Theta(1-x^2) \times \frac{1}{4}\frac{v^2-x^2}{(1-x^2)^2}\frac{(-e^2m^2/\pi^2)}{(q^2+m_D^2 Q_2(x)/2)^2 + \pi^2 m_D^4 x^2/16}. \tag{55}
$$

This is the same expression we found for the mass correction of the soft sector in Eq. (39), as expected.

V. RESULTS AND DISCUSSION

The final expression of the collisional energy loss is obtained after adding the hard and soft contributions. Then, the poles $1/\epsilon$ and the dependence on the renormalization scale ν cancel out. For $m = 0$ we reach to the same expression first found by Braaten and Thoma [6] in the regime $E \ll M^2/T$

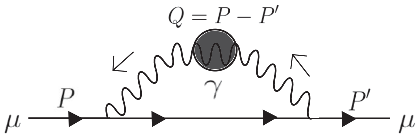

FIG. 2. One loop heavy fermion (μ) self-energy, dominated by an exchange of a virtual (resummed) photon (γ).

$$-\frac{dE}{dx}\bigg|_{\mathrm{BT}} = \frac{e^2 m_D^2}{8\pi}\left(\frac{1}{v} - \frac{1-v^2}{2v^2}\ln\frac{1+v}{1-v}\right) \times \left\{\ln\frac{E}{M} + \ln\frac{1}{e} + A(v)\right\}. \quad (56)$$

The extra finite pieces generated in the computation of the hard and soft contributions using DR also cancel out, so that the function $A(v)$ is the same as that using a cutoff for the computation. Note that Eq. (56) is not valid for neither the $v \to 0$ or $v \to 1$ limits, because of the kinematical constraints used in the evaluation of the momentum integrals. In particular, we assumed that the velocity of the heavy fermion is always smaller than that of the plasma constituents. Taking into account those limits can be done after a proper modification of the kinematical constraints, see Refs. [6,10]. Further, in the case $v \to 1$ Compton scattering also contributes at the same order as the one here computed [22].

The fermion mass correction to the above result is also obtained after adding the corresponding hard and soft contributions we computed. Then, the pole and the dependence on the renormalization scale also cancel out, and to leading logarithmic accuracy we obtain for $m \ll T \ll M$

$$-\frac{dE}{dx}\bigg| = -\frac{dE}{dx}\bigg|_{\mathrm{BT}} + \frac{e^4 m^2}{16\pi^3}\left(\frac{3}{v} - \frac{v^2-3}{2v^2}\ln\frac{1+v}{1-v}\right)\ln\left(\frac{1}{e}\right). \quad (57)$$

We have not computed mass corrections beyond logarithmic accuracy, as most likely the genuine perturbative corrections to the energy loss are more relevant in the regime where our assumptions are valid.

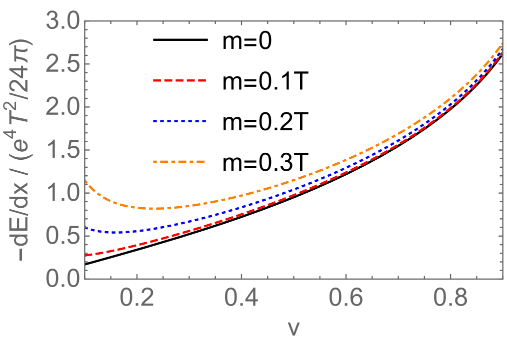

FIG. 3. Values of the collisional energy loss in QED for the different values of the mass of the fermion constituents of the plasma. The black line corresponds to the massless case, the red dashed line for $m = 0.1T$, the blue dashed line for $m = 0.2T$, and the orange dot-dashed line $m = 0.3T$.

We have represented in Fig. 3 the value of the collisional energy loss for different values of the fermion mass, so as to estimate how relevant its effect could be. We note that the effects of a fermion mass seem to be quite relevant already for values of $m = 0.3T$. It might thus seem interesting to evaluate also the energy loss for values of the fermion mass close to T, where our approximations are not valid. Note that the assumption $m \ll T$ allows us to compute the collisional energy loss analytically, which is always a good initial step to assess the effect we are considering. We have provided all the ingredients to carry out the computation for values of m getting close to T, but we defer the careful study of that case for future projects, as it requires a much more detailed analysis. The main difficulty for such a computation is the evaluation of the soft sector, as one should generalize the Braaten-Pisarski resummation program in the presence of massive fermions. The explicit form of the photon polarization tensor needed in that case to construct the resummed propagators is given in Appendix C.

Although our computation was initially performed for a QED plasma, it can be extended to QCD. In fact, retaining mass fermion corrections in QCD can be fully justified, and it was our ultimate motivation. For instance, in the context of heavy ion collisions, it may be reasonable to disregard the masses of up and down quarks, but neglecting the mass of the strange quark may not be such a good approximation. The contribution of the mass effects in QCD can be obtained from the corresponding QED calculation at logarithmic accuracy by simple substitution, while further corrections would be needed beyond this accuracy. Note that the mass corrections to the HTL gluon polarization tensor are the same as those of the photon polarization in QED, only some color and flavor factors have to be taken into account. Similarly, in the evaluation of the scattering matrix element of a heavy quark with a light quark in the t-channel, the one that is IR sensitive, only some color and flavor factors are to be considered. At leading logarithmic accuracy the corrections associated to a massive quark to the QCD collisional energy loss are also given by the QED result, replacing e^2 by g^2, the strong coupling constant, and taking into account the factor $2/3$. More explicitly

$$\frac{g^4 m^2}{24\pi^3}\left(\frac{3}{v} - \frac{v^2-3}{2v^2}\ln\frac{1+v}{1-v}\right)\ln\left(\frac{1}{g}\right). \quad (58)$$

We have evaluated the impact of including the strange quark mass corrections to the collisional energy loss of a charm and bottom quark (see Figs. 2 and 3 of Ref. [7]), when $T = 250$ MeV, and assuming that the strong fine structure constant is $\alpha_s = 0.2$. Taking the strange quark mass as $m = 100$ MeV, so $m = 0.4T$, we note that in this case the mass corrections are in the 1 to 2 percent level. The effect is certainly not as large as in QED because of two reasons. First, the gauge coupling constant is larger in QCD, and second, the contribution of one parton, no matter whether it is massless or massive, can never be too big as compared to the contribution associated to all partons. In any case, the mass effects here discussed are there and we have provided the tools to assess them.

ACKNOWLEDGMENTS

We thank Joan Soto for useful discussions. This work was supported by Ministerio de Ciencia, Investigación y Universidades (Spain) under the Project No. PID2019–110165GB-I00 (MCI/AEI/FEDER, UE), by Generalitat de Catalunya by the Project No. 2021-SGR-171 (Catalonia). This work was also partly supported by the Spanish program Unidad de Excelencia Maria de Maeztu CEX2020-001058-M, financed by No. MCIN/AEI/10.13039/501100011033.

APPENDIX A: INTEGRALS OF THE HARD CONTRIBUTION

When computing the hard contribution to the energy loss, we encounter three types of momentum transfer integrals in the region $0 < q < q_{\mathrm{in}}$, see Eq. (19). When computed in $d = 3 + 2\epsilon$, all of them give rise to Appell F_1 hypergeometric functions, due to the particular dependence on momentum transfer q of the function $\mathcal{K}_d(x, q, k)$ defined in Eq. (12). Explicitly, we compute the general formula

$$\nu^{3-d} \int_0^L dq q^{d-n} \left(1 - \left[\frac{q(x^2-1)}{2k} + \frac{xE_k}{k}\right]^2\right)^{\frac{(d-3)}{2}} = \frac{L^{d-n+1}}{d-n+1} \left(1 - \frac{x^2 E_k^2}{k^2}\right)^{\frac{(d-3)}{2}} \times F_1\left(1 + d - n, -\frac{d-3}{2}, -\frac{d-3}{2}, d - n + 2, \frac{1-x^2}{k + xE_k} L, -\frac{1-x^2}{k - xE_k} L\right), \tag{A1}$$

where $L \equiv 2(k - vE_k)/(1 - v^2)$ and $F_1(a; b_1, b_2; c; z_1, z_2)$ is the so called Appell hypergeometric function of the first kind. For $n = 5$, 4, 3 we obtain the required integrals for the evaluation of the hard contribution. The above results can be simplified expressing F_1 by its infinite series representation

$$F_1(a; b_1, b_2; c; z_1, z_2) = \sum_{m=0}^{\infty} \sum_{n=0}^{\infty} \frac{(a)_{m+n} (b_1)_m (b_2)_n}{m! n! (c)_{m+n}} z_1^m z_2^n, \tag{A2}$$

where $(\alpha)_n = \Gamma(n + \alpha)/\Gamma(\alpha)$ is a Pochhammer symbol, and realizing that in $d = 3 + 2\epsilon$ only the first terms of the series are non-vanishing. Following this procedure, we obtain Eqs. (20) and (21) setting $n = 5$ and $n = 4$ in Eq. (A1) respectively. As stated in Sec. II the last case $n = 3$ is not necessary for the evaluation of the hard contribution. In order to see it, we use Eq. (A2) to write the Appell function as

$$F_1\left(d - 2, -\frac{d-3}{2}, -\frac{d-3}{2}, d - 1, \frac{k - vE_k}{k + xE_k} \frac{1-x^2}{1-v^2}, \frac{k - vE_k}{k - xE_k} \frac{1-x^2}{1-v^2}\right) = 1 + \mathcal{O}(d-3). \tag{A3}$$

Note that Eq. (A1) is finite in three spatial dimensions when $n = 3$. Then, since in $d = 3$ the measure of Eq. (19) is even in x, the corresponding terms vanish due to antisymmetry in x. Let us now write the results needed for the evaluation of the hard contribution at $m = 0$, i.e., Eq. (23). The integral in energy transfer gives

$$\int_{-v}^{v} dx (1 - x^2/v^2)^{(d-3)/2} (1 - x^2)^{(d-3)/2} \left\{3x^2 + \frac{x^2(1-v^2)}{x^2 - 1} + (d-3)x^2\right\} = 2v^2 \left\{\left(\frac{1}{v} + \frac{v^2 - 1}{2v^2} \ln\frac{1+v}{1-v}\right) + \epsilon \frac{2v}{3} + \epsilon \frac{P(v)}{v^2} + \mathcal{O}(\epsilon^2)\right\}, \tag{A4}$$

where $P(v)$ was previously defined in Eq. (26). The result for the k integral may be written as

$$2e^4 \nu^{3-d} C_d \int_0^{\infty} dk\, k^{d-2} \left(\frac{2k}{(1+v)\nu}\right)^{d-3} n_F(k) = \frac{e^2 m_{D,3+2\epsilon}^2}{16\pi} \left\{1 + \left[1 + \gamma_E + \frac{\zeta'(2)}{\zeta(2)} + \ln 2 + \frac{1}{2} \ln\frac{4T^2}{(1+v)^2 \bar{\nu}^2}\right] 2\epsilon + \mathcal{O}(\epsilon^2)\right\}. \tag{A5}$$

When writing the above result, we used the Debye mass in $d = 3 + 2\epsilon$ dimensions defined in Eq. (25). Multiplying the series Eq. (A4) by Eq. (A5) we eventually reach the result for the hard contribution to the energy loss at $m = 0$, i.e., Eq. (24).

Let us now discuss how to properly regularize the momentum integrals for the mass corrections of the hard contribution, i.e., the k integrals of Eq. (29). Explicitly, moving to the dimensionless variable $y = k/T$ and setting $d = 3 + 2\epsilon$, the IR integral to evaluate is

$$e^4 m^2 C_{3+2\epsilon}\left(\frac{T}{\nu}\right)^{2\epsilon}\int_0^\infty dy\, y^{-1+2\epsilon}\left(\frac{2T}{(1+v)\nu}y\right)^{2\epsilon} n_F(y). \tag{A6}$$

In DR, the small parameter ϵ acts as a regulator of the divergence, playing a similar role as a cutoff would do. In order to properly regularize Eq. (A6) we must distinguish the regulator of the IR divergence in momentum transfer from the regulator of the IR divergence in k, that we denote as ϵ_k. So, instead of Eq. (A6) we need to evaluate

$$\begin{aligned} &e^4 m^2 C_{3+2\epsilon}\left(\frac{T}{\nu}\right)^{2\epsilon}\int_0^\infty dy\, y^{-1+2\epsilon_k}\left(\frac{2T}{(1+v)\nu}y\right)^{2\epsilon} n_F(y) \\ &= e^4 m^2 C_{3+2\epsilon}\left(\frac{T}{\nu}\right)^{2\epsilon}\left(\frac{2T}{(1+v)\nu}\right)^{2\epsilon}(1-2^{1-2\epsilon-2\epsilon_k})\Gamma(2\epsilon+2\epsilon_k)\zeta(2\epsilon+2\epsilon_k). \end{aligned} \tag{A7}$$

Taking the limit $\epsilon_k \to 0$ above and then expanding for $\epsilon \to 0$ we get Eq. (30). In this way, the piece that was initially IR divergent in k also has a contribution to the pole in ϵ, i.e., the regulator of the IR divergence in momentum transfer. Applying the same procedure we can compute the other necessary integral in momentum of Eq. (29), which gives

$$e^4 m^2 \nu^{3-d} C_d \int_0^\infty dk\, k^{d-3}\left(\frac{2k}{(1+v)\nu}\right)^{d-3}\frac{1}{2}\frac{dn_F}{dk} = \frac{e^2}{16\pi}\frac{e^2 m^2}{2\pi^2}\left\{-1-\left(-2\gamma_E + 2\ln\pi + \ln\frac{T^2}{\bar{\nu}^2} + \ln\frac{4T^2}{(1+v)^2\bar{\nu}^2}\right)\epsilon + \mathcal{O}(\epsilon^2)\right\}. \tag{A8}$$

Although the result of the above integral is finite, intermediate steps in the computation require the evaluation of an IR divergent integral so that the same method for regularizing Eq. (30) must be used. If we do not distinguish between the regulators of the different divergences when evaluating the momentum integrals of the mass corrections, we would be unable to cancel the IR divergence in momentum transfer of the hard contribution with the UV divergence in momentum transfer of the soft contribution.

APPENDIX B: INTEGRALS OF THE SOFT CONTRIBUTION

The logarithmic ultraviolet divergence encountered in the soft region of the computation can be computed using DR regularization. One only needs to evaluate in $d = 3 + 2\epsilon$ [20]

$$\nu^{3-d}\int_0^\infty dq \frac{q^d}{(q^2 + m_D^2 a)^2 + m_D^4 b^2} = -\frac{1}{2}\left\{\frac{1}{\epsilon} - \ln\left(\frac{\nu^2}{m_D^2}\right) + \frac{1}{2}\ln(a^2+b^2) + \frac{a}{b}\arccos\left(\frac{a}{\sqrt{a^2+b^2}}\right)\right\} + \mathcal{O}(\epsilon). \tag{B1}$$

APPENDIX C: HTL POLARIZATION TENSOR FOR GENERIC FERMION MASS *m*

We have previously mentioned that Eqs. (22) and (50) should be valid for the evaluation of the hard and soft contribution to the energy loss respectively, if the fermions in the plasma have mass m, which is assumed to be at most of order T. However, the computation of the soft contribution with generic mass demands that the HTL resummation technique has to be done assuming massive fermions. We give here the expressions of the HTL polarization tensors in such a case. These can be evaluated, for example, in the real time formalism of thermal field theory, following the same steps as in Ref. [14] but with massive particles. After carrying out the integral in frequency one then arrives to the expression

$$\Pi^{\mu\nu}(L) = e^2\nu^{3-d}\int\frac{d^dq}{(2\pi)^d}\frac{1-2n_F(E_q)}{E_q}\left\{\frac{2E_qv^\mu v^\nu - v^\mu L^\nu - v^\nu L^\mu + g^{\mu\nu}(v\cdot L)}{v\cdot L - L^2/2E_q + i\mathrm{sgn}(E_q - l_0)0^+}\right.$$
$$\left. - \frac{2E_q\tilde{v}^\mu\tilde{v}^\nu + \tilde{v}^\mu L^\nu + \tilde{v}^\nu L^\mu - g^{\mu\nu}(\tilde{v}\cdot L)}{\tilde{v}\cdot L + L^2/2E_q + i\mathrm{sgn}(E_q + l_0)0^+}\right\}. \tag{C1}$$

Here $L = (l_0, l)$ is the external photon momentum, $v^\mu = (1, \boldsymbol{q}/E_q)$ and $\tilde{v}^\mu = (1, -\boldsymbol{q}/E_q)$ are the velocity of the massive fermions and antifermions, respectively, with $E_q = \sqrt{q^2 + m^2}$ and $\mathrm{sgn}(x)$ is the sign function. Under the assumption that external momenta obeys $L \ll Q$, after a change of variables to express the antiparticle contribution as the particle one, it is possible to approximate the expression to find

$$\Pi^{\mu\nu}(L) \approx 2e^2\nu^{3-d}\int\frac{d^dq}{(2\pi)^d}\frac{1-2n_F(E_q)}{E_q}\left(g^{\mu\nu} - \frac{v^\mu L^\nu + v^\nu L^\mu}{v\cdot L} + \frac{L^2 v^\mu v^\nu}{(v\cdot L)^2}\right). \tag{C2}$$

Note that in the limit $m = 0$, one reproduces the correct well-known limit for the HTL. This final result is the one that one would obtain from classical transport theory. Unfortunately, there is not a simple analytical expression of the polarization tensor for a generic value m. The generalization of the Braaten-Pisarski resummation program in this case would most likely to be implemented numerically.

[1] D. d'Enterria, Landolt-Bornstein **23**, 471 (2010).
[2] J. Casalderrey-Solana and C. A. Salgado, Acta Phys. Pol. B **38**, 3731 (2007).
[3] A. Majumder and M. Van Leeuwen, Prog. Part. Nucl. Phys. **66**, 41 (2011).
[4] G. Y. Qin and X. N. Wang, Int. J. Mod. Phys. E **24**, 1530014 (2015).
[5] J. D. Bjorken, Report No. FERMILAB-PUB-82-059-THY.
[6] E. Braaten and M. H. Thoma, Phys. Rev. D **44**, 1298 (1991).
[7] E. Braaten and M. H. Thoma, Phys. Rev. D **44**, R2625 (1991).
[8] R. D. Pisarski, Phys. Rev. Lett. **63**, 1129 (1989).
[9] E. Braaten and R. D. Pisarski, Nucl. Phys. **B337**, 569 (1990).
[10] S. Peigne and A. Peshier, Phys. Rev. D **77**, 014015 (2008).
[11] S. Peigne and A. Peshier, Phys. Rev. D **77**, 114017 (2008).
[12] J. Ghiglieri, A. Kurkela, M. Strickland, and A. Vuorinen, Phys. Rep. **880**, 1 (2020).
[13] C. Manuel, J. Soto, and S. Stetina, Phys. Rev. D **94**, 025017 (2016); **96**, 129901(E) (2017).
[14] S. Carignano, C. Manuel, and J. Soto, Phys. Lett. B **780**, 308 (2018).
[15] S. Carignano and C. Manuel, Phys. Rev. D **104**, 056031 (2021).
[16] S. Carignano, M. E. Carrington, and J. Soto, Phys. Lett. B **801**, 135193 (2020).
[17] T. Gorda, A. Kurkela, J. Österman, R. Paatelainen, S. Säppi, P. Schicho, K. Seppänen, and A. Vuorinen, Phys. Rev. D **107**, 036012 (2023).
[18] A. Ekstedt, arXiv:2302.04894.
[19] M. Comadran and C. Manuel, Phys. Rev. D **104**, 076006 (2021).
[20] S. Carignano and C. Manuel, Phys. Rev. D **103**, 116002 (2021).
[21] M. Le Bellac, *Thermal Field Theory* (Cambridge University Press, Cambridge, England, 1996).
[22] S. Peigne and A. V. Smilga, Phys. Usp. **52**, 659 (2009).

3 On-shell effective field theory and quantum transport for hard photons

In this section one can find the publication [26].

On-shell effective field theory and quantum transport for hard photons

Marc Comadran [1,2,3,*] and Cristina Manuel [1,2,†]

[1] *Instituto de Ciencias del Espacio (ICE, CSIC), C. Can Magrans s.n., 08193 Cerdanyola del Vallès, Spain*
[2] *Institut d'Estudis Espacials de Catalunya (IEEC), 08860 Castelldefels (Barcelona), Spain*
[3] *Departament de Física Quàntica i Astrofísica and Institut de Ciències del Cosmos, Universitat de Barcelona (IEEC-UB), Martí i Franqués 1, 08028 Barcelona, Spain*

(Received 9 September 2024; accepted 4 November 2024; published 27 November 2024)

We develop an effective field theory for the description of high energetic or hard photons, the on-shell effective theory (OSEFT). The OSEFT describes the so-called eikonal or semiclassical optical limit, allowing for corrections organized in a systematic expansion on inverse powers of the photon energy. We derive the OSEFT from the Maxwell Lagrangian and study its different properties, such as the gauge symmetry and reparametrization invariance. The theory can be finally formulated in terms of a gauge invariant vector gauge field, without the need to introduce gauge-fixing. We then use the OSEFT to compute corrections to the Wigner photon function and derive its associated side jump effect from reparametrization invariance. Finally, we discuss how to properly define the Stokes parameters from transport theory once quantum effects are considered, so as to preserve their well-defined properties under Lorentz transformations.

DOI: 10.1103/PhysRevD.110.096024

I. INTRODUCTION

Effective field theories are one of the most useful and advantageous tools in physics. They rely on the idea that in order to describe some phenomena at a given energy scale it is enough to identify the degrees of freedom that operate at that scale and uncover the Lagrangian that governs their dynamics, exploiting the symmetries of the problem. The effective Lagrangian is then organized in operators of increasing dimension over powers of the high energy scale. A different set of effective field theories have been proposed to describe a wide variety of physical phenomena; see the excellent reviews [1–3] to discuss the most relevant technical details and most used effective field theories for vacuum physics.

In this manuscript we will focus on the so called on-shell effective field theory (OSEFT) [4–10], which was first developed to describe energetic chiral fermions, with the main aim to describe quantum corrections to the classical transport equations [4]. The OSEFT also proved to be useful to compute power corrections to photon self-energy diagrams in high temperature T plasmas [5], or mass corrections to the same amplitudes [10], taking profit of the natural hierarchy of energy scales that appear in these systems.

Our focus in this manuscript is to describe the OSEFT associated to high energetic or hard photons. This presents different challenges, among them, a proper description respectful with the gauge symmetry of the photon degrees of freedom. We first present the complete OSEFT associated to an electromagnetic field, as being derived from the Maxwell Lagrangian. As we will discuss, the leading order Lagrangian in a high energy expansion describes the so-called eikonal or optical limit, while higher order terms in such an expansion would describe quantum corrections to the eikonal limit. Notably, the effective field theory can be formulated without imposing any gauge fixing condition. The nonphysical components of the vector gauge field potential can be eliminated, after integrating out and using local field redefinitions. Remarkably, we will show that the final OSEFT Lagrangian only contains one vector degree of freedom and demonstrate its invariance under gauge transformations that respect the energy scaling of the effective photon field. By studying the reparametrization invariance (RI) of the theory, we also check that the OSEFT for photons is respectful with the Lorentz symmetry.

Then, we also consider a many-body system, such as a thermal plasma. By employing the OSEFT for photons and well-established thermal field theory techniques, we derive the quantum kinetic equations obeyed by the photon Wigner function. Also, we show that the OSEFT allows us to systematically compute quantum corrections associated to the photon Wigner function.

*Contact author: mcomadca60@alumnes.ub.edu
†Contact author: cristina.manuel@csic.es

The polarization space components of the photon Wigner function can be related to the so-called Stokes parameters [11]. While the Stokes parameters are not Lorentz invariant, some ratios of them are [12,13]. For example, the percentage of circular polarization of a system is expected to be a Lorentz invariant. In this work, we will see that when quantum corrections are taken into consideration, the classical definition of the polarization ratio is no longer Lorentz invariant. This is related to the fact that in quantum kinetic theory, Lorentz transformations acquire nontrivial modifications when quantum effects are taken into account [14]. The unusual transformation properties have meaningful physical implications, for instance the so-called side jump effect [15,16]. Hence, we propose how to generalize the definition of the Stokes parameters, so as to preserve the Lorentz invariance of the polarization ratios when small quantum effects are taken into account. As we will discuss, the modification is relevant when the frame of reference of observation is not at rest with the thermal ensemble where the photon radiation is produced. For instance, this could be realized in many astrophysical and cosmological settings, where those conditions are usually met.

This manuscript is organized as follows, in Sec. II we develop the OSEFT associated to highly energetic photons. In Sec. II A we derive the OSEFT vacuum propagator and the dispersion relation, also, in Sec. II B we construct an effective gauge field for almost on-shell photons and in Sec. II C we discuss how the gauge symmetry is realized in the OSEFT. Then, in Sec. II D we introduce a polarization basis in the effective field theory, while Sec. II E is devoted to the study of the RI of the theory. In Sec. II F we explain the relation between the full theory and OSEFT variables. Then we employ the OSEFT in Sec. III to develop a quantum kinetic theory for hard photons. Using those results, in Sec. III A we construct the photon Wigner function while in Sec. III B a derivation of the side jump effect for photons from first principles is presented. In addition, in Sec. IV we discuss the Lorentz transformation properties of the Stokes parameters when small quantum effects are taken into account, from a quantum kinetic theory perspective. We present our conclusions in Sec. V. Finally, we elaborate in Appendix A a simplified operator notation used throughout the paper and explain some operator identities used in this work. In Appendix B we give general RI transformations for the effective photons fields which are too lengthy to include in the main text.

We use natural units $c = \hbar = k_B = 1$, metric conventions $\mathrm{diag}(g^{\mu\nu}) = (1, -1, -1, -1)$ and the normalization $\epsilon^{0123} = 1$ for the Levi-Civita tensor. Sometimes we will use the shortened notations $A^{(\mu}B^{\nu)} = A^\mu B^\nu + A^\nu B^\mu$ and $A^{[\mu}B^{\nu]} = A^\mu B^\nu - A^\nu B^\mu$. We employ boldface letters for three-dimensional vectors e.g. $A^\mu = (A^0, A^i) = (A^0, \boldsymbol{A})$.

II. ON-SHELL EFFECTIVE FIELD THEORY FOR PHOTONS

In this section we develop the OSEFT associated to hard or energetic photons. It fully corresponds to an effective field theory treatment of the so-called eikonal or optical limit. The eikonal approximation is considered as a sort of semiclassical approach, valid when the wavelength of the photon is much shorter than any other length scale in the problem. The OSEFT allows us to study corrections to the pure classical term as a series of operators of increasing dimension over powers of the photon energy, which is the inverse of the photon wavelength. These will represent quantum corrections to the semiclassical picture, an explicit example of which will be presented in the manuscript.

Our starting point is the Lagrangian describing the propagation of free electromagnetic fields,[1]

$$\mathcal{L} = -\frac{1}{4} F_{\mu\nu} F^{\mu\nu}. \tag{1}$$

Here, $F^{\mu\nu}(x) = \partial^\mu A^\nu(x) - \partial^\nu A^\mu(x)$ is the electromagnetic field strength tensor, and $A^\mu(x)$ is the vector gauge field potential. The momentum of an almost on-shell photon in the frame characterized by the timelike vector u^μ (satisfying $u^2 = 1$), can be decomposed into on-shell and residual parts as follows:

$$q^\mu = p^\mu + k^\mu = E v^\mu + k^\mu, \tag{2}$$

being $E = p \cdot u$ the energy of the photon in that frame, v^μ a lightlike vector ($v^2 = 0$) and k^μ the so-called residual momentum. The above decomposition assumes $k^\mu \ll E v^\mu$, so that one can identify the photon energy E as the hard scale. We define another lightlike vector $\tilde{v}^\mu$ ($\tilde{v}^2 = 0$) satisfying $v \cdot \tilde{v} = 2$, such that

$$u^\mu = \frac{v^\mu + \tilde{v}^\mu}{2}. \tag{3}$$

Moreover, it will be useful to introduce an additional spacelike vector,

$$n^\mu = \frac{\tilde{v}^\mu - v^\mu}{2}, \tag{4}$$

which satisfies $n^2 = -1$. Then, the momentum splitting of Eq. (2) is performed at the Lagrangian level,

$$\mathcal{L}_{E,v} = -\frac{1}{4} (\partial^\mu A_v^\nu - \partial^\nu A_v^\mu)^2, \tag{5}$$

[1] It is possible to generalize this procedure for electromagnetic field propagation in a medium characterized by a refractive index, as long as the space of variation of the index is much larger than the photon wavelength. We will leave this case for future studies.

and we factor out the hard momenta of the vector gauge field potential as

$$A_v^\mu(x) = e^{-iEv\cdot x}\xi^\mu(x) + e^{iEv\cdot x}\xi^{\mu\dagger}(x). \tag{6}$$

The above decomposition then assumes that the field $\xi^\mu(x)$ only has a dependence on the residual momenta. In terms of this field we can rewrite the Lagrangian of Eq. (5) as

$$\begin{aligned}\mathcal{L}_{E,v} = \frac{1}{2}\xi^{\mu\dagger}(g_{\mu\nu}\Box - \partial_\mu\partial_\nu - 2iEg_{\mu\nu}(v\cdot\partial) + E^2 v_\mu v_\nu \\ + iE(v_\mu\partial_\nu + \partial_\mu v_\nu))\xi^\nu + \text{H.c.},\end{aligned} \tag{7}$$

where the oscillating terms $\sim e^{\pm 2iEv\cdot x}$ have been dropped, also, we use $\Box = \partial^\mu\partial_\mu$ and H.c. stands for Hermitian conjugate. However, we can as well construct an artificial covariant derivative by introducing

$$\mathcal{D}^\mu \equiv \partial^\mu - iEv^\mu, \tag{8}$$

and rewrite the Lagrangian in the compact form,

$$\mathcal{L}_{E,v} = \frac{1}{2}\xi^{\mu\dagger}(g_{\mu\nu}\mathcal{D}^2 - \mathcal{D}_\mu\mathcal{D}_\nu)\xi^\nu + \text{H.c.}, \tag{9}$$

with $\mathcal{D}^2 = \mathcal{D}^\mu\mathcal{D}_\mu = \Box - 2iE(v\cdot\partial)$. The $\xi^\mu(x)$ field contains both physical and nonphysical components. At the classical level, this last can be eliminated for instance by imposing gauge fixing conditions. Below we will show that, under the above assumptions, the nonphysical components can be eliminated from the Lagrangian using effective field theory techniques, with no need of gauge-fixing.

Let us start by introducing the transverse projector to v^μ and $\tilde{v}^\mu$,

$$P_\perp^{\mu\nu} = g^{\mu\nu} - \frac{1}{2}(v^\mu\tilde{v}^\nu + \tilde{v}^\mu v^\nu), \tag{10}$$

which obeys

$$P_\perp^{\mu\nu}P_{\perp,\mu\rho} = P^\nu_{\perp,\rho}, \qquad P_\perp^2 = 2. \tag{11}$$

Note that in the rest frame, where $u^\mu = (1,\mathbf{0})$, one has $v^\mu = (1,\boldsymbol{v})$, $\tilde{v}^\mu = (1,-\boldsymbol{v})$ and $n^\mu = (0,-\boldsymbol{v})$, so that the transverse projector only has spatial components in that frame and is perpendicular to $\boldsymbol{v}$. Using the transverse projector, we can split the $\xi^\mu(x)$ field into different components,

$$\xi^\mu(x) = \xi_\perp^\mu(x) + v^\mu\phi(x) + n^\mu\lambda(x), \tag{12}$$

where each component is clearly identified

$$\xi_\perp^\mu(x) = P_\perp^{\mu\nu}\xi_\nu(x), \quad \phi(x) = (u\cdot\xi)(x), \quad \lambda(x) = (v\cdot\xi)(x). \tag{13}$$

The $\xi_\perp^\mu(x)$ field describes transverse degrees of freedom to v^μ and $\tilde{v}^\mu$, while the remaining longitudinal and scalar degrees of freedom are both described by the $\lambda(x)$ and $\phi(x)$ fields. There is a certain freedom in the decomposition of the nontransverse part of Eq. (12). We have chosen the one that singles out the component that is still transverse to the frame vector u^μ, that is $\lambda(x)$ (since $u\cdot n = 0$). The suitability of this choice will be explained throughout the paper. In terms of these components, the Lagrangian can be written as

$$\begin{aligned}\mathcal{L}_{E,v} = \frac{1}{2}\Big\{&\xi_\perp^{\mu\dagger}(g_{\mu\nu}\mathcal{D}^2 - \partial_\mu\partial_\nu)\xi_\perp^\nu - \phi^\dagger(v\cdot\partial)^2\phi \\ &- \lambda^\dagger(\mathcal{D}^2 + (n\cdot\mathcal{D})^2)\lambda - \xi_\perp^{\mu\dagger}\partial_\mu(v\cdot\partial)\phi \\ &- \phi^\dagger(v\cdot\partial)\partial_\mu\xi_\perp^\mu - \xi_\perp^{\mu\dagger}\partial_\mu(n\cdot\mathcal{D})\lambda - \lambda^\dagger(n\cdot\mathcal{D})\partial_\mu\xi_\perp^\mu \\ &+ \phi^\dagger(\mathcal{D}^2 - (v\cdot\partial)(n\cdot\mathcal{D}))\lambda \\ &+ \lambda^\dagger(\mathcal{D}^2 - (v\cdot\partial)(n\cdot\mathcal{D}))\phi\Big\} + \text{H.c.}\end{aligned} \tag{14}$$

Above, one can see that the operators accounting for the propagation of the various components do not have the same power counting in energy E, for instance $\mathcal{D}^2 \sim E$ and $(n\cdot\mathcal{D})^2 \sim E^2$. Hence, we identify the $\lambda(x)$ field as the degree of freedom that can be integrated out using its classical equation of motion,

$$\begin{aligned}\lambda(x) = -\frac{1}{\mathcal{D}^2 + (n\cdot\mathcal{D})^2}[(n\cdot\mathcal{D})\partial_\mu\xi_\perp^\mu(x) \\ - (\mathcal{D}^2 - (v\cdot\partial)(n\cdot\mathcal{D}))\phi(x)].\end{aligned} \tag{15}$$

The resulting Lagrangian may be written as

$$\begin{aligned}\mathcal{L}_{E,v} = \frac{1}{2}\Big\{&\xi_\perp^{\mu\dagger}\left(g_{\mu\nu}\mathcal{D}^2 - \partial_\mu\partial_\nu\frac{\mathcal{D}^2}{\mathcal{D}^2 + (n\cdot\mathcal{D})^2}\right)\xi_\perp^\nu \\ &- \xi_\perp^{\mu\dagger}\partial_\mu\frac{\mathcal{D}^2(u\cdot\mathcal{D})}{\mathcal{D}^2 + (n\cdot\mathcal{D})^2}\phi - \phi^\dagger\frac{\mathcal{D}^2(u\cdot\mathcal{D})}{\mathcal{D}^2 + (n\cdot\mathcal{D})^2}\partial_\mu\xi_\perp^\mu \\ &+ \phi^\dagger\frac{\partial_\perp^2\mathcal{D}^2}{\mathcal{D}^2 + (n\cdot\mathcal{D})^2}\phi\Big\} + \text{H.c.},\end{aligned} \tag{16}$$

where we defined $\partial_\perp^\mu \equiv P_\perp^{\mu\nu}\partial_\nu$. In the above Lagrangian and for the rest of the paper, we will use a compact operator notation that we elaborate in Appendix A. Subsequently, the above operators are expanded and organized in inverse powers of the hard scale $(1/E)^n$, yielding an infinite series of Lagrangians $\mathcal{L}_{E,v}^{(n)}$, each of them encompassing operators that increase in dimension with the power of n. Specifically, using the expansions,

$$\frac{\mathcal{D}^2}{\mathcal{D}^2 + (n\cdot\mathcal{D})^2} = \frac{2i(v\cdot\partial)}{E} + \mathcal{O}\left(\frac{1}{E^2}\right), \tag{17a}$$

$$\frac{\mathcal{D}^2(u\cdot\mathcal{D})}{\mathcal{D}^2 + (n\cdot\mathcal{D})^2} = 2(v\cdot\partial) + \frac{i}{E}(\partial_\perp^2 - (v\cdot\partial)^2) + \mathcal{O}\left(\frac{1}{E^2}\right), \tag{17b}$$

we can write down the first 3 orders,

$$\mathcal{L}_{E,v}^{(-1)} = -E\xi_\perp^{\mu\dagger} g_{\mu\nu}(iv\cdot\partial)\xi_\perp^\nu + \text{H.c.}, \tag{18a}$$

$$\mathcal{L}_{E,v}^{(0)} = \frac{1}{2}\xi_\perp^{\mu\dagger} g_{\mu\nu}\Box\xi_\perp^\nu - \xi_\perp^{\mu\dagger}\partial_\mu(v\cdot\partial)\phi - \phi^\dagger(v\cdot\partial)\partial_\mu\xi_\perp^\mu + \text{H.c.}, \tag{18b}$$

$$\mathcal{L}_{E,v}^{(1)} = \frac{i}{E}\bigg(-\xi_\perp^{\mu\dagger}\partial_\mu(v\cdot\partial)\partial_\nu\xi_\perp^\nu - \frac{1}{2}\xi_\perp^{\mu\dagger}\partial_\mu(\partial_\perp^2 - (v\cdot\partial)^2)\phi - \frac{1}{2}\phi^\dagger(\partial_\perp^2 - (v\cdot\partial)^2)\partial_\mu\xi_\perp^\mu + \phi^\dagger\partial_\perp^2(v\cdot\partial)\phi\bigg) + \text{H.c.} \tag{18c}$$

Beyond the leading order, scalar and longitudinal degrees of freedom endure, indicated by the presence of terms with the $\phi(x)$ field. However, we can eliminate those terms through the application of local field redefinitions. Indeed, the following transformation:

$$\xi_\perp^\mu(x) \to \tau_\perp^\mu(x) = \xi_\perp^\mu(x) - \frac{i\partial_\perp^\mu}{E}\phi(x) - \frac{(v\cdot\partial + \tilde{v}\cdot\partial)\partial_\perp^\mu}{2E^2}\phi(x), \tag{19}$$

completely eliminates all terms with the $\phi(x)$ field from Eqs. (18b) and (18c). We have demonstrated here a specific case of a much broader scenario. In general, to eliminate the $\phi(x)$ field from the nth order Lagrangian, one needs to apply the following field redefinition:

$$\xi_\perp^\mu(x) \to \tau_\perp^\mu(x) = \xi_\perp^\mu(x) - \frac{\partial_\perp^\mu}{u\cdot\mathcal{D}}\phi(x), \tag{20}$$

with the operators expanded up to $(n+1)$th order in inverse powers of E. In this way, the $\phi(x)$ field can be eliminated at all orders in the energy expansion and the final Lagrangian can be written in terms of the locally redefined field only as

$$\mathcal{L}'_{E,v} = \frac{1}{2}\tau_\perp^{\mu\dagger}\left(g_{\mu\nu}\mathcal{D}^2 - \partial_\mu\partial_\nu\frac{\mathcal{D}^2}{\mathcal{D}^2 + (n\cdot\mathcal{D})^2}\right)\tau_\perp^\nu + \text{H.c.} \tag{21}$$

The final OSEFT Lagrangian only contains the vector degree of freedom $\tau_\perp^\mu(x)$, corresponding to transverse, almost on-shell photons. Note however, that we did not impose any particular gauge to derive it, in fact, we demonstrate in Sec. II C that it enjoys a gauge symmetry. Notably, the equivalence principle [2,17,18] guarantees that the on-shell quantities after the local field redefinition of Eq. (20) remain unaffected.

Expanding now to the lowest orders we have

$$\mathcal{L}_{E,v}^{\prime(-1)} = -E\tau_\perp^{\mu\dagger} g_{\mu\nu}(iv\cdot\partial)\tau_\perp^\nu + \text{H.c.}, \tag{22a}$$

$$\mathcal{L}_{E,v}^{\prime(0)} = \frac{1}{2}\tau_\perp^{\mu\dagger} g_{\mu\nu}\Box\tau_\perp^\nu + \text{H.c.}, \tag{22b}$$

$$\mathcal{L}_{E,v}^{\prime(1)} = -\frac{1}{E}\tau_\perp^{\mu\dagger}\partial_\mu(iv\cdot\partial)\partial_\nu\tau_\perp^\nu + \text{H.c.} \tag{22c}$$

$$\mathcal{L}_{E,v}^{\prime(2)} = \frac{1}{2E^2}\tau_\perp^{\mu\dagger}\partial_\mu(\Box - 4(u\cdot\partial)(v\cdot\partial))\partial_\nu\tau_\perp^\nu + \text{H.c.} \tag{22d}$$

The leading order Lagrangian describes the so-called eikonal limit, while the higher order Lagrangians capture the corrections to this limit. Let us discuss how the above Lagrangian should be interpreted, as in an effective field theory, one has to solve the theory order by order. For example, naively, the equation of motion as derived from Eqs. (22a)–(22d) reads

$$\left(-g_{\mu\nu}(2Eiv\cdot\partial - \Box) - \partial_\mu\left(\frac{2iv\cdot\partial}{E} - \frac{\Box - 4(u\cdot\partial)(v\cdot\partial)}{E^2}\right)\partial_\nu\right) \times\tau_\perp^\nu(x) = 0. \tag{23}$$

However, one can always use the equation of motion at a given order in $1/E$ as a constraint for the operators appearing at the next order. For instance, the equation of motion at leading order $i(v\cdot\partial)\tau_\perp^\mu(x) = 0$ can be used to simplify the operator $\Box\tau_\perp^\mu(x) = \partial_\perp^2\tau_\perp^\mu(x) + \mathcal{O}(1/E)$ appearing at the next order. Performing this process at a fixed order in $1/E$, one can always show without much difficulty that all structures proportional to $\partial^\mu\partial^\nu$ vanish, so that the equation of motion only contains the tensor structure $g^{\mu\nu}$ and can be formally written as

$$-(2Eiv\cdot\partial - \Box)\tau_\perp^\mu(x) = 0, \tag{24}$$

or as $\mathcal{D}^2\tau_\perp^\mu(x) = 0$, by employing the operator in Eq. (8).

A. Vacuum propagator and dispersion relation

The OSEFT Green function in vacuum, that we define as $\mathcal{G}_\perp^{\mu\nu}(x,y) = \langle 0|\mathcal{T}\tau_\perp^{\mu\dagger}(x)\tau_\perp^\nu(y)|0\rangle$, where $\mathcal{T}$ denotes time-ordering, obeys

$$\mathcal{D}_x^2\mathcal{G}_\perp^{\mu\nu}(x,y) = P_\perp^{\mu\nu}\delta(x-y), \tag{25}$$

as can be deduced from Eq. (24). The above equation can be easily inverted in (residual) momentum space, yielding to

$$\mathcal{G}_\perp^{\mu\nu}(k) = \frac{-P_\perp^{\mu\nu}}{2E(v\cdot k) + k^2 + i0^+}. \tag{26}$$

The dispersion equation is $2E(v\cdot k) + k^2 = 0$, which has to be solved order by order in the energy expansion (see for instance Refs. [4–6]). Doing so up to order $1/E$, one gets

$$2E(v\cdot k) + k_\perp^2 - \frac{(\tilde{v}\cdot k)k_\perp^2}{2E} = 0, \tag{27}$$

so that in the rest frame, using the notation $k^\mu = (k_0, \boldsymbol{k})$ for the residual momentum, the denominator of the propagator can be written as $2E(k_0 - \mathrm{f}(\boldsymbol{k})) + i0^+$ where $\mathrm{f}(\boldsymbol{k})$ is the dispersion relation of the OSEFT, given by

$$\mathrm{f}(\boldsymbol{k}) = \boldsymbol{v}\cdot\boldsymbol{k} + \frac{\boldsymbol{k}_\perp^2}{2E} - \frac{(\boldsymbol{v}\cdot\boldsymbol{k})\boldsymbol{k}_\perp^2}{2E^2} + \mathcal{O}\left(\frac{1}{E^3}\right), \tag{28}$$

where we used the fact that in the rest frame one has $k_\perp^2 = -\boldsymbol{k}_\perp^2$ and $\tilde{v}\cdot k \approx 2(\boldsymbol{v}\cdot\boldsymbol{k})$.

B. Effective gauge field for almost on-shell photons

It is interesting to relate our starting effective field $\xi^\mu(x)$ with the locally redefined field of the OSEFT Lagrangian $\tau_\perp^\mu(x)$. In order to do so, we first insert the equation of motion of the $\lambda(x)$ field into Eq. (12), in addition, by writing $\partial_\perp^\mu = \partial^\mu - v^\mu(u\cdot\partial) - n^\mu(v\cdot\partial)$ in the field redefinition of Eq. (20) and using the operator identity of Eq. (A2), we find that an effective gauge field for almost on-shell photons is

$$\xi^\mu(x) = \left(g^\mu_\nu - n^\mu\partial_\nu\frac{n\cdot\mathcal{D}}{\mathcal{D}^2 + (n\cdot\mathcal{D})^2}\right)\tau_\perp^\nu(x) + \frac{\mathcal{D}^\mu}{u\cdot\mathcal{D}}\phi(x). \tag{29}$$

Actually, it is relatively easy to derive again the OSEFT Lagrangian in very few steps, by directly plugging the above relation into Eq. (9) and noting that all terms with the $\phi(x)$ field vanish due to $(g_{\mu\nu}\mathcal{D}^2 - \mathcal{D}_\mu\mathcal{D}_\nu)\mathcal{D}^\mu = 0$.

The above expression is quite useful in computations, for instance, in Sec. III we will use it to construct the photon Wigner function in a semiclassical approximation; furthermore, it will help to understand the physical picture underlying the OSEFT. This last question will be elaborated throughout the manuscript, in particular in the next section, where we discuss how the gauge symmetry is realized in the effective field theory.

C. OSEFT gauge transformations

In effective field theories, where there is a well defined hierarchy of scales, it is common to separate the gauge transformations for each sector of the theory according to their scale, respecting such a separation. One particular example of this fact occurs in SCET, where one talks on a gauge symmetry associated to the hard (or collinear) gluon fields, and another one associated to the soft gluon fields [3]. An additional multipole expansion of the different fields might be needed to respect the energy separation [19]. An analogous situation is expected in the OSEFT for photons. In this work, we only consider the hard sector of the theory, ignoring the soft gauge fields, as they do not interact. Further, we are not considering the interaction with matter particles neither. All of them could be incorporated, following the same SCET techniques. Here we will discuss the gauge symmetry associated to hard photons. The Lagrangian of Eq. (5) enjoys the gauge symmetry,

$$A_v^\mu(x) \to A_v^\mu(x) + \partial^\mu\theta_v(x), \tag{30}$$

for an arbitrary function $\theta_v(x)$ that respects the energy scaling of the gauge field. Hence, the OSEFT Lagrangian of Eq. (21) should also posses a gauge symmetry. By writing $\theta_v(x) = e^{-iEv\cdot x}\eta(x) + \text{H.c.}$, we can deduce how the different components of the photon field transform under a gauge transformation. Explicitly, one then finds that the OSEFT vector gauge field transforms as

$$\xi^\mu(x) \to \xi^\mu(x) + \mathcal{D}^\mu\eta(x), \tag{31}$$

and thus,

$$\xi_\perp^\mu(x) \to \xi_\perp^\mu(x) + \partial_\perp^\mu\eta(x), \tag{32a}$$

$$\phi(x) \to \phi(x) + (u\cdot\mathcal{D})\eta(x), \tag{32b}$$

$$\lambda(x) \to \lambda(x) + (v\cdot\partial)\eta(x). \tag{32c}$$

Then, we can show that the final OSEFT Lagrangian is gauge invariant. To prove it, we note that the locally redefined field is itself invariant under the above set of gauge transformations. Indeed,

$$\begin{aligned}\tau_\perp^\mu(x) &\to \xi_\perp^\mu(x) + \partial_\perp^\mu\eta(x) - \frac{\partial_\perp^\mu}{u\cdot\mathcal{D}}[\phi(x) + (u\cdot\mathcal{D})\eta(x)]\\ &= \tau_\perp^\mu(x).\end{aligned} \tag{33}$$

Let us conclude this section with the following observation. Taking the four divergence in Eq. (6) and resorting to Eq. (29) one can show that

$$\partial_\mu A_v^\mu = \frac{\mathcal{D}^2}{(u\cdot\mathcal{D})}\phi(x)e^{-iEv\cdot x} + \text{H.c.} \tag{34}$$

Thus, if we had not carried out the local field redefinition and rather we would have fixed the gauge as $\phi(x) = 0$ in the initial Lagrangian, that would imply that the gauge field obeys $u_\mu A_v^\mu = 0$ and $\partial_\mu A_v^\mu = 0$. In conclusion, the resulting framework in the OSEFT if we impose that $\phi(x) = 0$ is equivalent to the Coulomb gauge. However, let us stress that in this work we perform a local field redefinition to eliminate the nonphysical $\phi(x)$ component of the gauge field from the Lagrangian, which allows us to work without choosing any particular gauge.

D. Polarization vectors

The field $\tau_\perp^\mu(x)$ is transverse to v^μ and $\tilde{v}^\mu$. Thus, in the rest frame, it only has spatial components and is transverse to $\boldsymbol{v}$. It is suggesting then to introduce polarization vectors in the effective field theory.

Let us define a linear polarization basis, as $\{e_i^\mu\}$ with $i = \{1, 2\}$, satisfying $(e_i^\mu)^* = e_i^\mu$, also

$$v \cdot e_i = \tilde{v} \cdot e_i = 0, \qquad e_i \cdot e_j = g_{ij} = -\delta_{ij}, \tag{35}$$

so that they are unitary and spacelike. We shall, however, work with circular polarization vectors, that we introduce as $\{e_h^\mu\}$ with $h = \{+, -\}$, obeying the properties,

$$v \cdot e_h = \tilde{v} \cdot e_h = 0, \qquad e_h^* \cdot e_{h'} = -\delta_{hh'}. \tag{36}$$

Their relation with the linear polarization vectors is

$$e_h^\mu = \frac{1}{\sqrt{2}}(e_1^\mu + ih e_2^\mu), \tag{37}$$

so that $(e_h^\mu)^* = e_{-h}^\mu$. Note that both the linear and circular polarization vectors are also transverse to u^μ and n^μ. We can relate the polarization vectors with the transverse projector and spin tensor (introduced below) as

$$P_\perp^{\mu\nu} = g^{\mu\nu} - \frac{1}{2}(v^\mu \tilde{v}^\nu + \tilde{v}^\mu v^\nu) = -e_+^{*\mu} e_+^\nu - e_-^{*\mu} e_-^\nu, \tag{38a}$$

$$S_\perp^{\mu\nu} = i\epsilon^{\mu\nu\alpha\beta} v_\alpha u_\beta = e_+^{*\mu} e_+^\nu - e_-^{*\mu} e_-^\nu. \tag{38b}$$

The spin tensor obeys $S_\perp^2 = -2$, but it is not a good projector, since $S_\perp^{\mu\nu} S_{\perp,\mu\rho} = -P_{\perp,\rho}^\nu$. Thus, it is useful to introduce the right ($h = +$) and left ($h = -$) projectors,

$$P_h^{\mu\nu} = \frac{1}{2}(P_\perp^{\mu\nu} - h S_\perp^{\mu\nu}) = -e_h^{*\mu} e_h^\nu, \tag{39}$$

satisfying the properties,

$$P_\pm^2 = 0, \qquad P_\pm^{\mu\nu} P_{\mp,\mu\nu} = 1,$$
$$P_\pm^{\mu\nu} P_{\pm,\mu\rho} = 0, \qquad P_\pm^{\mu\nu} P_{\mp,\mu\rho} = -P_{\mp,\rho}^\nu. \tag{40}$$

Now, the field $\tau_\perp^\mu(x)$ can be decomposed in the circular polarization basis as

$$\tau_\perp^\mu(x) = \sum_{h=\pm} e_h^\mu \tau_h(x). \tag{41}$$

Hence, the components $\tau_h(x) = -(e_h^* \cdot \tau_\perp)(x)$ correspond to right $(h = +)$ and left $(h = -)$ handed circularly polarized photons respectively.

E. Reparametrization invariance

In general, an effective field theory should remain invariant under infinitesimal transformations of the parameters used to describe the theory. The invariance under these types of transformations is called reparametrization invariance (RI), and it was first discussed in the context of heavy quark effective field theory (HQEFT) [20], and later on generalized for massless degrees of freedom in the context of soft collinear effective field theory (SCFT) [21].

RI is the symmetry associated with the ambiguity of the decomposition of the full momentum q^μ in Eq. (2). A small shift in the velocity v^μ could be reabsorbed in the definition of the residual momentum k^μ, while the physics should remain unchanged. On the other hand, the explicit choices of the vectors v^μ and $\tilde{v}^\mu$ seem to imply an apparent breaking of the Lorentz symmetry. Checking the RI of the theory ultimately confirms that Lorentz symmetry is respected in the effective field theory.

RI has been extensively studied also in the OSEFT for fermions in [7,9]. We will discuss how to generalize these concepts for the photon fields here. The main idea is that the field $A_v^\mu(x)$ should not change under infinitesimal transformations of the parameters used to construct the effective field theory. Then, under a RI transformation one should have

$$A_v^\mu(x) \xrightarrow{\Lambda} A_{v'}^\mu(x) = A_v^\mu(x), \tag{42}$$

where we introduced the label $\Lambda = \{\mathrm{I}, \mathrm{II}, \mathrm{III}\}$ for the three types of RI transformations [21]. Thus, the OSEFT Lagrangian should enjoy the following symmetries:

$$(\mathrm{I}): \begin{cases} v^\mu \to v^\mu + \Delta_\perp^\mu \\ \tilde{v}^\mu \to \tilde{v}^\mu \end{cases}, \qquad (\mathrm{II}): \begin{cases} v^\mu \to v^\mu \\ \tilde{v}^\mu \to \tilde{v}^\mu + \tilde{\Delta}_\perp^\mu \end{cases},$$
$$(\mathrm{III}): \begin{cases} v^\mu \to (1+\alpha) v^\mu \\ \tilde{v}^\mu \to (1-\alpha)\tilde{v}^\mu \end{cases}, \tag{43}$$

where $\{\Delta_\perp^\mu, \tilde{\Delta}_\perp^\mu, \alpha\}$ are five infinitesimal parameters, satisfying

$$\Delta_\perp \cdot v = \Delta_\perp \cdot \tilde{v} = \tilde{\Delta}_\perp \cdot v = \tilde{\Delta}_\perp \cdot \tilde{v} = 0. \tag{44}$$

In Tables I and II we show the transformation rules for the projected fields and other relevant quantities of the effective

TABLE I. Transformation rules for the projected fields $\xi_\perp^\mu(x)$, $\lambda(x)$ and $\phi(x)$. We dropped the space time arguments to enlighten the notation.

	Type (I)	Type (II)	Type (III)
$\xi_\perp^\mu$	$\xi_\perp^\mu - \Delta_\perp^\mu \phi + \frac{1}{2}\Delta_\perp^\mu \lambda - \frac{1}{2} v^\mu (\Delta_\perp \cdot \xi)$	$\xi_\perp^\mu - \frac{1}{2} v^\mu (\tilde{\Delta}_\perp \cdot \xi) - \frac{1}{2}\tilde{\Delta}_\perp^\mu \lambda$	$\xi_\perp^\mu$
ϕ	$\phi + \frac{1}{2}(\Delta_\perp \cdot \xi)$	$\phi + \frac{1}{2}(\tilde{\Delta}_\perp \cdot \xi)$	$(1-\alpha)\phi + \alpha\lambda$
λ	$\lambda + \Delta_\perp \cdot \xi$	λ	$(1+\alpha)\lambda$

TABLE II. Transformation rules for the operators of the effective field theory and the OSEFT polarization vectors. The transformation rules for the negative energy sector of the theory can be easily recovered after replacing $E \to -E$ and $h \to -h$.

	Type (I)	Type (II)	Type (III)
E	E	E	$(1-\alpha)E$
∂^μ	$\partial^\mu + iE\Delta_\perp^\mu$	∂^μ	∂^μ
$\partial_\perp^\mu$	$\partial_\perp^\mu - \frac{1}{2}(\Delta_\perp \cdot \partial)\tilde{v}^\mu - \frac{1}{2}(\tilde{v}\cdot\mathcal{D})\Delta_\perp^\mu$	$\partial_\perp^\mu - \frac{1}{2}(\tilde{\Delta}_\perp \cdot \partial)v^\mu - \frac{1}{2}(v\cdot\partial)\tilde{\Delta}_\perp^\mu$	$\partial_\perp^\mu$
$\mathcal{D}^\mu$	$\mathcal{D}^\mu$	$\mathcal{D}^\mu$	$\mathcal{D}^\mu$
$u\cdot\mathcal{D}$	$u\cdot\mathcal{D} + \frac{1}{2}(\Delta_\perp\cdot\partial)$	$u\cdot\mathcal{D} + \frac{1}{2}(\tilde{\Delta}_\perp\cdot\partial)$	$u\cdot\mathcal{D} - \alpha(n\cdot\mathcal{D})$
$n\cdot\mathcal{D}$	$n\cdot\mathcal{D} - \frac{1}{2}(\Delta_\perp\cdot\partial)$	$n\cdot\mathcal{D} + \frac{1}{2}(\tilde{\Delta}_\perp\cdot\partial)$	$n\cdot\mathcal{D} - \alpha(u\cdot\mathcal{D})$
$\partial_\perp^2$	$\partial_\perp^2 - (\Delta_\perp\cdot\partial)(\tilde{v}\cdot\mathcal{D})$	$\partial_\perp^2 - (\tilde{\Delta}_\perp\cdot\partial)(v\cdot\partial)$	$\partial_\perp^2$
e_h	$e_h - \frac{1}{2}(e_h\cdot\Delta_\perp)\tilde{v}^\mu$	$e_h - \frac{1}{2}(e_h\cdot\tilde{\Delta}_\perp)v^\mu$	e_h

field theory respectively. Polarization vectors also change under RI transformations, as can be seen in the last row of Table II, so that they preserve their transversality to v^μ and $\tilde{v}^\mu$.

After integrating out, the transformations in Table I with the presence of the $\lambda(x)$ field have to be modified. We derive and discuss the general expressions for those transformations, i.e. valid at any order in $1/E$, in Appendix B. Remarkably, it can also be shown that the OSEFT Lagrangian, obtained after the local field redefinition to eliminate the $\phi(x)$ field, is RI invariant. In order to prove it, one just needs to know how the field $\tau_\perp^\mu(x)$, introduced in Eq. (20), changes under each type of transformation. We also give the general form of these last transformations in Appendix B.

Hence, using Eqs. (B8)–(B10), it is possible to check that

$$\delta_{(\mathrm{I})}\mathcal{L}_{E,v} = \delta_{(\mathrm{II})}\mathcal{L}_{E,v} = \delta_{(\mathrm{III})}\mathcal{L}_{E,v} = 0, \tag{45}$$

or in other words, the OSEFT Lagrangian is RI invariant. It is worth mentioning that all nontransverse structures in these last transformations are not necessary to proof the RI invariance of the Lagrangian, as those pieces always vanish when contracted with transverse tensors. However, they would be necessary to derive the transformation rules for other quantities, such as currents. The general transformations for $\tau_\perp^\mu(x)$ are quite simple when expanded in powers of $1/E$. Precisely, keeping terms up to first order in the energy expansion we find

$$\tau_\perp^\mu \xrightarrow{(\mathrm{I})} \tau_\perp^\mu - \frac{i\partial_\perp^\mu}{2E}(\Delta_\perp\cdot\tau_\perp) - \frac{i\Delta_\perp^\mu}{2E}(\partial\cdot\tau_\perp) - \frac{\tilde{v}^\mu}{2}(\Delta_\perp\cdot\tau_\perp), \tag{46a}$$

$$\tau_\perp^\mu \xrightarrow{(\mathrm{II})} \tau_\perp^\mu - \frac{i\partial_\perp^\mu}{2E}(\tilde{\Delta}_\perp\cdot\tau_\perp) + \frac{i\tilde{\Delta}_\perp^\mu}{2E}(\partial\cdot\tau_\perp) - \frac{v^\mu}{2}(\tilde{\Delta}_\perp\cdot\tau_\perp), \tag{46b}$$

$$\tau_\perp^\mu \xrightarrow{(\mathrm{III})} \tau_\perp^\mu. \tag{46c}$$

Employing the expressions above, we derive in Sec. III the transformation rules for the distribution function for photons at $1/E$ accuracy, in particular using type (II) transformations one can derive the so-called side jump effect.

F. Going backward to the full theory variables

When constructing the OSEFT, we decomposed the photon momentum q^μ as in Eq. (2), introducing the effective field theory variables E, v^μ and k^μ. Any quantity computed from the OSEFT depends on these variables. However, it is desirable to be able to reexpress the results in terms of the full theory momentum q^μ.

This is a well established process which has been extensively discussed in the literature of the OSEFT, see e.g. Refs. [5–9], so we just recall here the relevant expressions needed for this work. First, we will need the expression of the on-shell velocity v_q^μ in the effective field theory, which reads

$$v_q^\mu = v^\mu + \frac{k_\perp^\mu}{E} - \frac{(\tilde{v}\cdot k)k_\perp^\mu}{2E^2} - \frac{k_\perp^2 n^\mu}{2E^2} + \mathcal{O}\left(\frac{1}{E^3}\right). \tag{47}$$

It follows that $\tilde{v}_q^\mu = 2u^\mu - v_q^\mu$, while the frame vector u^μ does not change when moving back to the full theory. Also, it is useful to define a spacelike vector in the full theory, such that

$$n_q^\mu = \frac{\tilde{v}_q^\mu - v_q^\mu}{2} = n^\mu - \frac{k_\perp^\mu}{E} + \frac{(\tilde{v}\cdot k)k_\perp^\mu}{2E^2} + \frac{k_\perp^2 n^\mu}{2E^2} + \mathcal{O}\left(\frac{1}{E^3}\right). \tag{48}$$

Let us introduce the polarization vectors of the full theory in the circular basis as $\{e_{q,h}^\mu\}$ with the suffix (q) indicating that they are functions of momentum and $h = \{+,-\}$. We can relate them with the OSEFT polarization vectors $\{e_h^\mu\}$ using the following trick. By requiring that at each order in $1/E$,

$$u\cdot e_{q,h} = v_q\cdot e_{q,h} = \tilde{v}_q\cdot e_{q,h} = 0, \qquad e_{q,h}\cdot e_{q,h'} = -\delta_{hh'}, \tag{49}$$

holds, it is not difficult to realize that

$$e^{\mu}_{q,h} = e^{\mu}_{h} - \frac{e_h \cdot k_\perp}{E} n^\mu + \frac{(e_h \cdot k_\perp)}{2E^2}(k^\mu_\perp + (\tilde{v}\cdot k)n^\mu) + \mathcal{O}\left(\frac{1}{E^3}\right). \tag{50}$$

Then, we can introduce the transverse projector and spin tensor of the full theory as

$$P^{\mu\nu}_{\perp,q} = g^{\mu\nu} - \frac{1}{2}(v^\mu_q \tilde{v}^\nu_q + \tilde{v}^\mu_q v^\nu_q) = -e^{*\mu}_{q,+}e^{\nu}_{q,+} - e^{*\mu}_{q,-}e^{\nu}_{q,-}, \tag{51a}$$

$$S^{\mu\nu}_{\perp,q} = \frac{i\epsilon^{\mu\nu\alpha\beta}q_\alpha u_\beta}{u\cdot q} = e^{*\mu}_{q,+}e^{\nu}_{q,+} - e^{*\mu}_{q,-}e^{\nu}_{q,-}, \tag{51b}$$

respectively. In the definitions above, $q^\mu = (E_q, \boldsymbol{q})$ is the on-shell momentum (with $E_q = u\cdot q$), also $v^\mu_q = (1, \boldsymbol{q}/E_q)$ and $\tilde{v}^\mu_q = (1, -\boldsymbol{q}/E_q)$. They can also be expressed in terms of the OSEFT variables, either by using Eqs. (47) or (50). For instance, we can write

$$P^{\mu\nu}_{\perp,q} = P^{\mu\nu}_{\perp} - \frac{1}{E}n^{(\mu}k^{\nu)}_\perp + \frac{(\tilde{v}\cdot k)}{2E^2}n^{(\mu}k^{\nu)}_\perp + \frac{1}{E^2}(k^\mu_\perp k^\nu_\perp + k^2_\perp n^\mu n^\nu) + \mathcal{O}\left(\frac{1}{E^3}\right), \tag{52a}$$

$$S^{\mu\nu}_{\perp,q} = S^{\mu\nu}_{\perp} + \frac{1}{E}n^{[\mu}S^{\nu]\alpha}_\perp k_\alpha - \frac{1}{2E^2}k^{[\mu}_\perp S^{\nu]\alpha}_\perp k_\alpha - \frac{(\tilde{v}\cdot k)}{2E^2}n^{[\mu}S^{\nu]\alpha}_\perp k_\alpha + \mathcal{O}\left(\frac{1}{E^3}\right). \tag{52b}$$

III. QUANTUM KINETIC THEORY FOR PHOTONS FROM THE OSEFT

In the previous section we derived the OSEFT associated to an energetic photon field. Here we will consider a many body system, such as a plasma, characterized by a temperature T. Then, one should consider that there are many electromagnetic fields with energy scales of the order or much larger than T, which then admit an OSEFT description. The electromagnetic fields with typical energy scales lower than T can be then treated as classical gauge fields. This can be justified by the fact that the Bose-Einstein distribution function is well approximated by a classical field distribution function at low energies.

In this section we derive photon quantum kinetic equations from the effective field theory developed in Sec. II, that is, we assume that we are describing the high energetic photons in the system. To this aim, apart from the OSEFT for photons we employ the Schwinger-Keldysh formalism of thermal field theory [22–24]; see also Refs. [25,26] for recent reviews on the subject. We will consider a collisionless medium, that it, we will ignore the interactions of photons with the electrons/positrons in the plasma, which occur at a typical length scale $\sim 1/e^4 T$ [27] [up to $\ln(e)$]. Thus, the kinetic equations derived in this manuscript are valid for distances shorter than the λ scale, and timescales associated to the inverse of that length. We will also neglect the effect of any other background field.

Let us emphasize that in the OSEFT, we have performed a local field redefinition to eliminate the nonphysical component of the photon field from the Lagrangian [c.f. Eq. (20)]. Notably, as the equivalence theorem was extended to finite density and then to general thermodynamic observables in Ref. [28], doing a similar reasoning as in Sec. II allows us to work with the locally redefined field with no need to worry about affecting any on-shell quantity.

The main object in the Schwinger-Keldysh formalism is the Green function, which is expressed as a matrix in the complex time path contour. Similarly, in the OSEFT, one can define for positive energy photons,

$$\mathcal{G}^{\mu\nu}_\perp(x,y) = \begin{pmatrix} \mathcal{G}^{c,\mu\nu}_\perp(x,y) & \mathcal{G}^{<,\mu\nu}_\perp(x,y) \\ \mathcal{G}^{>,\mu\nu}_\perp(x,y) & \mathcal{G}^{a,\mu\nu}_\perp(x,y) \end{pmatrix} = \begin{pmatrix} \langle \mathcal{T}_C \tau^\mu_\perp(x)\tau^{\nu\dagger}_\perp(y)\rangle & \langle \tau^{\nu\dagger}_\perp(y)\tau^\mu_\perp(x)\rangle \\ \langle \tau^\mu_\perp(x)\tau^{\nu\dagger}_\perp(y)\rangle & \langle \tilde{\mathcal{T}}_C \tau^\mu_\perp(x)\tau^{\nu\dagger}_\perp(y)\rangle \end{pmatrix}, \tag{53}$$

where $\mathcal{T}_C$ and $\tilde{\mathcal{T}}_C$ denote time and antitime ordering along the complex time contour respectively, while $\langle\ldots\rangle$ denotes thermal average over an ensemble of states. Analogous definitions can be done for the negative energy sector of the theory. Indeed, we can also define

$$\tilde{\mathcal{G}}^{\mu\nu}_\perp(x,y) = \begin{pmatrix} \tilde{\mathcal{G}}^{c,\mu\nu}_\perp(x,y) & \tilde{\mathcal{G}}^{<,\mu\nu}_\perp(x,y) \\ \tilde{\mathcal{G}}^{>,\mu\nu}_\perp(x,y) & \tilde{\mathcal{G}}^{a,\mu\nu}_\perp(x,y) \end{pmatrix} = \begin{pmatrix} \langle \mathcal{T}_C \tau^{\mu\dagger}_\perp(x)\tau^{\nu}_\perp(y)\rangle & \langle \tau^{\nu}_\perp(y)\tau^{\mu\dagger}_\perp(x)\rangle \\ \langle \tau^{\mu\dagger}_\perp(x)\tau^{\nu}_\perp(y)\rangle & \langle \tilde{\mathcal{T}}_C \tau^{\mu\dagger}_\perp(x)\tau^{\nu}_\perp(y)\rangle \end{pmatrix}. \tag{54}$$

Our interest is in the lesser (or greater) components of the Green functions, as these are related with the photon phase-space distribution function after a Wigner transform. From their definition, it follows that the lesser and greater components of each sector of the theory are related by

$$\mathcal{G}^{<,\mu\nu}_\perp(x,y) = \tilde{\mathcal{G}}^{>,\nu\mu}_\perp(y,x), \tag{55}$$

and satisfy the hermiticity property,

$$(\mathcal{G}^{<,\mu\nu}_\perp(x,y))^* = \tilde{\mathcal{G}}^{>,\mu\nu}_\perp(x,y) = \mathcal{G}^{<,\nu\mu}_\perp(y,x). \tag{56}$$

Let us focus on the positive energy sector of the theory. We define the OSEFT Wigner function for positive energy photons as

$$\mathcal{G}_{\perp}^{<,\mu\nu}(X,k) = \int d^4 s e^{ik\cdot s} \mathcal{G}_{\perp}^{<,\mu\nu}(x,y), \tag{57}$$

where $X^\mu = (x^\mu + y^\mu)/2$ and $s^\mu = x^\mu - y^\mu$ are the central and relative coordinate respectively, while k^μ is the residual momentum. We can build kinetic equations to the desired order in $1/E$ by adding and subtracting the Wigner transformed equations of motion. Precisely, taking into account Eq. (25), we can define

$$(I_\pm)^{\mu\nu} = -\frac{1}{2}\int d^4 s e^{ik\cdot s}(\mathcal{D}_x^2 \pm \mathcal{D}_y^2)\mathcal{G}_{\perp}^{<,\mu\nu}(x,y) = 0.$$

Performing the Wigner transform, the dispersion $(I_+)^{\mu\nu} = 0$ and transport $(I_-)^{\mu\nu} = 0$ equations give

$$\left(2E(v\cdot k) + k^2 - \frac{\partial^2}{4}\right)\mathcal{G}_{\perp}^{<,\mu\nu}(X,k) = 0, \tag{58a}$$

$$(Eiv\cdot\partial + ik\cdot\partial)\mathcal{G}_{\perp}^{<,\mu\nu}(X,k) = 0, \tag{58b}$$

respectively. Above and for the rest of the paper, we will use the shortened notation $\partial^\mu = \partial_X^\mu$ when all derivatives in the expressions are respect to the center coordinate. The kinetic equations can also be written in the following form, obtained after solving the theory order by order in $1/E$ (see the remarks in Sec. II),

$$\left(2E(v\cdot k) + k_\perp^2 - \frac{\partial_\perp^2}{4} - \frac{(\tilde{v}\cdot k)k_\perp^2}{2E} + \frac{(\tilde{v}\cdot k)\partial_\perp^2}{8E} + \frac{(k_\perp\cdot\partial)(\tilde{v}\cdot\partial)}{4E}\right)\mathcal{G}_{\perp}^{<,\mu\nu}(X,k) = 0, \tag{59a}$$

$$\left(Eiv\cdot\partial + i(k_\perp\cdot\partial) - \frac{ik_\perp^2(\tilde{v}\cdot\partial)}{4E} + \frac{i(\tilde{v}\cdot\partial)\partial_\perp^2}{16E} - \frac{i(\tilde{v}\cdot k)(k_\perp\cdot\partial)}{2E}\right)\mathcal{G}_{\perp}^{<,\mu\nu}(X,k) = 0. \tag{59b}$$

In addition, one should complement the kinetic equations with the following constraints which, by construction, are obeyed at any order in $1/E$:

$$v_\mu \mathcal{G}_{\perp}^{<,\mu\nu} = \tilde{v}_\mu \mathcal{G}_{\perp}^{<,\mu\nu} = v_\nu \mathcal{G}_{\perp}^{<,\mu\nu} = \tilde{v}_\nu \mathcal{G}_{\perp}^{<,\mu\nu} = 0. \tag{60}$$

Analogous kinetic equations and constraints can be derived for the negative energy sector, just by replacing $E \to -E$ and $\mathcal{G} \to \tilde{\mathcal{G}}$. The above constraints suggest that the OSEFT Wigner function can be decomposed into the polarization basis introduced in Sec. II C as

$$\mathcal{G}_{\perp}^{<,\mu\nu}(X,k) = \sum_{h,h'=\pm} e_h^\mu e_{h'}^{*\nu} \mathcal{G}^{<,hh'}(X,k). \tag{61}$$

In the remaining part of the paper we will assume that there is no polarization mixing in the photon ensemble and thus write

$$\mathcal{G}_{\perp}^{<,\mu\nu}(X,k) = \sum_{h=\pm} e_h^\mu e_h^{*\nu} \mathcal{G}^{<,h}(X,k). \tag{62}$$

The polarization space components are defined as the Wigner transform of the corresponding Green function as

$$\mathcal{G}^{<,h}(X,k) = \int d^4 s e^{ik\cdot s} \mathcal{G}^{<,h}(x,y), \tag{63}$$

where $\mathcal{G}^{<,h}(x,y) = \langle \tau_h^\dagger(y)\tau_h(x)\rangle$. After the Wigner transform, their general structure is

$$\mathcal{G}^{<,h}(X,k) = 2\pi\delta(K_h) f^h(X,k), \tag{64}$$

where we denote with $f^h(X,k)$ the off-shell distribution function for right/left circular polarized photons of positive energy, while K_h is the function that governs the dispersion relation, given by the expression inside the parenthesis in Eq. (58a). Again, similar definitions can be done for the negative energy sector, e.g. $\tilde{\mathcal{G}}^{<,h}(X,k) = 2\pi\delta(\tilde{K}_h)\tilde{f}^h(X,k)$.

A. Wigner function for photons

Transport equations associated to the photon Wigner function were studied in the literature long ago; see for example [29]. The photon Wigner function can be determined in several ways, for instance by using the Fourier decomposition of the vector field gauge potential or by directly solving the quantum kinetic equations [27,30,31]. Here we present yet an alternative derivation using the OSEFT developed in Sec. II.

The lesser component of the Wigner function for photons is defined as

$$G^{<,\mu\nu}(X,q) = \int d^4 s e^{iq\cdot s}\langle A^\nu(y)A^\mu(x)\rangle. \tag{65}$$

Then, plugging the ansatz for the photon field of Eq. (6) onto the above equation and using the momentum decomposition $q^\mu = \pm Ev^\mu + k^\mu$ for the positive/negative energy sector of the theory respectively, one can write

$$G^{<,\mu\nu}(X,q) = \int d^4 s e^{ik\cdot s}\{\langle \xi^{\nu\dagger}(y)\xi^\mu(x)\rangle + \langle \xi^\nu(y)\xi^{\mu\dagger}(x)\rangle\}, \tag{66}$$

where we used that

$$\langle \xi^\nu(y)\xi^\mu(x)\rangle = \langle \xi^{\nu\dagger}(y)\xi^{\mu\dagger}(x)\rangle = 0, \tag{67}$$

which is equivalent to impose causality preserving commutation relations between creation and annihilation operators. Then, for free photons we can directly use Eq. (29) to write the Wigner function as follows:

$$G^{<,\mu\nu}(X,q) = \int d^4 s e^{ik\cdot s}\{(\mathcal{O}^\mu_\alpha)_x(\mathcal{O}^\nu_\beta)^*_y \mathcal{G}^{<,\alpha\beta}_\perp(x,y) + (\mathcal{O}^\mu_\alpha)^*_x(\mathcal{O}^\nu_\beta)_y \tilde{\mathcal{G}}^{<,\alpha\beta}_\perp(x,y)\}, \quad (68)$$

where $\mathcal{G}^{<,\alpha\beta}_\perp(x,y)$ and $\tilde{\mathcal{G}}^{<,\alpha\beta}_\perp(x,y)$ are the OSEFT Green functions for positive and negative energies introduced in Eqs. (53) and (54) respectively, and we used the shortened notation,

$$\mathcal{O}^\mu_\nu = g^\mu_\nu - n^\mu \partial_\nu \frac{n\cdot\mathcal{D}}{\mathcal{D}^2 + (n\cdot\mathcal{D})^2}. \quad (69)$$

Note that in Eq. (68), we assumed that

$$\langle\phi^\dagger(y)\tau^\mu_\perp(x)\rangle = \langle\tau^{\mu\dagger}_\perp(y)\phi(x)\rangle = \langle\phi^\dagger(y)\phi(x)\rangle = 0, \quad (70)$$

which can be justified by noting that in the Lagrangian of Eq. (21) there are no terms that couple those fields. Then, using the expansion $\mathcal{O}^\mu_\nu \approx g^\mu_\nu - \frac{i}{E} n^\mu \partial_\nu$ and decomposing the OSEFT Wigner functions onto the circular polarization basis, we reach to

$$G^{<,\mu\nu}(X,q) = \sum_{h=\pm}\int d^4 s e^{ik\cdot s}\left\{\left(e^\mu_h e^{*\nu}_h + \frac{i}{E}(e^\mu_h n^\nu(e^*_h\cdot\partial_y) - n^\mu e^{*\nu}_h(e_h\cdot\partial_x))\right)\mathcal{G}^{<,h}(x,y) + \left(e^{*\mu}_h e^\nu_h - \frac{i}{E}(e^{*\mu}_h n^\nu(e_h\cdot\partial_y) - n^\mu e^\nu_h(e^*_h\cdot\partial_x))\right)\tilde{\mathcal{G}}^{<,h}(x,y)\right\}. \quad (71)$$

By writing $\partial^\mu_x = \frac{1}{2}\partial^\mu_X + \partial^\mu_s$ and $\partial^\mu_y = \frac{1}{2}\partial^\mu_X - \partial^\mu_s$ above, we can easily perform the Wigner transform, as $\partial^\mu_s \to -ik^\mu$ after integrating by parts. The result may be written as

$$G^{<,\mu\nu}(X,q) = \sum_{h=\pm}(\Pi^{\mu\nu}_h(k)\mathcal{G}^{<,h}(X,k) + \tilde{\Pi}^{\mu\nu}_h(k)\tilde{\mathcal{G}}^{<,h}(X,k)), \quad (72)$$

where we defined the tensor,

$$\Pi^{\mu\nu}_h(k) = e^\mu_h e^{*\nu}_h - \frac{1}{E}(e^\mu_h n^\nu(e^*_h\cdot k) + n^\mu e^{*\nu}_h(e_h\cdot k)) + \frac{i}{2E}(e^\mu_h n^\nu(e^*_h\cdot\partial) - n^\mu e^{*\nu}_h(e_h\cdot\partial)), \quad (73)$$

while $\tilde{\Pi}^{\mu\nu}_h(k)$ can be obtained after replacing $E\to -E$ and $h\to -h$ in the above expression. Note that in the above tensor we are reproducing the expansion of the full theory polarization vectors of Eq. (50). The tensor $\Pi^{\mu\nu}_h(k)$ can also be written in terms of the transverse projector and the spin tensor,

$$\Pi^{\mu\nu}_h(k) = -\frac{1}{2}\left(P^{\mu\nu}_\perp + hS^{\mu\nu}_\perp - \frac{1}{E}n^{(\mu}k^{\nu)}_\perp + \frac{h}{E}n^{[\mu}S^{\nu]\alpha}_\perp k_\alpha - \frac{i}{2E}n^{[\mu}\partial^{\nu]}_\perp + \frac{ih}{2E}n^{(\mu}S^{\nu)\alpha}_\perp\partial_\alpha\right), \quad (74)$$

after resorting to Eq. (39). Above, it can be easily seen that we are reproducing the expansions of the full theory transverse projector and spin tensor of Eqs. (52a) and (52b) up to first order in $1/E$; additionally, we produce quantum corrections to the Wigner function.

Now we would like to reexpress the Wigner function in terms of the full theory variables. At this expansion order we can associate

$$\mathcal{G}^{<,h}(X,k) = 2\pi\delta(K_h)f^h(X,k) \to 4\pi\delta(q^2)\theta(u\cdot q)f^h(X,q), \quad (75a)$$

$$\tilde{\mathcal{G}}^{<,h}(X,k) = 2\pi\delta(\tilde{K}_h)\tilde{f}^h(X,k) \to -4\pi\delta(q^2)\theta(-u\cdot q) \times f^h(X,q), \quad (75b)$$

where $f^h(X,q)$ is the off-shell distribution for right-/left-handed circularly polarized photons of the full theory. If, for instance, one considers that the photon ensemble is at thermal equilibrium and that there is no CP violating effect, so that one can assume $f^+(X,q) = f^-(X,q) \equiv f_{\rm eq}(q_0)$, the distribution function takes the form $f_{\rm eq}(q_0) = (e^{q_0/T}-1)^{-1}$ in the rest frame of the medium, being T the equilibrium temperature. In that scenario, one has

$$f_{\rm eq}(q_0) = \begin{cases} n_B(\boldsymbol{q}), & \text{if } q_0 = |\boldsymbol{q}| \\ -[1+n_B(\boldsymbol{q})], & \text{if } q_0 = -|\boldsymbol{q}| \end{cases}, \quad (76)$$

where $n_B(\boldsymbol{q}) = (e^{|\boldsymbol{q}|/T}-1)^{-1}$ is the Bose-Einstein distribution function. The tensors $\Pi^{\mu\nu}_h(k)$ and $\tilde{\Pi}^{\mu\nu}_h(k)$ both translate to $\Pi^{\mu\nu}_h(q)$, which may be written either in terms of the polarization vectors or the transverse projector and spin tensor as (see Sec. II F)

$$\Pi_h^{\mu\nu}(q) = e^{\mu}_{q,h} e^{*\nu}_{q,h} + \frac{i}{2E_q}\left(e^{\mu}_{q,h} n^{\nu}_q (e^*_{q,h}\cdot\partial) - n^{\mu}_q e^{*\nu}_{q,h}(e_{q,h}\cdot\partial)\right), \tag{77a}$$

$$\Pi_h^{\mu\nu}(q) = -\frac{1}{2}\left(P^{\mu\nu}_{\perp,q} + hS^{\mu\nu}_{\perp,q} - \frac{i}{2E_q} n_q^{[\mu}\partial_{\perp,q}^{\nu]} + \frac{ih}{2E_q} n_q^{(\mu} S_{\perp,q}^{\nu)\alpha}\partial_\alpha\right), \tag{77b}$$

where we recall that $n^\mu_q = u^\mu - v^\mu_q$, being $v^\mu_q = q^\mu/E_q$ the photon on-shell velocity. Then, after moving back to the full theory variables, one can write the Wigner function for photons at $1/E_q$ accuracy as

$$G^{<,\mu\nu}(X,q) = 4\pi\sum_{h=\pm}\Pi_h^{\mu\nu}(q)\delta(q^2)\mathrm{sgn}(u\cdot q) f^h(X,q), \tag{78}$$

with $\mathrm{sgn}(x)$ denoting the sign function. The kinetic equations obeyed by the photon Wigner function can be deduced from Eqs. (58a) and (58b). In terms of the full theory variables they read

$$q^2 G^{<,\mu\nu}(X,q) = 0, \tag{79a}$$

$$(q\cdot\partial) G^{<,\mu\nu}(X,q) = 0. \tag{79b}$$

In Eq. (79a) we dropped a piece proportional to $\sim\partial^2$ to be consistent with the gradient expansion assumed here. Although the $1/E$ and gradient expansions are fundamentally different approximations, at the order we work and in the absence of background fields both approximations agree. We note that at this expansion order the following constraints are satisfied:

$$\left(\frac{1}{2}\partial_\mu - iq_\mu\right)\Pi_h^{\mu\nu}(q) = \left(\frac{1}{2}\partial_\nu + iq_\nu\right)\Pi_h^{\mu\nu}(q) = 0, \tag{80}$$

and also,

$$u_\mu \Pi_h^{\mu\nu}(q) = u_\nu \Pi_h^{\mu\nu}(q) = 0, \tag{81}$$

so that the Wigner function obeys the Coulomb gauge-fixing conditions. We note that the Wigner function of Eq. (78) coincides exactly with that encountered in Refs. [27,30,31]. However, let us remark that we did not impose any gauge fixing condition to achieve this result, which means that the Wigner function associated to the high-energy modes, when computed in a semiclassical approach, is a gauge invariant quantity, provided that the gauge transformations are respectful with the separation of energy scales.

B. Side jumps from reparametrization invariance

In a semiclassical approach to describe massless chiral fermions the Lorentz transformations need to be modified in the presence of small quantum effects in order to preserve the frame independence of the theory [14]. This is related to the fact that the total angular momentum of a relativistic spinning particle is ambiguous, because the definition of the spin part is nonunique. The issue is resolved by imposing the condition $u_\mu S^{\mu\nu}_{\perp,q} = q_\mu S^{\mu\nu}_{\perp,q} = 0$, so that the spin tensor is uniquely fixed in the inertial frame, and is given then by Eq. (51). Consequently, when moving from frame u^μ to u'^μ the particle position also changes, so that the total angular momentum is conserved. The shift on the particle position when changing between inertial frames is the so-called side jump effect [14,15]. In the context of chiral kinetic theory, describing a system of massless fermions, this effect is manifested by the fact that the fermion distribution function is no longer a Lorentz scalar.

In chiral kinetic theory, the side jump effect can naturally be derived from OSEFT, and it is linked with the reparametrization invariance of the theory. This was checked for massless fermions in [7,8]. As we will see, the same applies to photons. Note that while it has been widely accepted that this side jump effect would affect also other massless spinning particles [32], and not only fermions, we are however unaware of any explicit proof of this side jump effect from quantum field theory.

In order to derive the side jump effect, we first need to know the RI transformations of the polarization space components of the Wigner function. Those can be derived from

$$\mathcal{G}^{<,h}(X,k) = e^*_{h,\mu} e_{h,\nu}\int d^4s\, e^{ik\cdot s}\langle \tau_\perp^{\dagger\nu}(y)\tau^\mu_\perp(x)\rangle, \tag{82}$$

by employing the transformation rules of Eqs. (46a)–(46c). Under a type (II) transformation one finds

$$\begin{aligned}\delta_{(\mathrm{II})}\mathcal{G}^{<,h}(X,k) &= \frac{i}{2E} e^*_{h,\mu} e_{h,\nu}\int d^4s\, e^{ik\cdot s}\Big((\partial_x+\partial_y)^\mu\tilde{\Delta}^\nu_\perp \\ &\quad - \tilde{\Delta}^\mu_\perp(\partial_x+\partial_y)^\nu\Big)\mathcal{G}^{<,h}(x,y) \\ &= \frac{ih}{2E} S^{\mu\nu}_\perp \tilde{\Delta}_{\perp,\nu}\partial_\mu \mathcal{G}^{<,h}(X,k).\end{aligned} \tag{83}$$

The contribution from the negative energy sector, $\delta_{(\mathrm{II})}\tilde{\mathcal{G}}^{<,h}(X,k)$, is the same as above, as can be seen by replacing $E\to -E$ and $h\to -h$. After adding the positive and negative energy sector contribution, we can deduce the transformation rule for the photon distribution function under a type (II) transformation, which reads

$$f^h(X,q)\xrightarrow{(\mathrm{II})} f^h(X,q) + \frac{ih}{2E_q} S^{\mu\nu}_{\perp,q}\tilde{\Delta}_{\perp,\nu}\partial_\mu f^h(X,q), \tag{84}$$

after moving back to the full theory variables, which is the expected side jump effect. Note that Eq. (84) gives the infinitesimal change of the distribution function, where one has to take into account that $\tilde{\Delta}^{\mu}_{\perp}/2 = u'^{\mu} - u^{\mu}$.

Doing a similar reasoning as above, one can show that at $1/E_q$ accuracy $S^{\mu\nu}_{\perp,q}$ and $f^h(X,q)$ are both invariant under a type (I) and a type (III) RI transformation, so that there is no side jump effect in those cases.

IV. STOKES PARAMETERS WITH QUANTUM CORRECTIONS

By projecting the Wigner function of Eq. (78) onto the circular polarization basis, we can build a naive photon current associated to every helicity state. Precisely, in the absence of polarization mixing in the photon ensemble, we can define

$$j^{h,\mu}(X) = \int \frac{d^4q}{(2\pi)^4} q^{\mu} G^h(X,q), \quad h = \pm, \tag{85}$$

where we dropped the lesser symbol ($<$) from the Wigner function to enlighten the notation. Also, we introduced

$$G^h(X,q) = 4\pi\delta(q^2)\mathrm{sgn}(u\cdot q) f^h(X,q). \tag{86}$$

The polarization space components of the Wigner function (or the zeroth component of the photon current), can be directly related to the Stokes parameters [11,33]. Then, with this setting, the naive Stokes parameters matrix can be defined as

$$\begin{aligned}\rho(X) &= \begin{pmatrix} j_0^+(X) & 0 \\ 0 & j_0^-(X) \end{pmatrix} \\ &= \begin{pmatrix} j_0^I(X) - j_0^V(X) & 0 \\ 0 & j_0^I(X) + j_0^V(X) \end{pmatrix},\end{aligned} \tag{87}$$

where $j_0^I = (j_0^+ + j_0^-)/2$ and $j_0^V = -(j_0^+ - j_0^-)/2$ give the values of the intensity and degree of polarization of the photon ensemble, respectively. It is well-known that the Stokes parameters are not Lorentz invariant, but the percentage of circulation polarization, obtained as the ratio of the degree of circular polarization over the intensity; i.e. j_0^V/j_0^I, is usually regarded in the literature as a Lorentz invariant [12,13].

However, in a semiclassical approach to photon propagation based on quantum kinetic theory, as soon as quantum corrections are considered, and due to the side jump effect discussed in Sec. III B this is no longer the case. Modification of the definition of the Stokes parameters is then needed in order to restore the Lorentz invariance of the polarization ratios.

The above issue is related to the fact that the naive current of Eq. (88) does not transform as a Lorentz vector when quantum corrections are taken into account, because the photon distribution function is no longer a Lorentz scalar. A solution was found in Ref. [14], by including a magnetization contribution to the naive helicity current one can restore its frame independence in the collisionless limit. Indeed, one can define a frame independent photon current in the collisionless limit as

$$J^{h,\mu}(X) = \int \frac{d^4q}{(2\pi)^4} (q^{\mu} - ihS^{\mu\nu}_{\perp,q}\partial_{\nu}) G^h(X,q). \tag{88}$$

From the above current, we can define new Stokes parameters as $J_0^I = (J_0^+ + J_0^-)/2$ and $J_0^V = -(J_0^+ - J_0^-)/2$, so that the Lorentz invariance of the polarization ratio J_0^V/J_0^I is restored. Hence, we can write the intensity and the degree of polarization of the photon ensemble as

$$\begin{aligned}J_0^I(X) = \int \frac{d^4q}{(2\pi)^3} & 2\delta(q^2)\mathrm{sgn}(u\cdot q) \\ &\times \left(q_0 f^I(X,q) + \frac{\boldsymbol{u}\times\boldsymbol{q}}{u\cdot q}\cdot \boldsymbol{\nabla} f^V(X,q)\right),\end{aligned} \tag{89}$$

$$\begin{aligned}J_0^V(X) = \int \frac{d^4q}{(2\pi)^3} & 2\delta(q^2)\mathrm{sgn}(u\cdot q) \\ &\times \left(q_0 f^V(X,q) + \frac{\boldsymbol{u}\times\boldsymbol{q}}{u\cdot q}\cdot \boldsymbol{\nabla} f^I(X,q)\right),\end{aligned} \tag{90}$$

respectively, where the we have defined

$$f^I(X,q) = \frac{f^+(X,q) + f^-(X,q)}{2}, \tag{91}$$

$$f^V(X,q) = -\frac{f^+(X,q) - f^-(X,q)}{2}. \tag{92}$$

Note that in the rest frame of the medium ($\boldsymbol{u} = \boldsymbol{0}$) or in the frames satisfying $\boldsymbol{u}\times\boldsymbol{q} = 0$, the naive polarization percentage j_0^V/j_0^I is still a Lorentz invariant quantity, even in the presence of small quantum effects.

Let us emphasize that the frame independence of the current of Eq. (88) is only valid under the assumption of a collisionless medium. Nevertheless, under certain circumstances this program can also be generalized in the presence of collisions [15], so that further modification of the Stokes parameters would be required in that scenario.

V. DISCUSSION

In this manuscript we have fully developed the OSEFT associated to photons, generalizing previous work carried out for chiral fermions. Assuming a high energy expansion, we derived the Lagrangian associated to the high energy or hard photons from the free Maxwell Lagrangian. By splitting the vector gauge field into different components, we identified the degree of freedom that can be integrated out from the Lagrangian using its classical equation of motion, given in Eq. (15). Subsequently, we showed that the remaining nonphysical degree of freedom can be eliminated employing the local field redefinition of Eq. (20). After this last step, we obtained an effective field theory that only contains a transverse vector gauge field [cf. Eq. (21)].

Generally, in the context of effective field theories, it is common to split the fields into different components, according to their energy scale (e.g. into hard and soft parts). In a gauge theory then one expects a gauge symmetry associated to each sector of the theory which is respectful with the energy scaling of such decomposition. In this work, a gauge symmetry associated to the hard part of the photon field has been presented, and we demonstrated that the OSEFT Lagrangian enjoys that symmetry. We have also proven the RI of the theory, which basically means that the OSEFT is respectful with the Lorentz symmetry. Using the RI transformations, a first principles derivation of the so-called side jump effect for photons has been provided [see Eq. (84)].

Since at high energies, or when the photon wavelength is much shorter than any length scale in the system, electromagnetic waves can be accurately studied under the so-called eikonal limit, the OSEFT seems a suitable tool to study how the physics beyond the eikonal approximation is corrected. For instance, we used the OSEFT and the Schwinger-Keldysh formalism of thermal field theory to construct a quantum kinetic theory for photons. We have shown how to use the OSEFT to systematically compute quantum corrections to the semiclassical photon Wigner function, and we explicitly computed the leading order quantum correction [see Eqs. (77a), (77b), and (78)]. In addition, we derived the quantum kinetic equations obeyed by the photon Wigner function in the collisionless limit, given by Eqs. (79a) and (79b). Our results agree with those found in Refs. [27,30,31]. However, as in the effective field theory approach we separate the gauge field into physical and nonphysical components, in OSEFT computations one can clearly identify which modes contribute at each order in the energy expansion, thus providing valuable insight.

We have then elaborated on the proper definition of the Stokes parameters as deduced from quantum kinetic theory. At the classical level, the percentage of circular polarization in a system is a Lorentz invariant quantity. However, we have shown that as soon as quantum corrections are considered, the definition of the Stokes parameters needs to be modified in order to preserve the Lorentz invariance of the percentage of circular polarization. We have given such a definition in Eqs. (89) and (90) for the intensity and degree of circular polarization. Let us recall that we assumed the absence of polarization mixing in the photon ensemble. It would be interesting to generalize the discussion in the presence of such polarization modes, as they are known to be generated in relevant cosmological physical scenarios.

Finally, let us mention that the OSEFT for photons could be used also for the computation of power corrections to different sort of Feynman diagrams, for example, at high temperature and/or density. One could extend the study we carry out by allowing interactions of the hard photons with either hard and soft fermions, and proceed with the same methods for the study of the effects of these interactions, as it was done for the contribution of hard fermions in [5,6].

ACKNOWLEDGMENTS

We thank Joan Soto and Stefano Carignano for discussions. This work was supported by Ministerio de Ciencia, Investigación y Universidades (Spain) MCIN/AEI/10.13039/501100011033/ FEDER, UE, under the Project No. PID2022-139427NB-I00, by Generalitat de Catalunya by the Project No. 2021-SGR-171 (Catalonia). This work was also partly supported by the Spanish program Unidad de Excelencia Maria de Maeztu CEX2020-001058-M.

DATA AVAILABILITY

No data were created or analyzed beyond what is included in this article.

APPENDIX A: OPERATOR NOTATION AND IDENTITIES

In this manuscript we use a simplified operator notation in order to shorten the length of the expressions. When we write one over a differential operator we mean the inverse of the differential operator in the denominator. To compactify even more the notation, we often write fractions of different differential operators. For example it should be understood the following:

$$\frac{n\cdot\mathcal{D}}{\mathcal{D}^2+(n\cdot\mathcal{D})^2}\partial_\mu\xi^\mu_\perp \to \frac{1}{\mathcal{D}^2+(n\cdot\mathcal{D})^2}(n\cdot\mathcal{D})\partial_\mu\xi^\mu_\perp. \tag{A1}$$

Also, in most of the derivations presented in this work, we used the fact that some combinations of operators, which appear acting on the $\phi(x)$ field, vanish identically. For instance, when deriving Eq. (29) we used the fact that

$$\frac{n\cdot\mathcal{D}}{\mathcal{D}^2+(n\cdot\mathcal{D})^2}\frac{\partial^2_\perp}{u\cdot\mathcal{D}} - \frac{\mathcal{D}^2-(v\cdot\partial)(n\cdot\mathcal{D})}{\mathcal{D}^2+(n\cdot\mathcal{D})^2} + \frac{v\cdot\partial}{u\cdot\mathcal{D}} = 0. \tag{A2}$$

Similarly, one can show other operator identities which are relevant in our derivations,

$$\frac{u\cdot\mathcal{D}}{\mathcal{D}^2+(n\cdot\mathcal{D})^2}\frac{\mathcal{D}^2}{n\cdot\mathcal{D}} - \frac{\mathcal{D}^2-(v\cdot\partial)(n\cdot\mathcal{D})}{\mathcal{D}^2+(n\cdot\mathcal{D})^2} - \frac{v\cdot\partial}{n\cdot\mathcal{D}} = 0, \tag{A3a}$$

$$\frac{(u\cdot\mathcal{D})(n\cdot\mathcal{D})(\mathcal{D}^2-(v\cdot\partial)(n\cdot\mathcal{D}))}{\mathcal{D}^2+(n\cdot\mathcal{D})^2}-(\mathcal{D}^2-(v\cdot\partial)(u\cdot\mathcal{D}))+\frac{\mathcal{D}^2\partial_\perp^2}{\mathcal{D}^2+(n\cdot\mathcal{D})^2}=0. \tag{A3b}$$

APPENDIX B: RI TRANSFORMATIONS

As we explained in Sec. II E, the transformation rules are modified after integrating out the $\lambda(x)$ field. Precisely, for the transverse field we find

$$\xi_\perp^\mu \xrightarrow{(\mathrm{I})} \xi_\perp^\mu-\frac{\Delta_\perp^\mu}{2}\left(1+\frac{(u\cdot\mathcal{D})(n\cdot\mathcal{D})}{\mathcal{D}^2+(n\cdot\mathcal{D})^2}\right)\phi-\frac{\Delta_\perp^\mu}{2}\frac{(n\cdot\mathcal{D})(\partial\cdot\xi_\perp)}{\mathcal{D}^2+(n\cdot\mathcal{D})^2}-\frac{v^\mu}{2}(\Delta_\perp\cdot\xi)-n^\mu\delta_{(\mathrm{I})}\lambda, \tag{B1}$$

$$\xi_\perp^\mu \xrightarrow{(\mathrm{II})} \xi_\perp^\mu+\frac{\tilde{\Delta}_\perp^\mu}{2}\left(\frac{(n\cdot\mathcal{D})(\partial\cdot\xi_\perp)}{\mathcal{D}^2+(n\cdot\mathcal{D})^2}-\frac{\mathcal{D}^2-(v\cdot\partial)(n\cdot\mathcal{D})}{\mathcal{D}^2+(n\cdot\mathcal{D})^2}\phi\right)-\frac{v^\mu}{2}(\tilde{\Delta}_\perp\cdot\xi)-n^\mu\delta_{(\mathrm{II})}\lambda, \tag{B2}$$

$$\xi_\perp^\mu \xrightarrow{(\mathrm{III})} \xi_\perp^\mu-\alpha n^\mu\left(\frac{(n\cdot\mathcal{D})(\partial\cdot\xi_\perp)}{\mathcal{D}^2+(n\cdot\mathcal{D})^2}-\frac{\mathcal{D}^2-(v\cdot\partial)(n\cdot\mathcal{D})}{\mathcal{D}^2+(n\cdot\mathcal{D})^2}\phi\right)-n^\mu\delta_{(\mathrm{III})}\lambda. \tag{B3}$$

In the above transformations, we defined the quantities $\delta_{(\Lambda)}\lambda$ for $\Lambda=\{\mathrm{I},\mathrm{II},\mathrm{III}\}$ given by

$$\begin{aligned}\delta_{(\mathrm{I})}\lambda=&\frac{1}{2}\frac{\mathcal{D}^2+2(n\cdot\mathcal{D})^2}{\mathcal{D}^2+(n\cdot\mathcal{D})^2}(\Delta_\perp\cdot\xi_\perp)+\frac{1}{2}\frac{\mathcal{D}^2}{(\mathcal{D}^2+(n\cdot\mathcal{D})^2)^2}(\Delta_\perp\cdot\partial_\perp)(\partial\cdot\xi_\perp)\\&+\frac{1}{2}\left(\frac{(n\cdot\mathcal{D})(\mathcal{D}^2-(v\cdot\partial)(n\cdot\mathcal{D}))}{(\mathcal{D}^2+(n\cdot\mathcal{D})^2)^2}+\frac{v\cdot\partial}{\mathcal{D}^2+(n\cdot\mathcal{D})^2}\right)(\Delta_\perp\cdot\partial)\phi,\end{aligned} \tag{B4}$$

$$\begin{aligned}\delta_{(\mathrm{II})}\lambda=&\frac{1}{2}\frac{\mathcal{D}^2}{\mathcal{D}^2+(n\cdot\mathcal{D})^2}(\tilde{\Delta}_\perp\cdot\xi_\perp)-\frac{1}{2}\frac{\mathcal{D}^2}{(\mathcal{D}^2+(n\cdot\mathcal{D})^2)^2}(\tilde{\Delta}_\perp\cdot\partial_\perp)(\partial\cdot\xi_\perp)\\&-\frac{1}{2}\left(\frac{(n\cdot\mathcal{D})(\mathcal{D}^2-(v\cdot\partial)(n\cdot\mathcal{D}))}{(\mathcal{D}^2+(n\cdot\mathcal{D})^2)^2}+\frac{v\cdot\partial}{\mathcal{D}^2+(n\cdot\mathcal{D})^2}\right)(\tilde{\Delta}_\perp\cdot\partial)\phi,\end{aligned} \tag{B5}$$

$$\begin{aligned}\delta_{(\mathrm{III})}\lambda=&-\alpha\left(\frac{n\cdot\mathcal{D}}{\mathcal{D}^2+(n\cdot\mathcal{D})^2}(\partial\cdot\xi_\perp)-\frac{\mathcal{D}^2-(v\cdot\partial)(n\cdot\mathcal{D})}{\mathcal{D}^2+(n\cdot\mathcal{D})^2}\phi\right)+\alpha\frac{\mathcal{D}^2(u\cdot\mathcal{D})}{(\mathcal{D}^2+(n\cdot\mathcal{D})^2)^2}(\partial\cdot\xi_\perp)\\&+\alpha\left(\frac{(u\cdot\mathcal{D})(n\cdot\mathcal{D})(\mathcal{D}^2-(v\cdot\partial)(n\cdot\mathcal{D}))}{(\mathcal{D}^2+(n\cdot\mathcal{D})^2)^2}-\frac{\mathcal{D}^2-(v\cdot\partial)(u\cdot\mathcal{D})}{\mathcal{D}^2+(n\cdot\mathcal{D})^2}\right)\phi,\end{aligned} \tag{B6}$$

which account for the infinitesimal variations of the operators on the equation of motion of $\lambda(x)$ [c.f Eq. (15)]. For the $\phi(x)$ field, only the transformation rule under type (III) needs to be modified,

$$\phi\xrightarrow{(\mathrm{III})}(1-\alpha)\phi-\alpha\left(\frac{n\cdot\mathcal{D}}{\mathcal{D}^2+(n\cdot\mathcal{D})^2}(\partial\cdot\xi_\perp)-\frac{\mathcal{D}^2-(v\cdot\partial)(n\cdot\mathcal{D})}{\mathcal{D}^2+(n\cdot\mathcal{D})^2}\phi\right). \tag{B7}$$

Remarkably, using Eqs. (B1)–(B3) and the corresponding transformations for the $\phi(x)$ field, one can show that the Lagrangian of Eq. (16), obtained after integrating out the hard field $\lambda(x)$, is RI invariant. Finally, let us conclude by writing down the general transformations for the locally redefined field of Eq. (20), they read

$$\begin{aligned}\tau_\perp^\mu\xrightarrow{(\mathrm{I})}\tau_\perp^\mu&-\frac{\partial_\perp^\mu}{2(u\cdot\mathcal{D})}(\Delta_\perp\cdot\tau_\perp)-\frac{\Delta_\perp^\mu}{2}\frac{n\cdot\mathcal{D}}{\mathcal{D}^2+(n\cdot\mathcal{D})^2}(\partial\cdot\tau_\perp)-\frac{v^\mu}{2}(\Delta_\perp\cdot\tau_\perp)\\&-\frac{n^\mu}{2}\left(\frac{\mathcal{D}^2+2(n\cdot\mathcal{D})^2}{\mathcal{D}^2+(n\cdot\mathcal{D})^2}(\Delta_\perp\cdot\tau_\perp)+\frac{\mathcal{D}^2}{(\mathcal{D}^2+(n\cdot\mathcal{D})^2)^2}(\Delta_\perp\cdot\partial)(\partial\cdot\tau_\perp)\right),\end{aligned} \tag{B8}$$

$$\tau_\perp^\mu \xrightarrow{\text{(II)}} \tau_\perp^\mu - \frac{\partial_\perp^\mu}{2(u\cdot\mathcal{D})}(\tilde{\Delta}_\perp\cdot\tau_\perp) + \frac{\tilde{\Delta}_\perp^\mu}{2}\frac{n\cdot\mathcal{D}}{\mathcal{D}^2+(n\cdot\mathcal{D})^2}(\partial\cdot\tau_\perp) - \frac{v^\mu}{2}(\tilde{\Delta}_\perp\cdot\tau_\perp),$$
$$-\frac{n^\mu}{2}\left(\frac{\mathcal{D}^2}{\mathcal{D}^2+(n\cdot\mathcal{D})^2}(\tilde{\Delta}_\perp\cdot\tau_\perp) - \frac{\mathcal{D}^2}{(\mathcal{D}^2+(n\cdot\mathcal{D})^2)^2}(\tilde{\Delta}_\perp\cdot\partial)(\partial\cdot\tau_\perp)\right), \tag{B9}$$

$$\tau_\perp^\mu \xrightarrow{\text{(III)}} \tau_\perp^\mu + \alpha\frac{\partial_\perp^\mu}{u\cdot\mathcal{D}}\frac{n\cdot\mathcal{D}}{\mathcal{D}^2+(n\cdot\mathcal{D})^2}(\partial\cdot\tau_\perp) + \alpha n^\mu\frac{\mathcal{D}^2(u\cdot\mathcal{D})}{(\mathcal{D}^2+(n\cdot\mathcal{D})^2)^2}(\partial\cdot\tau_\perp). \tag{B10}$$

[1] A. V. Manohar, Lect. Notes Phys. **479**, 311 (1997).
[2] A. V. Manohar, Introduction to effective field theories, in *Effective Field Theory in Particle Physics and Cosmology: Lecture Notes of the Les Houches Summer School*, edited by Sacha Davidson *et al.* (Oxford Academic, Oxford, 2020), Vol. 108.
[3] T. Becher, A. Broggio, and A. Ferroglia, Lect. Notes Phys. **896**, 1 (2015).
[4] C. Manuel and J. M. Torres-Rincon, Phys. Rev. D **90**, 076007 (2014).
[5] C. Manuel, J. Soto, and S. Stetina, Phys. Rev. D **94**, 025017 (2016); **96**, 129901(E) (2017).
[6] C. Manuel, J. Soto, and S. Stetina, EPJ Web Conf. **137**, 07014 (2017).
[7] S. Carignano, C. Manuel, and J. M. Torres-Rincon, Phys. Rev. D **98**, 076005 (2018).
[8] S. Carignano, C. Manuel, and J. M. Torres-Rincon, Phys. Rev. D **102**, 016003 (2020).
[9] C. Manuel and J. M. Torres-Rincon, Phys. Rev. D **103**, 096022 (2021).
[10] M. Comadran and C. Manuel, Phys. Rev. D **104**, 076006 (2021).
[11] J. D. Jackson, *Classical Electrodynamics* (John Wiley and Sons, New York, 1999).
[12] W. J. Cocke and D. A. Holm, Nature (London), Phys. Sci. **240**, 161 (1972).
[13] D. Han, Y. S. Kim, and M. E. Noz, Phys. Rev. E **56**, 6065 (1997).
[14] J. Y. Chen, D. T. Son, M. A. Stephanov, H. U. Yee, and Y. Yin, Phys. Rev. Lett. **113**, 182302 (2014).
[15] J. Y. Chen, D. T. Son, and M. A. Stephanov, Phys. Rev. Lett. **115**, 021601 (2015).
[16] M. Stone, V. Dwivedi, and T. Zhou, Phys. Rev. Lett. **114**, 210402 (2015).
[17] R. Haag, Phys. Rev. **112**, 669 (1958).
[18] S. R. Coleman, J. Wess, and B. Zumino, Phys. Rev. **177**, 2239 (1969).
[19] M. Beneke and T. Feldmann, Phys. Lett. B **553**, 267 (2003).
[20] M. E. Luke and A. V. Manohar, Phys. Lett. B **286**, 348 (1992).
[21] A. V. Manohar, T. Mehen, D. Pirjol, and I. W. Stewart, Phys. Lett. B **539**, 59 (2002).
[22] J. I. Kapusta and C. Gale, *Finite-Temperature Field Theory: Principles and Applications* (Cambridge University Press, Cambridge, England, 2011), ISBN 978-0-521-17322-3, 978-0-521-82082-0, 978-0-511-22280-1.
[23] M. L. Bellac, *Thermal Field Theory* (Cambridge University Press, Cambridge, England, 2011), ISBN 978-0-511-88506-8, 978-0-521-65477-7.
[24] M. Laine and A. Vuorinen, Lect. Notes Phys. **925**, 1 (2016).
[25] J. Ghiglieri, A. Kurkela, M. Strickland, and A. Vuorinen, Phys. Rep. **880**, 1 (2020).
[26] M. G. Mustafa, Eur. Phys. J. Special Topics **232**, 1369 (2023).
[27] S. Lin, Phys. Rev. D **105**, 076017 (2022).
[28] R. J. Furnstahl, H. W. Hammer, and N. Tirfessa, Nucl. Phys. **A689**, 846 (2001).
[29] D. Vasak, M. Gyulassy, and H. T. Elze, Ann. Phys. (N.Y.) **173**, 462 (1987).
[30] K. Hattori, Y. Hidaka, N. Yamamoto, and D. L. Yang, J. High Energy Phys. 02 (2021) 001.
[31] X. G. Huang, P. Mitkin, A. V. Sadofyev, and E. Speranza, J. High Energy Phys. 10 (2020) 117.
[32] X. G. Huang and A. V. Sadofyev, J. High Energy Phys. 03 (2019) 084.
[33] M. Beneke and C. Fidler, Phys. Rev. D **82**, 063509 (2010).

4 Photon quantum kinetic equations and collective modes in an axion background

In this section one can find the publication [27].

Photon quantum kinetic equations and collective modes in an axion background

Marc Comadran[1,2,3,*] and Cristina Manuel[1,2,†]

[1]Instituto de Ciencias del Espacio (ICE, CSIC), C. Can Magrans s.n., 08193 Cerdanyola del Vallès, Spain
[2]Institut d'Estudis Espacials de Catalunya (IEEC), Ed. RDIT, Campus UPC, 08860 Castelldefels, Barcelona, Spain
[3]Departament de Física Quàntica i Astrofísica and Institut de Ciències del Cosmos, Universitat de Barcelona (IEEC-UB), Martí i Franqués 1, 08028 Barcelona, Spain

(Received 2 March 2024; accepted 8 April 2024; published 2 May 2024)

We develop a quantum kinetic theory for photons in the presence of an axion background and in the collisioness limit. In deriving the classical regime of our quantum kinetic equations, we observe that they capture well-known features of axion electrodynamics. By projecting the Wigner function onto a polarization basis, relating the Wigner matrix function with the Stokes parameters, we establish the dispersion relations and transport equations for each polarization space component. Additionally, we investigate how the axion background affects the dispersion relations of photon collective modes within an electron-positron plasma at equilibrium temperature T. While the plasmon remains unaffected, we find that the axion background breaks the degeneracy of transverse collective modes at order $eg_{a\gamma}T(\partial a)$, where e represents the electron charge, $g_{a\gamma}$ denotes the photon-axion coupling, and ∂a represents the scale associated with variations in the axion field.

DOI: 10.1103/PhysRevD.109.096003

I. INTRODUCTION

The exploration of axion electrodynamics holds interest in various domains of physics. Originally conceived within the realm of high-energy physics to address the so called CP problem of QCD [1–4], the term axion is nowadays more generically used to refer to a broader class of light pseudoscalar particles, regardless or not they are related to QCD. Axions naturally manifest in extensions of the Standard Model of particle physics, thus deserving serious consideration as potential candidates for dark matter. There are several intense experimental programs to search for these elusive particles, both in the laboratory an in astrophysical scenarios (see, for example, [5,6], and references therein). Concurrently, analogous axion-photon couplings manifest in certain condensed matter systems [7], giving account of topological magnetoelectric phenomena.

In this article we will consider photon properties in a plasma when there is also an axion background. A plasma is typically characterized by either a temperature T and/or chemical potential μ. We will consider that the axion wavelength is much greater than any of these scales T, μ which describe the medium. The interactions between axions and photons are described by the Lagrangian,

$$\mathcal{L}_{\text{int}} = \frac{1}{4} g_{a\gamma} a F_{\mu\nu} \tilde{F}^{\mu\nu}. \tag{1}$$

Here $\tilde{F}^{\mu\nu} = \frac{1}{2}\epsilon^{\mu\nu\alpha\beta}F_{\alpha\beta}$ is the dual of the electromagnetic tensor $F^{\mu\nu} = \partial^\mu A^\nu - \partial^\nu A^\mu$, being $\epsilon^{\mu\nu\rho\sigma}$ the Levi-Civita tensor, the fields $A^\mu(x)$ and $a(x)$ are associated to photons and axions respectively, and $g_{a\gamma}$ is the axion-photon coupling [6]. This coupling suggests that an axion background acts as an effective chiral medium. There has been a renewed interest in the last decade on chiral media, with the discovery of a variety of new quantum chiral transport phenomena [8], such as the chiral magnetic effect. A clear parallelism among axion electrodynamics and chiral media has been stressed [9].

Quantum field theory methods have been developed for the study of relativistic plasmas [10]. It is by now well-understood that the particle fields of different energy scales have to be treated differently (see, for example [11]). Effective field theories have been designed for that purpose. For momenta scales of the order of the temperature T or higher, the photons are treated as quasiparticles, which are more efficiently described with transport equations. For momenta much lower than the temperature T the photon

*mcomadca60@alumnes.ub.edu
†cmanuel@ice.csic.es

fields are then described as classical background fields, whose properties are then modified by the medium. Collective modes then emerge for those scales, with the appearance of the so called plasmon mode [12,13], which is absent in vacuum.

The purpose of this article is to study how an axion background modifies both the photon transport equation and also the collective modes of a thermal plasma. We will assume that the time and spatial scales of variation of the axion are much less than the photon momentum. While our study would be valid for astrophysical and cosmological plasmas, it can be also of used for other condensed matter systems. We will use well-established quantum field theory methods to study these two effects. Similar photon transport equations have been derived [14,15]. We will comment later on differences with Ref. [14], while in Ref. [15] the axions are considered as quasiparticles and not as a background. Therefore, there the axions interact with the photons through the collision term, allowing for the conversion of axions into photons in the background of a magnetic field, as those commonly found in astrophysical plasmas. In this work, we ignore these processes, while they could be easily incorporated by including a proper collision term to our transport equations.

The paper is structured as follows. In Sec. II we derive quantum kinetic equations for photons in the presence of an axion background using the Keldysh-Schiwgner formalism and in Sec. III we address the effect of the axion background onto the collective modes of photons. Finally in Sec. IV we discuss our findings and make contact with other approaches found in the literature. We also give some details on the derivation of the kinetic equations in Appendix A. Appendix B is devoted to provide the transport equations in a linear polarization basis.

Let us establish our notations and conventions. We use the signature $\mathrm{diag}(g^{\mu\nu}) = (1, -1, -1, -1)$, and the normalization $\epsilon^{0123} = -\epsilon_{0123} = 1$ for the Levi-Civita tensor. Rising or lowering spatial indices produces a minus sign e.g. if $A^\mu = (A^0, A^i)$ is a vector in Minkowski space, we have $A^i = -A_i$. Boldface letters will be used to denote three-dimensional vectors $A^i = \boldsymbol{A}$. The four gradient is $\partial_\mu = (\partial_0, \partial_i)$, where $\partial_i = \nabla$. The Minkowski product between A^μ and B^μ is defined as $A \cdot B = g_{\mu\nu} A^\mu B^\mu = A^0 B^0 - \boldsymbol{A} \cdot \boldsymbol{B}$. Natural units $\hbar = c = k_B = 1$ are used throughout.

II. QUANTUM KINETIC EQUATIONS FOR PHOTONS IN AN AXION BACKGROUND

The Keldysh-Schwinger formulation of quantum field theory has become a well-established tool to study relativistic plasmas, whether they are at or far to thermal equilibrium [16]. In the Keldysh-Schwigner formalism, nonequilibrium Green functions are defined as 2×2 matrix in the complex, closed time path contour, see e.g. Ref. [17] for a recent review. In the case of photons one defines,

$$\boldsymbol{G}^{\mu\nu}(x, y) = \begin{pmatrix} G^{c,\mu\nu}(x, y) & G^{<,\mu\nu}(x, y) \\ G^{>,\mu\nu}(x, y) & G^{a,\mu\nu}(x, y) \end{pmatrix} = \begin{pmatrix} \langle \mathcal{T} A^\mu(x) A^\nu(y) \rangle & \langle A^\nu(y) A^\mu(x) \rangle \\ \langle A^\mu(x) A^\nu(y) \rangle & \langle \tilde{\mathcal{T}} A^\mu(x) A^\nu(y) \rangle \end{pmatrix}, \tag{2}$$

where $\mathcal{T}$ and $\tilde{\mathcal{T}}$ denote time and anti-time ordering along the complex path, respectively, and $\langle \ldots \rangle$ stands for average over an ensemble of states. In order to derive kinetic equations it is sufficient to study the dynamics of the lesser (or greater) component of the Green function $G^{<,\mu\nu}(x, y)$ (or $G^{>,\mu\nu}(x, y)$), as this is related to the photon phase space density after a Wigner transformation.

A relevant problem that emerges in the present formulation is that the components of the Green function in Eq. (2) are not gauge invariant quantities, and they contain nontransverse degrees of freedom. There are various ways to circumvent this inconvenience, the usual prescription is to impose gauge-fixing conditions, although there are other approaches, such as defining a gauge-invariant two-point Green function [18]. In a forthcoming publication, we will explore alternative possibilities by employing effective field theory techniques. In this work, we adopt the former and impose the Lorentz gauge $\partial^\mu A_\mu = 0$, which leads to the following gauge conditions for the lesser component of the Green function:

$$\partial_{x,\mu} G^{<,\mu\nu}(x, y) = 0, \tag{3a}$$

$$\partial_{y,\nu} G^{<,\mu\nu}(x, y) = 0. \tag{3b}$$

The equations of motion obeyed by each component of the Green function can be deduced from the Kadanoff-Baym equations [19]. In the collisionless limit and allowing photons to interact with the axion background through the coupling in Eq. (1), the Kadanoff-Baym equations take the simple form,

$$(g_{\mu\lambda} \Box - g_{a\gamma} \epsilon_{\mu\lambda\alpha\beta} (\partial^\alpha a) \partial^\beta)_x G^{<,\mu\nu}(x, y) = 0, \tag{4a}$$

$$(g_{\mu\nu} \Box - g_{a\gamma} \epsilon_{\mu\nu\alpha\beta} (\partial^\alpha a) \partial^\beta)_y G^{<,\lambda\mu}(x, y) = 0. \tag{4b}$$

Where $\Box = \partial^\mu \partial_\mu$ and the suffix $(\ldots)_x$ indicates that all operators act on the coordinate x^μ. The second equation above, in which the operators act on y^μ, is easily obtained by considering the equation of motion obeyed by the greater two-point Green function, renaming $x^\mu \leftrightarrow y^\mu$ and using the property,

$$G^{>,\nu\mu}(y, x) = G^{<,\mu\nu}(x, y). \tag{5}$$

The phase space density, also called Wigner function, is defined as the Wigner transform of the Green function,

$$G^{<,\mu\nu}(X,q) = \int d^4 s e^{iq\cdot s} G^{<,\mu\nu}(X+s/2, X-s/2), \quad (6)$$

where $X^\mu = (x^\mu + y^\mu)/2$ and $s^\mu = x^\mu - y^\mu$ are the center and relative coordinates, respectively. Let us recall, as said in the introduction, that we assume that $|\partial_\mu a|/|a| \ll q_\mu$. Adding and subtracting the Wigner transformed equations of motion of Eqs. (4a) and (4b) one finds the collisionless equations,

$$\left(q^2 - \frac{\partial^2}{4}\right) G^{\mu\nu} + \frac{g_{a\gamma}}{2}\left(\epsilon^{\mu\rho\alpha\beta} A_{\alpha\beta} G_\rho{}^\nu + \epsilon^{\nu\rho\alpha\beta} A^*_{\alpha\beta} G^\mu{}_\rho\right) = 0, \quad (7a)$$

$$(iq\cdot\partial) G^{\mu\nu} + \frac{g_{a\gamma}}{2}\left(\epsilon^{\mu\rho\alpha\beta} A_{\alpha\beta} G_\rho{}^\nu - \epsilon^{\nu\rho\alpha\beta} A^*_{\alpha\beta} G^\mu{}_\rho\right) = 0, \quad (7b)$$

which have to be complemented with the Wigner-transformed gauge conditions of Eqs. (3a) and (3b)

$$\left(\frac{1}{2}\partial_\mu - iq_\mu\right) G^{\mu\nu} = \left(\frac{1}{2}\partial_\mu + iq_\mu\right) G^{\nu\mu} = 0, \quad (8)$$

and the additional condition, necessary to eliminate the residual ambiguity of the Lorentz gauge,

$$u_\mu G^{\mu\nu} = u_\mu G^{\nu\mu} = 0, \quad (9)$$

where u^μ is a time-like vector representing the velocity of the reference frame, satisfying $u^2 = 1$. When writing the above equations, we used the notation $\partial^\mu = \partial/\partial X_\mu$ and dropped the lesser symbol and the arguments of the Wigner function to enlighten the notation, $G^{\mu\nu} = G^{<,\mu\nu}(X,q)$. Additionally, we establish

$$A_{\alpha\beta} G_\rho{}^\nu \equiv \sum_{n=0}^{\infty} \frac{(-i\Delta)^n}{n!} \partial_\alpha a(X) \left(\frac{1}{2}\partial_\beta - iq_\beta\right) G_\rho{}^\nu(X,q), \quad (10)$$

being $\Delta = \frac{1}{2}\frac{\partial}{\partial q}\cdot\frac{\partial}{\partial X}$. For details regarding the derivation of the kinetic equations, we refer to Appendix A. In the absence of an axion background, we reproduce the photon quantum kinetic equations found in Refs. [20–22]. The Keldysh-Schwinger formalism could also be used to reproduce the collision term in the photon transport equation. We will not add a collision term in this reference, but refer to [15] for that purpose.

A. Classical transport equation in the polarization basis

It is convenient to obtain the classical limit of the photon transport equations, which are easier to handle and are enough to study the physics at large scales. For that purpose, one should carry out a gradient expansion, assuming that variations of the Wigner function on the scale associated to the center coordinate are much less than those on the relative coordinate i.e. $\partial_X^\mu \ll \partial_s^\mu$. That this corresponds to a classical limit can be seen by going to momentum space in the relative coordinate and restoring $\hbar$, as one then assumes $\hbar\partial_X^\mu \ll q^\mu$ when performing the gradient expansion. In a thermal plasma, as most photons have momenta of the order of the temperature T, this simply implies to look for variations at scales larger than the inverse of the temperature. Thus, we perform a gradient expansion of Eqs. (7a) and (7b) and the Wigner function,

$$G^{\mu\nu}(X,q) = G^{\mu\nu}_{(0)}(X,q) + G^{\mu\nu}_{(1)}(X,q) + \mathcal{O}(\partial_X^2), \quad (11)$$

where $G^{\mu\nu}_{(0)}(X,q)$ should be understood as the classical limit of the Wigner function, while higher-order terms in the gradient expansion correspond to the quantum corrections. As we will only consider the classical limit in this work, we drop the subindex (0), and understand that we only keep the $G^{\mu\nu}_{(0)}$ in the expansion. In the classical limit the kinetic equations read,

$$q^2 G^{\mu\nu} - \frac{ig_{a\gamma}}{2}(\partial_\alpha a) q_\beta \left(\epsilon^{\mu\rho\alpha\beta} G_\rho{}^\nu - \epsilon^{\nu\rho\alpha\beta} G^\mu{}_\rho\right) = 0, \quad (12a)$$

$$(iq\cdot\partial) G^{\mu\nu} - \frac{ig_{a\gamma}}{2}(\partial_\alpha a) q_\beta \left(\epsilon^{\mu\rho\alpha\beta} G_\rho{}^\nu + \epsilon^{\nu\rho\alpha\beta} G^\mu{}_\rho\right) = 0, \quad (12b)$$

and the classical Wigner function is constrained by

$$q_\mu G^{\mu\nu} = q_\mu G^{\nu\mu} = u_\mu G^{\mu\nu} = u_\mu G^{\nu\mu}. \quad (13)$$

After imposing the condition that the Wigner function is orthogonal to u^μ, the resulting framework is essentially identical to adopting the Coulomb gauge [20]. Yet another way to eliminate the residual gauge ambiguity of the Lorentz gauge is to project the Wigner function into the physical space, using transverse projectors [23].

It is convenient to write the transport equation in a polarization basis. If we introduce a two dimensional basis of polarization vectors (e.g. ϵ_a^μ with $a = \{1,2\}$) satisfying, $\epsilon_a^* \cdot \epsilon_b = \delta_{ab}$, and $\epsilon_a \cdot u = \epsilon_a \cdot q = 0$, then the Wigner function can be expressed as

$$G^{\mu\nu}(X,q) = \sum_{a,b=1,2} \epsilon_a^{*\mu} \epsilon_b^\nu G^{ab}(X,q). \quad (14)$$

Projecting Eqs. (12a) and (12b) onto the polarization basis we easily obtain the kinetic equations obeyed by the polarization space components of the Wigner function,

$$q^2 G^{ab} - \frac{ig_{a\gamma}}{2}\epsilon_{\mu\nu\alpha\beta}(\partial^\alpha a) q^\beta \left(\epsilon_c^{*\mu}\epsilon_a^\nu G^{cb} - \epsilon_c^\mu \epsilon_b^{*\nu} G^{ac}\right) = 0, \quad (15a)$$

$$(iq\cdot\partial) G^{ab} - \frac{ig_{a\gamma}}{2}\epsilon_{\mu\nu\alpha\beta}(\partial^\alpha a) q^\beta \left(\epsilon_c^{*\mu}\epsilon_a^\nu G^{cb} + \epsilon_c^\mu \epsilon_b^{*\nu} G^{ac}\right) = 0, \quad (15b)$$

where summation over repeated indices should be understood. It is simpler to solve the transport equations in a circular polarization basis, since the polarization space components of the Wigner function then decouple. Explicitly, we introduce the polarization basis vectors $\epsilon_a^\mu = \{\epsilon_+^\mu, \epsilon_-^\mu\}$, characterized by the properties,

$$\epsilon_\pm^* \cdot \epsilon_\pm = 0, \qquad \epsilon_\pm^* \cdot \epsilon_\mp = 1, \qquad (\epsilon_\pm^\mu)^* = \epsilon_\mp^\mu. \tag{16}$$

Let us elaborate on the physical interpretation of the Wigner function components in the circular polarization basis. Since $G^{\mu\nu}$ is invariant under basis rotations, i.e. $\epsilon_\pm^{\mu'} \to e^{\pm i\theta}\epsilon_\pm^\mu$, the polarization space components of the Wigner function transform as [23]

$$G^{\pm\pm'} \to G^{\pm\pm}, \qquad G^{\pm\mp'} \to e^{\pm 2i\theta} G^{\pm\mp}, \tag{17}$$

which reveals that $G^{\pm\pm}$ and $G^{\pm\mp}$ have null ($s = 0$) and integer ($s = \pm 2$) spin, respectively. Moreover, the polarization space components of the Wigner function can be directly related to the Stokes parameters [24], their relation in the circular basis is

$$G^{ab} = \begin{pmatrix} G^{++} & G^{+-} \\ G^{-+} & G^{--} \end{pmatrix} = \begin{pmatrix} G^I - G^V & G^Q - iG^U \\ G^Q + iG^U & G^I + G^V \end{pmatrix}. \tag{18}$$

Hence, the diagonal components of the Wigner function $G^{\pm\pm}$ relate to the intensity G^I and degree of circular polarization G^V of the photon ensemble, while the off-diagonal components $G^{\pm\mp}$, decomposed into the Stokes parameters G^Q and G^U, give information on the polarization phases and are related to the so called E and B polarization modes [23].

The kinetic equations for each polarization space component of the Wigner function in the circular basis can be simplified after using the identity [25],

$$i(\epsilon_-^{*\mu}\epsilon_-^\nu - \epsilon_+^{*\mu}\epsilon_+^\nu) = \frac{1}{\kappa}\epsilon^{\mu\nu\alpha\beta}u_\beta q_\alpha, \tag{19}$$

where we defined $\kappa = \sqrt{(u\cdot q)^2 - q^2}$. Hence, for the diagonal components G^{++} and G^{--}, corresponding to right- and left-handed circularly polarized photons respectively, we find

$$\left(q^2 \pm \frac{g_{a\gamma}}{\kappa}[(q\cdot\partial a)(u\cdot q) - q^2(u\cdot\partial a)]\right)G^{\pm\pm} = 0, \tag{20a}$$

$$iq\cdot\partial G^{\pm\pm} = 0. \tag{20b}$$

As for the off-diagonal components G^{+-} and G^{-+}, reflecting the correlation of different polarization in the photon ensemble, we get

$$q^2 G^{\pm\mp} = 0, \tag{21a}$$

$$\left(iq\cdot\partial \pm \frac{g_{a\gamma}}{\kappa}[(q\cdot\partial a)(u\cdot q) - q^2(u\cdot\partial a)]\right)G^{\pm\mp} = 0. \tag{21b}$$

The form of Eqs. (20a) and (21a) suggest that the general structure of the Wigner function is

$$G^{ab}(X,q) = 4\pi\delta(Q_{ab}^2)\mathrm{sgn}(u\cdot q)f^{ab}(X,q), \tag{22}$$

where $a, b = +, -$ and $\mathrm{sgn}(x)$ is the sign function, the quantities Q_{ab}^2 govern the dispersion relations and $f^{ab}(X,q)$ are the off shell distribution functions for each polarization space component of the Wigner function. The transport equations obeyed by the on-shell distribution functions are derived finding the dispersion relations and imposing the resulting on shell conditions. Let us show how this is realized in the rest frame of the medium $u^\mu = (1, \mathbf{0})$.
In this frame, the dispersion relations are obtained as solutions to the equations,

$$Q_{\pm\pm}^2 = \omega^2 - |\boldsymbol{q}|^2 \pm g_{a\gamma}[|\boldsymbol{q}|\partial_0 a + \omega(\hat{\boldsymbol{q}}\cdot\nabla a)] = 0, \tag{23a}$$

$$Q_{\pm\mp}^2 = \omega^2 - |\boldsymbol{q}|^2 = 0, \tag{23b}$$

and the transport equations read,

$$(i\omega\partial_0 + i\boldsymbol{q}\cdot\nabla)G^{\pm\pm} = 0, \tag{24a}$$

$$(i\omega\partial_0 + i\boldsymbol{q}\cdot\nabla \pm g_{a\gamma}[|\boldsymbol{q}|\partial_0 a + \omega(\hat{\boldsymbol{q}}\cdot\nabla a)])G^{\pm\mp} = 0, \tag{24b}$$

where we used the notation $q^\mu = (\omega, \boldsymbol{q})$ for the photon momentum and defined $\hat{\boldsymbol{q}} = \boldsymbol{q}/|\boldsymbol{q}|$. Then, we see that the presence of the axion induces a different dispersion relation for the diagonal components of the Wigner function G^{++} and G^{--}, while both off-diagonal components G^{+-} and G^{-+} obey a free dispersion relation, unaffected by the axion. Explicitly, solving Eqs. (23a) and (23b) we find the following dispersion relations:

$$\omega_{\pm\pm}(\boldsymbol{q}) \approx |\boldsymbol{q}| \mp \frac{1}{2}g_{a\gamma}(\partial_0 a + \hat{\boldsymbol{q}}\cdot\nabla a), \tag{25a}$$

$$\omega_{\pm\mp}(\boldsymbol{q}) = |\boldsymbol{q}|. \tag{25b}$$

The first equation above coincides with the result first found by Harari and Sikivie [26], note that we approximated $\omega_{\pm\pm}(\boldsymbol{q})$ at linear order in $g_{a\gamma}$. There are also negative energy solutions,

$$\tilde{\omega}_{\pm\pm}(\boldsymbol{q}) \approx -|\boldsymbol{q}| \pm \frac{1}{2}g_{a\gamma}(\partial_0 a - \hat{\boldsymbol{q}}\cdot\nabla a), \tag{26a}$$

$$\tilde{\omega}_{\pm\mp}(\boldsymbol{q}) = -|\boldsymbol{q}|. \tag{26b}$$

Imposing the on shell conditions dictated by Eqs. (25a) and (25b) onto Eqs. (24a) and (24b) respectively leads to the transport equations obeyed by the on-shell distribution functions, that we formally define as

$$f^{\pm\pm}(X,\boldsymbol{q}) = f^{\pm\pm}(X,q)|_{q_0=\omega_{\pm\pm}(\boldsymbol{q})}, \tag{27a}$$

$$f^{\pm\mp}(X,\boldsymbol{q}) = f^{\pm\mp}(X,q)|_{q_0=|\boldsymbol{q}|}, \tag{27b}$$

for the positive energy solutions. Thus, at first order in the gradient expansion and at linear order in $g_{a\gamma}$ we find,

$$(i\partial_0 + i\hat{\boldsymbol{q}}\cdot\nabla)f^{\pm\pm}(X,\boldsymbol{q}) = 0, \tag{28a}$$

$$(i\partial_0 + i\hat{\boldsymbol{q}}\cdot\nabla \pm g_{a\gamma}(\partial_0 a + \hat{\boldsymbol{q}}\cdot\nabla a))f^{\pm\mp}(X,\boldsymbol{q}) = 0. \tag{28b}$$

Please note that the effective velocity appearing in Eq. (28a) is $\boldsymbol{v}_{\mathrm{eff}} = \hat{\boldsymbol{q}} + \mathcal{O}(\partial_X)$, which consistently ignores the effects of the axion, as it would enter as quantum effect, at second order in the gradient expansion. Similar distribution functions and transport equations can be defined for the negative energy solutions.

The conditions we assumed in this work are equivalent to those carried out in the so called eikonal approximation [27]. It has been argued that in the eikonal approximation there is no chiral bending of light in the presence of an axion background in vacuum [27], as the index of refraction of both left- and right-handed waves is one in this approximation. Please note that in this gradient expansion we found that the dispersion law of the right-/left-handed photons might be also written down as $(q \pm \frac{g_{a\gamma}}{2}\partial a)^2 \approx 0$, so that the photons travel at the speed of light, as also found in [27].

The photon current associated to the polarized photons can be defined as

$$J^{\mu,ab}(X) = (n^{ab}, \boldsymbol{j}^{ab}) = \int \frac{d^4q}{(2\pi)^4} q^\mu G^{ab}(X,q). \tag{29}$$

In a plasma at thermal equilibrium, and in the frame at rest with the medium, the right and left-handed photon distribution function is the Bose-Einstein distribution function $f_{\mathrm{B}}(\omega) = 1/(e^{\omega/T} - 1)$. Then, by direct computation one finds that the difference between equilibrium densities of right- and left-handed photons is proportional to the temporal variation of the axion field,

$$n^{++} - n^{--} = \frac{g_{a\gamma}T^2}{3}\partial_0 a + \mathcal{O}(g_{a\gamma}^2). \tag{30}$$

Similarly, one finds

$$\boldsymbol{j}^{++} - \boldsymbol{j}^{--} = \frac{g_{a\gamma}T^2}{9}\nabla a + \mathcal{O}(g_{a\gamma}^2), \tag{31}$$

such that the spatial gradient of the axion field induces a difference in the right- and left-handed photon currents. On the other hand, from Eq. (28b) we see that the axion induces a rotation on the E and B modes, if there are such polarizations modes. If $X_0^\mu = (t_0, \boldsymbol{X}_0)$ denotes an initial coordinate, then one finds that at a final state $X_f^\mu = (t_f, \boldsymbol{X}_f)$,

$$f^{\pm\mp}(X_f,\boldsymbol{q}) = f^{\pm\mp}(X_0,\boldsymbol{q})\exp\{\mp i g_{a\gamma}[a(X_f) - a(X_0)]\}. \tag{32}$$

As these components have spin 2, the angle of rotation of these modes is $g_{a\gamma}(\Delta a)/2$. This accounts for the rotation of the polarization vector first discussed in [28,29]. In particular, if the initial configuration only contains E polarization modes, the axion background induces the appearance of B-modes. This is an effect that has also already been discussed in the literature [30,31], and that our transport equation properly encodes.

III. COLLECTIVE MODES OF PHOTONS IN AN AXION BACKGROUND

The momentum of most quasiparticles that constitute an electromagnetic plasma is of the order of the equilibrium temperature T and/or the chemical potential μ. Collective modes then emerge as perturbations whose typical momentum, that we denote by Q_μ, is much lesser than those scales, of the order of the Debye mass $Q_\mu \sim m_D \ll T$, μ. In the previous section, we assumed that the variations of the axion field are much less than the momentum of the photons $|\partial_\mu a|/|a| \ll q_\mu \sim T$, μ, which allowed us to treat the axion as a background field and the photons as quasiparticles. We also emphasize that if the variations of the axion field are of the same order of the photon momentum, then axions should also be treated as quasiparticles. The interaction between the collective modes and the axion field has also to be addressed differently according to the hierarchy between their typical scales. We will assume that the variations of the axion field are much less than the momentum of the collective modes $|\partial_\mu a|/|a| \ll Q_\mu \sim m_D$, so that the axion still can be effectively described as a background field.

In the absence of an axion background or any CP violating effect in the medium, there is a transverse collective mode that is degenerate and a longitudinal collective mode, the so called plasmon, which is absent in vacuum. The impact of the axion background on the dispersion relations of collective modes is reflected in the dynamics of the dressed propagator $\hat{G}^{\mu\nu}(x,y)$, whose inverse reads in momentum space,

$$\hat{G}^{-1}_{\mu\nu}(Q) = -Q^2 g_{\mu\nu} + \Pi_{\mu\nu}(Q) + i g_{a\gamma}\epsilon_{\mu\nu\alpha\beta}(\partial^\alpha a)Q^\beta. \tag{33}$$

Within the frame of reference in which the medium is in motion with velocity u^μ, one can establish three independent projectors which are orthogonal to both Q^μ and u^μ as [25]

$$P_T^{\mu\nu} = \tilde{g}^{\mu\nu} - P_L^{\mu\nu}, \;\; P_L^{\mu\nu} = \frac{\tilde{u}^\mu \tilde{u}^\nu}{\tilde{u}^2}, \;\; P_P^{\mu\nu} = \frac{i}{\kappa}\epsilon^{\mu\nu\alpha\beta} Q_\alpha u_\beta, \quad (34)$$

where

$$\tilde{u}^\mu = \tilde{g}^{\mu\nu} u_\nu, \qquad \tilde{g}^{\mu\nu} = g^{\mu\nu} - \frac{Q^\mu Q^\nu}{Q^2}, \quad (35)$$

and κ was given below Eq. (19) (now one should replace $q^\mu \to Q^\mu$). The projectors in Eq. (34) are called transverse, longitudinal, and parity-odd projectors, respectively. They satisfy the properties

$$P_L^2 = 1, \qquad P_T^2 = 2, \qquad P_P^2 = -2,$$
$$P_L^{\mu\nu} P_{T,\mu\nu} = P_L^{\mu\nu} P_{P,\mu\nu} = P_T^{\mu\nu} P_{P,\mu\nu} = 0. \quad (36)$$

As the effect of a parity odd source, either due to the axion background or the medium, is to split the otherwise degenerate right- and left-circular polarization modes of the photon [25], it is convenient to introduce additional right (+) and left (−) projectors,

$$P_h^{\mu\nu} = \frac{1}{2}(P_T^{\mu\nu} + h P_P^{\mu\nu}), \quad h = \pm, \quad (37)$$

in terms of which, the polarization tensor can be decomposed as

$$\Pi^{\mu\nu} = \sum_{h=\pm} P_h^{\mu\nu}(\Pi_T + h\Pi_P) - \frac{Q^2}{\kappa^2} P_L^{\mu\nu} \Pi_L. \quad (38)$$

Note that if $\Pi_P = 0$ one recovers the usual decomposition of the polarization tensor into its transverse and longitudinal component. The inverse of the dressed propagator in Eq. (33) can be decomposed in terms of the projectors $P_+^{\mu\nu}$, $P_-^{\mu\nu}$, and $P_L^{\mu\nu}$ too and then inverted, which gives,

$$\hat{G}^{\mu\nu}(Q) = -\frac{\kappa^2}{Q^2}\frac{P_L^{\mu\nu}}{\kappa^2 + \Pi_L} - \sum_{h=\pm} \frac{P_h^{\mu\nu}}{Q^2 - \Pi_T + h(\Pi_P + \frac{g_{a\gamma}}{\kappa}[(Q\cdot\partial a)(u\cdot Q) - Q^2(u\cdot\partial a)])}. \quad (39)$$

The poles in the dressed propagator above determine the dispersion relations obeyed by the collective modes within the medium. It is worth mentioning that the longitudinal collective mode remains unaffected by the interaction of photons with the axion background. The projectors used to decompose the dressed propagator can be related to the polarization vectors,

$$P_+^{\mu\nu} = -\epsilon_+^{*\mu}\epsilon_+^\nu, \quad P_-^{\mu\nu} = -\epsilon_-^{*\mu}\epsilon_-^\nu, \quad P_L^{\mu\nu} = -\epsilon_L^\mu \epsilon_L^\nu, \quad (40)$$

where we introduced the longitudinal polarization vector as [25]

$$\epsilon_L^\mu = \frac{\tilde{u}^\mu}{\sqrt{-\tilde{u}^2}}. \quad (41)$$

Thus, we may write the dressed propagator in terms of the polarization basis vectors,

$$\hat{G}^{\mu\nu}(Q) = \frac{\kappa^2}{Q^2}\frac{\epsilon_L^\mu \epsilon_L^\nu}{\kappa^2 + \Pi_L} + \sum_{h=\pm} \frac{\epsilon_h^{*\mu}\epsilon_h^\nu}{Q^2 - \Pi_T + h(\Pi_P + \frac{g_{a\gamma}}{\kappa}[(Q\cdot\partial a)(u\cdot Q) - Q^2(u\cdot\partial a)])}. \quad (42)$$

Let us now assume a QED plasma at very high temperature, such that one can neglect the electron mass. The Debye mass is then $m_D^2 = e^2T^2/3$ where e is the electron charge so that the momentum of the collective modes is of order $Q_\mu \sim eT$. The values of the longitudinal Π_L and transverse Π_T polarization tensors components are then well-known, and given by the so called hard thermal loop (HTL) expressions [10]. Certainly, the axion background also affects the polarization tensor through its coupling to electrons. We ignore those contributions here, but they would be required for a more complete analysis. Then, assuming $\Pi_P = 0$ and moving to the rest frame of the plasma $u^\mu = (1, \mathbf{0})$, the dispersion relations associated to the two transverse collective modes are obtained as solutions to the equations,

$$\omega^2 - |\boldsymbol{q}|^2 - \frac{m_D^2\omega^2}{2|\boldsymbol{q}|^2}\left[1 - \left(1 - \frac{|\boldsymbol{q}|^2}{\omega^2}\right)\frac{\omega}{2|\boldsymbol{q}|}\ln\left(\frac{\omega + |\boldsymbol{q}|}{\omega - |\boldsymbol{q}|}\right)\right]$$
$$\pm g_{a\gamma}[|\boldsymbol{q}|\partial_0 a + \omega(\hat{\boldsymbol{q}}\cdot\nabla a)] = 0, \quad (43)$$

where we used the notation $Q^\mu = (\omega, \boldsymbol{q})$. The effect of the axion background then comes in modifications of order $eTg_{a\gamma}\partial a$ to the dispersion laws. While these have to be solved numerically, it is possible to find simple analytical solutions in some cases. For instance, in the long wavelength limit $m_D \gg |\boldsymbol{q}|$ we find the solutions,

$$\omega_\pm^2 \approx \frac{m_D^2}{3} \mp \frac{g_{a\gamma} m_D}{\sqrt{3}} (\hat{\boldsymbol{q}} \cdot \nabla a), \tag{44}$$

implying that right- and left-handed circularly polarized collective modes oscillate with different plasma frequencies, and at this expansion order also different from that of the plasmon mode, which is $\omega_L = m_D/\sqrt{3} \equiv \omega_{\rm pl}$ [10]. On the other hand, in the regime $m_D \ll |\boldsymbol{q}| \ll T$ one finds

$$\omega_\pm^2 \approx |\boldsymbol{q}|^2 + m_D^2 \mp g_{a\gamma}(\partial_0 a + \hat{\boldsymbol{q}} \cdot \nabla a), \tag{45}$$

so that the axion produces a different shift on the effective asymptotic masses for right- and left-handed modes. It is also interesting to study the limit $\omega \ll |\boldsymbol{q}|$, as in this regime, and due to Landau damping, there is an additional family of poles in the transverse modes which are purely imaginary. Let us assume without loss of generality that $\mathfrak{I}(\omega) > 0$ where $\mathfrak{I}$ denotes the imaginary part, then one finds the solutions,

$$\omega_\pm = -i \frac{4|\boldsymbol{q}|^3}{\pi m_D^2} \left(1 \mp \frac{g_{a\gamma} \partial_0 a}{|\boldsymbol{q}|}\right) = -i\gamma_\pm. \tag{46}$$

This has the same form of the chiral instabilities that are found in chiral media characterized by an imbalance in the population of right- and left-handed fermions [32]. In fact, it has the same form, after identifying the chiral chemical potential μ_5 with $g_{a\gamma}\partial_0 a/2\alpha$ [32,33]. The collective modes evolve in time as $\exp(-i\omega_\pm t) \sim \exp(-\gamma_\pm t)$, and they would become unstable if $\gamma_\pm$ becomes negative. As the sign of $\partial_0 a$ can be either positive or negative, this leads to the conditions $\pm g_{a\gamma}\partial_0 a > |\boldsymbol{q}|$, however, in this article we assumed that $|\partial_\mu a|/|a| \ll Q_\mu$, as the axion is treated as a background field. Therefore, taking this assumption into account and due to the smallness of the axion-photon coupling constant $g_{a\gamma}$, we conclude that $\gamma_\pm$ remains positive and there are no unstable modes in this case.

IV. DISCUSSION

We have developed a quantum kinetic theory in the collisionless limit for photons with the presence of an axion background, which is summarized in Eqs. (7)–(9). Performing a gradient expansion of the operators and the Wigner function (or phase-space distribution), we derived their classical limit and projected the resulting equations on a basis of polarization vectors, yielding Eqs. (12) and (13). A considerable advantage of this last projection is that the components of the Wigner function in polarization space can be directly related to the Stokes parameters, thus having a clear physical interpretation. Then, using a circular polarization basis of vectors, we derived the transport equations obeyed by the on shell distribution functions $f^{\pm\pm}$ and $f^{\pm\mp}$ in the rest frame of the medium, given by Eqs. (28a) and (28b) respectively, which is the central result of this article. Those equations properly encode features of axion electrodynamics, such that right- and left-handed circular polarized photons obey different dispersion relations, or the phase rotation of the polarization plane, which have been explored before in the literature.

A similar transport equation for photons in an axion background was derived in Ref. [14], there the authors derived a transport equation for the Stokes parameters in a time-dependent axion background. Our treatment is more general and fully covariant, and allows for the incorporation of different sort of corrections. For the comparison with Ref. [14] see Appendix B.

There are several ways in which our work could be extended, for instance, we could include the effects of collisions of photons with the quasiparticles of the thermal bath or compute quantum corrections to our classical transport equations. Another interesting generalization would be to consider that photons propagate through a nonflat space time, as considered in Ref. [23], as the presence of the axion background could provide new sources of B mode polarization.

We have also addressed the effects of the axion background on the photon collective oscillations within the medium through the photon-axion interaction. As expected, the axion background breaks the degeneracy of right- and left-handed circular polarized collective modes, while the plasmon remains unaffected. The contribution of the axion background is of order $e g_{a\gamma} T(\partial a)$, where ∂a is the scale associated to the variations of the axion field. We also considered limiting cases for the dispersion relations of the transverse collective modes; in the regime $m_D \gg |\boldsymbol{q}|$ the axion produces a shift on the oscillation frequencies of right- and left-handed polarized collective modes, see Eq. (44), while in the regime $m_D \ll |\boldsymbol{q}| \ll T$ the axion modifies their effective asymptotic masses [cf. Eq. (45)].

It has been argued that specific photon modes in chiral media may not propagate and experience instabilities [9]. However, under the considerations of this work, we have shown that if the chiral media consists of an axion background, both right- and left-handed photons are propagating modes, since the assumption that the axion field acts as a background prevents those instabilities to occur. We stress that the situation would change if the axions are considered as quanta, interacting with photons through the Lagrangian of Eq. (1). A similar reasoning and conclusion applies for the collective modes, that we have elaborated in Sec. II.

A relevant scenario, that we have not considered in this work, is when the variations of the axion field are comparable to the momentum scale of the collective modes, as in that case interactions between axions and collective modes can occur, leading to interesting phenomena and possible windows for detection [34–37].

ACKNOWLEDGMENTS

We thank Diego Blas for discussions. This work was supported by Ministerio de Ciencia, Investigación y Universidades (Spain) MCIN/AEI/10.13039/501100011033/FEDER, UE, under Projects No. PID2019–110165 GB-I00 and No. PID2022-139427NB-I00, by Generalitat de Catalunya by the Project No. 2021-SGR-171 (Catalonia). This work was also partly supported by the Spanish program Unidad de Excelencia Maria de Maeztu CEX2020-001058-M, financed by MCIN/AEI/10.13039/501100011033.

APPENDIX A: KINETIC EQUATIONS

In this section we give some details on how to derive the kinetic equations Eqs. (7a) and (7b). We start by defining the Wigner transform of the sum and difference of the equations of motion given by Eqs. (4a) and (4b) as

$$(I_\pm)_{\lambda\nu} = \int d^4 s e^{iq\cdot s}\{(g_{\mu\lambda}\Box - g_{a\gamma}\epsilon_{\mu\lambda\alpha\beta}(\partial^\alpha a)\partial^\beta)_x G^\mu{}_\nu(x,y) \pm (g_{\mu\nu}\Box - g_{a\gamma}\epsilon_{\mu\nu\alpha\beta}(\partial^\alpha a)\partial^\beta)_y G_\lambda{}^\mu(x,y)\}. \tag{A1}$$

Then, we move from configuration space variables x^μ and y^μ to Wigner space variables X^μ and s^μ using the relations

$$X^\mu = \frac{x^\mu + y^\mu}{2}, \qquad s^\mu = x^\mu - y^\mu, \tag{A2a}$$

$$\partial_x^\mu = \frac{1}{2}\partial_X^\mu + \partial_s^\mu, \qquad \partial_y^\mu = \frac{1}{2}\partial_X^\mu - \partial_s^\mu. \tag{A2b}$$

Doing so, we can write

$$(I_\pm)_{\lambda\nu} = \int d^4 s e^{iq\cdot s}\left\{\left[g_{\mu\lambda}\left(\partial_s\cdot\partial_X + \partial_s^2 + \frac{1}{4}\partial_X^2\right) - g_{a\gamma}\epsilon_{\mu\lambda\alpha\beta}A^{\alpha\beta}(X,s)\right]G^\mu{}_\nu(X+s/2, X-s/2) \pm \left[g_{\mu\nu}\left(-\partial_s\cdot\partial_X + \partial_s^2 + \frac{1}{4}\partial_X^2\right) - g_{a\gamma}\epsilon_{\mu\nu\alpha\beta}A^{\alpha\beta}(X,-s)\right]G^\mu{}_\lambda(X+s/2, X-s/2)\right\}. \tag{A3}$$

Where we defined the following operator, acting on the Wigner function,

$$A^{\alpha\beta}(X,s) = \left(\frac{1}{2}\partial_X^\alpha + \partial_s^\alpha\right)a(X+s/2)\left(\frac{1}{2}\partial_X^\beta + \partial_s^\beta\right). \tag{A4}$$

Now we perform a gradient expansion of the axion field,

$$a(X+s/2) = \sum_{n=0}^\infty \frac{1}{n!}\left(\frac{s\cdot\partial_X}{2}\right)^n a(X), \tag{A5}$$

and after the Wigner transformation, we find

$$(I_\pm)_{\lambda\nu} = \left\{\left[g_{\mu\lambda}\left(-iq\cdot\partial_X - q^2 + \frac{1}{4}\partial_X^2\right) - g_{a\gamma}\epsilon_{\mu\lambda\alpha\beta}A^{\alpha\beta}(X,q)\right]G^\mu{}_\nu(X,q) \pm \left[g_{\mu\nu}\left(iq\cdot\partial_X - q^2 + \frac{1}{4}\partial_X^2\right) - g_{a\gamma}\epsilon_{\mu\nu\alpha\beta}A^{*,\alpha\beta}(X,q)\right]G_\lambda{}^\mu(X,q)\right\}, \tag{A6}$$

where now $A^{\alpha\beta}(X,q)$ is given by Eq. (10), in which we neglected the arguments for simplicity. So finally, we find for the dispersion relation,

$$(I_+)_{\lambda\nu} = \left(-2q^2 + \frac{1}{2}\partial_X^2\right)G_{\lambda\nu}(X,q) - g_{a\gamma}\epsilon_{\mu\lambda\alpha\beta}A^{\alpha\beta}(X,q)G^\mu{}_\nu(X,q) - g_{a\gamma}\epsilon_{\mu\nu\alpha\beta}A^{*,\alpha\beta}(X,q)G_\lambda{}^\mu(X,q) = 0. \tag{A7}$$

While for the transport equation,

$$(I_-)_{\lambda\nu} = -2i(q\cdot\partial_X)G_{\lambda\nu}(X,q) - g_{a\gamma}\epsilon_{\mu\lambda\alpha\beta}A^{\alpha\beta}(X,q)G^\mu{}_\nu(X,q) + g_{a\gamma}\epsilon_{\mu\nu\alpha\beta}A^{*,\alpha\beta}(X,q)G_\lambda{}^\mu(X,q) = 0. \tag{A8}$$

Now we divide both Eqs. (A7) and (A8) by a factor of −2, also rising the indices in the Wigner function and the Levi-Civita tensor using the property $\epsilon_{\mu\nu\rho\sigma} = -\epsilon^{\mu\nu\rho\sigma}$ we reach,

$$\left(q^2 - \frac{1}{4}\partial_X^2\right)G^{\lambda\nu} - \frac{g_{a\gamma}}{2}(\epsilon^{\mu\lambda\alpha\beta}A_{\alpha\beta}G_\mu{}^\nu + \epsilon^{\mu\nu\alpha\beta}A^*_{\alpha\beta}G^\lambda{}_\mu) = 0,$$
$$(iq\cdot\partial_X)G^{\lambda\nu} - \frac{g_{a\gamma}}{2}(\epsilon^{\mu\lambda\alpha\beta}A_{\alpha\beta}G_\mu{}^\nu - \epsilon^{\mu\nu\alpha\beta}A^*_{\alpha\beta}G^\lambda{}_\mu) = 0, \tag{A9}$$

which exactly give Eqs. (7a) and (7b) after relabeling some indices and using the antisymmetry property of the Levi-Civita tensor.

APPENDIX B: CLASSICAL TRANSPORT EQUATION IN THE LINEAR-POLARIZATION BASIS

In this section we give the classical kinetic Eqs. (12a) and (12b) in a linear polarization basis and then write them in terms of the Stokes parameters. We start by introducing a linear-polarization basis vectors $\epsilon_a^\mu = \{\epsilon_1^\mu, \epsilon_2^\mu\}$, satisfying $\epsilon_a^*\cdot\epsilon_b = \delta_{ab}$ and $(\epsilon_a^\mu)^* = \epsilon_a^\mu$. The relation between the components of the Wigner function and the Stokes parameters in a linear polarization basis is [24]

$$G^{ab} = \begin{pmatrix} G^{11} & G^{12} \\ G^{21} & G^{22}\end{pmatrix} = \begin{pmatrix} G^I + G^Q & G^U - iG^V \\ G^U + iG^V & G^I - G^Q\end{pmatrix}, \tag{B1}$$

so that, after using the identity

$$\epsilon_1^\mu\epsilon_2^\nu - \epsilon_2^\mu\epsilon_1^\nu = \frac{1}{\kappa}\epsilon^{\mu\nu\alpha\beta}u_\beta q_\alpha, \tag{B2}$$

the dispersion laws for the Stokes parameters may be written as

$$q^2G^I - \frac{g_{a\gamma}}{\kappa}[(q\cdot\partial a)(u\cdot q) - q^2(u\cdot\partial a)]G^V = 0, \tag{B3a}$$

$$q^2G^V - \frac{g_{a\gamma}}{\kappa}[(q\cdot\partial a)(u\cdot q) - q^2(u\cdot\partial a)]G^I = 0, \tag{B3b}$$

$$q^2G^Q = 0, \tag{B3c}$$

$$q^2G^U = 0. \tag{B3d}$$

A problem with this formulation, that was not discussed in Ref. [14] is that the equations for G^I and G^V are coupled, so that they can not be treated individually as propagating modes. Instead, the propagating modes are the combinations $G^I \mp G^V$, corresponding to right- and left-handed photons, respectively, whose dispersion relations can be obtained by solving,

$$\left(q^2 \pm \frac{g_{a\gamma}}{\kappa}[(q\cdot\partial a)(u\cdot q) - q^2(u\cdot\partial a)]\right)(G^I \mp G^V) = 0, \tag{B4}$$

which yields to the solutions of Eqs. (25a) and (26a) in the rest frame. The transport equations in the linear polarization basis read,

$$(q\cdot\partial)(G^I \mp G^V) = 0, \tag{B5a}$$

$$(q\cdot\partial)G^Q + \frac{g_{a\gamma}}{\kappa}[(q\cdot\partial a)(u\cdot q) - q^2(u\cdot\partial a)]G^U = 0, \tag{B5b}$$

$$(q\cdot\partial)G^U - \frac{g_{a\gamma}}{\kappa}[(q\cdot\partial a)(u\cdot q) - q^2(u\cdot\partial a)]G^Q = 0. \tag{B5c}$$

The coupled equations for G^Q and G^U can be solved by applying the operator $(q\cdot\partial)$ on each equation and neglecting terms with two derivatives acting on the axion field. Thus, we find

$$(q\cdot\partial)^2G^Q + \frac{g_{a\gamma}^2}{\kappa^2}[(q\cdot\partial a)(u\cdot q) - q^2(u\cdot\partial a)]^2G^Q = 0, \tag{B6a}$$

$$(q\cdot\partial)^2G^U - \frac{g_{a\gamma}^2}{\kappa^2}[(q\cdot\partial a)(u\cdot q) - q^2(u\cdot\partial a)]^2G^U = 0. \tag{B6b}$$

Now, the general structure of the Stokes parameters is $G^{Q,U}(X,q) = 4\pi\delta(q^2)\mathrm{sgn}(u\cdot q)f^{Q,U}(X,q)$, being $f^{Q,U}(X,q)$ the corresponding off shell distribution functions. Moving to the rest frame and imposing the on-shell condition, we reach to

$$[(v\cdot\partial)^2 + \Omega^2]f^Q(X,\boldsymbol{q}) = 0, \tag{B7a}$$

$$[(v\cdot\partial)^2 - \Omega^2]f^U(X,\boldsymbol{q}) = 0, \tag{B7b}$$

where $f^{Q,U}(X,\boldsymbol{q})$ are the on shell distribution functions for the positive energy solutions, also we introduced the velocity vector $v^\mu = (1,\hat{\boldsymbol{q}})$ and the frequency $\Omega = g_{a\gamma}(v\cdot\partial a)$. Note that Ω coincides with the frequency defined in Ref. [14] when neglecting the gradient of the axion field (there is a difference of a factor of 2 due to our distinct definition of the dual of the electromagnetic tensor $\tilde{F}^{\mu\nu}$).

[1] R. D. Peccei and H. R. Quinn, Phys. Rev. Lett. **38**, 1440 (1977).
[2] R. D. Peccei and H. R. Quinn, Phys. Rev. D **16**, 1791 (1977).
[3] S. Weinberg, Phys. Rev. Lett. **40**, 223 (1978).
[4] F. Wilczek, Phys. Rev. Lett. **40**, 279 (1978).
[5] C. B. Adams, N. Aggarwal, A. Agrawal, R. Balafendiev, C. Bartram, M. Baryakhtar, H. Bekker, P. Belov, K. K. Berggren, A. Berlin *et al.*, arXiv:2203.14923.
[6] A. Caputo and G. Raffelt, Proc. Sci. 454 (**2024**) 041 [arXiv:2401.13728].
[7] A. Sekine and K. Nomura, J. Appl. Phys. **129**, 141101 (2021).
[8] D. E. Kharzeev, Prog. Part. Nucl. Phys. **75**, 133 (2014).
[9] Z. Qiu, G. Cao, and X. G. Huang, Phys. Rev. D **95**, 036002 (2017).
[10] M. L. Bellac, *Thermal Field Theory* (Cambridge University Press, Cambridge, England, 2011), ISBN 978-0-511-88506-8, 978-0-521-65477-7.
[11] D. F. Litim and C. Manuel, Phys. Rep. **364**, 451 (2002).
[12] V. P. Silin, Sov. Phys. JETP **11**, 1136 (1960).
[13] H. A. Weldon, Phys. Rev. D **26**, 1394 (1982).
[14] S. Shakeri and F. Hajkarim, J. Cosmol. Astropart. Phys. 04 (2023) 017.
[15] J. I. McDonald, B. Garbrecht, and P. Millington, J. Cosmol. Astropart. Phys. 12 (2023) 031.
[16] P. Danielewicz, Ann. Phys. (N.Y.) **152**, 239 (1984).
[17] S. Mrowczynski, B. Schenke, and M. Strickland, Phys. Rep. **682**, 1 (2017).
[18] D. Vasak, M. Gyulassy, and H. T. Elze, Ann. Phys. (N.Y.) **173**, 462 (1987).
[19] L. P. Kadanoff and G. Baym, *Quantum Statistical Mechanics* (The Benjamin/Cumming Publishing Company, Inc., Reading, MA, 1981).
[20] K. Hattori, Y. Hidaka, N. Yamamoto, and D. L. Yang, J. High Energy Phys. 02 (2021) 001.
[21] X. G. Huang, P. Mitkin, A. V. Sadofyev, and E. Speranza, J. High Energy Phys. 10 (2020) 117.
[22] S. Lin, Phys. Rev. D **105**, 076017 (2022).
[23] M. Beneke and C. Fidler, Phys. Rev. D **82**, 063509 (2010).
[24] J. D. Jackson, *Classical Electrodynamics* (Wiley, New York, 1998), ISBN 978-0-471-30932-1.
[25] J. F. Nieves and P. B. Pal, Phys. Rev. D **39**, 652 (1989); **40**, 2148(E) (1989).
[26] D. Harari and P. Sikivie, Phys. Lett. B **289**, 67 (1992).
[27] D. Blas, A. Caputo, M. M. Ivanov, and L. Sberna, Phys. Dark Universe **27**, 100428 (2020).
[28] S. M. Carroll, G. B. Field, and R. Jackiw, Phys. Rev. D **41**, 1231 (1990).
[29] S. M. Carroll, Phys. Rev. Lett. **81**, 3067 (1998).
[30] G. C. Liu, S. Lee, and K. W. Ng, Phys. Rev. Lett. **97**, 161303 (2006).
[31] G. C. Liu and K. W. Ng, Phys. Dark Universe **16**, 22 (2017).
[32] Y. Akamatsu and N. Yamamoto, Phys. Rev. Lett. **111**, 052002 (2013).
[33] S. Carignano and C. Manuel, Phys. Rev. D **99**, 096022 (2019).
[34] G. G. Raffelt, Phys. Rev. D **37**, 1356 (1988).
[35] N. V. Mikheev, D. A. Rumyantsev, and Y. E. Shkol‘nikova, Zh. Eksp. Teor. Fiz. **90**, 668 (2009).
[36] A. Caputo, A. J. Millar, and E. Vitagliano, Phys. Rev. D **101**, 123004 (2020).
[37] M. D. Redell, S. Mukherjee, and W. C. Lee, Phys. Rev. B **93**, 241201 (2016).

Chapter 3

Results and discussion

Here we summarize and discuss the results obtained in the works presented in this thesis. In our first work [23] we computed small mass $m \ll T$ corrections to the retarded component of the photon HTL polarization tensor. The computation of the mass corrections is non-trivial, as new IR divergent terms appear due to the small m expansion, which require regularization[1]. We used dimensional regularization (DR) to inspect these divergent terms, as it is a regularization method respectful with the Lorentz and gauge symmetries. After a subtle cancellation of the radial IR divergence with vanishing angular integrals, we found that the apparent IR divergent terms give a finite contribution to the mass corrections. Those last finite pieces are ultimately needed for the Ward-Takahashi identity to hold and can not be correctly reproduced using other regularization methods e.g a sharp cut-off for the radial IR divergent integral. We found that the longitudinal and transverse components, are corrected in the presence of a small mass as

$$\Pi_R^{L,m}(\ell_0,\boldsymbol{\ell}) = \frac{e^2m^2}{2\pi^2}\frac{\boldsymbol{\ell}^2}{\ell_0^2-\boldsymbol{\ell}^2}\ , \tag{3.1a}$$

$$\Pi_R^{T,m}(\ell_0,\boldsymbol{\ell}) = \frac{e^2m^2}{2\pi^2}\frac{\ell_0}{2|\boldsymbol{\ell}|}\ln\left(\frac{\ell_0+|\boldsymbol{\ell}|}{\ell_0-|\boldsymbol{\ell}|}\right)\ , \tag{3.1b}$$

[1] Many authors use Eqs.(5.51) in the book [19] for the small mass corrections to the HTL polarization tensor. Note that in those expressions the angular integrals have been carried out in $d=3$ spatial dimensions. Expanding them for small mass $m \ll T$ produces ill-defined integrals that require regularization. A cutoff regularization would then violate the Ward-Takahashi identity.

where $\ell_0 \to \ell_0 + i0^+$ for retarded boundary conditions. The above corrections should be compared with other corrections computed in the literature, e.g power and two-loop corrections (see Eq.(62) in [23]). While the HTL contribution is proportional to e^2T^2, the mass corrections, even if they do not depend on the temperature, should be viewed as a a correction of order m^2/T^2 with respect to the HTL. Similarly, the power corrections are of order ℓ^2/T^2, while the two-loop results are corrections of order e^2. These three corrections are of the same order if $m, \ell \sim eT$, and should be equally considered. However, if the mass is such that $eT < m \ll T$, then the mass corrections are dominant at soft scales ($\ell \sim eT$). A simple example can be found in Eq.(63) of [23], where we evaluate the impact of the mass correction on the screening mass. Let us recall that Eqs.(3.1a-3.1b) can also be generalized in the presence of a chemical potential. In addition, the mass corrections to the gluon HTL polarization tensor give the same result, after taking into account some color factors

In our second work, we evaluated the impact of including small mass corrections to the collisional energy loss experienced by a heavy and highly energetic fermion, i.e $E, M \gg T$, that traverses the EPP or QGP [25]. The first correct evaluation of the collisional energy loss was done by Braaten and Thoma (BT) [34], assuming massless fermions ($m = 0$). There the authors showed how to effectively separate the contributions from the hard and soft sectors, by introducing an intermediate cutoff separation scale q^* (satisfying $T \gg q^* \gg gT$) in the momentum transfer integrals. The hard sector was evaluated using the bare theory, while the evaluation of the soft sector required the use of HTL resummed propagators. Notably, the momentum transfer integrals of the hard and soft contribution were shown to be IR and UV divergent respectively, but when the two contributions were added both divergences and the dependence on the cut-off separation scale q^* canceled exactly, which led to a finite result. The separation of scales between the hard and soft sectors can also be implemented using DR without the need to introduce a separation scale q^* [39]. We also used this last method, because from the expertise gained in our first work [23] we knew that the Lorentz and gauge symmetries needed to be respected for the correct evaluation of the mass corrections. The inclusion of a small mass ($m \ll T$) in the evaluation of the collisional energy loss is involved, as new IR divergences appear in the radial integrals of the hard contribution, and the mass corrections to the HTL polarization tensor computed in our first work [23] are necessary for the evaluation of the soft contribution. Nevertheless, after a careful analysis of the IR divergent radial integrals of the hard contribution, we showed that they can be rendered finite and the only IR divergence that survives in the hard contribution comes from the momentum transfer integral, which in turn, vanishes with the UV divergence of the momentum transfer integral in the soft contribution. In the case of an EPP, we found that in the regime $E \ll M^2/T$, the leading order result of Braaten and Thoma (BT) [34], is corrected in the presence of a small mass ($m \ll T$) to logarithmic accuracy as

$$-\frac{dE}{dx}\bigg| = -\frac{dE}{dx}\bigg|_{\mathrm{BT}} + \frac{e^4 m^2}{16\pi^3}\left(\frac{3}{v} - \frac{v^2-3}{2v^2}\ln\frac{1+v}{1-v}\right)\ln\left(\frac{1}{e}\right) \ , \tag{3.2}$$

where $v \in [0,1]$ is the velocity of the heavy fermion. In Fig.3.1, we show the plot of the collisional energy loss for different values of the fermion constituent mass. Note that the mass corrections seem to be quite relevant already for values of $m = 0.3\,T$. This suggests that the mass effects in the regime $m \sim T$, where our approximations do not hold, could have a huge impact on the collisional energy loss in an EPP. Notably, we provided in [25] all the necessary tools for the evaluation of the collisional energy loss in that regime. Let us remark that the plot of Fig.3.1 should not be trusted neither in the $v \to 0$ or $v \to 1$ regions, because of the approximations used in the evaluation of the momentum integrals, both in the BT result and the mass corrections. Taking into account those limits can be done after a proper modification of the kinematical constraints [34, 40]. Although our computation was performed for an EPP, it can be extended to the QGP case. In fact, as we explained in Sec.(2), in the context of the QGP created in heavy ion-collisions, it may be reasonable to disregard the masses of up and down quarks, but neglecting the mass of the strange quark may not be such a good approximation. At leading logarithmic accuracy the corrections associated to a massive quark to the QCD collisional energy loss are also given by the QED result, replacing e^2 by g^2 and taking into account a color factor of 2/3. More explicitly

$$\frac{g^4 m^2}{24\pi^3}\left(\frac{3}{v} - \frac{v^2-3}{2v^2}\ln\frac{1+v}{1-v}\right)\ln\left(\frac{1}{g}\right) \ . \tag{3.3}$$

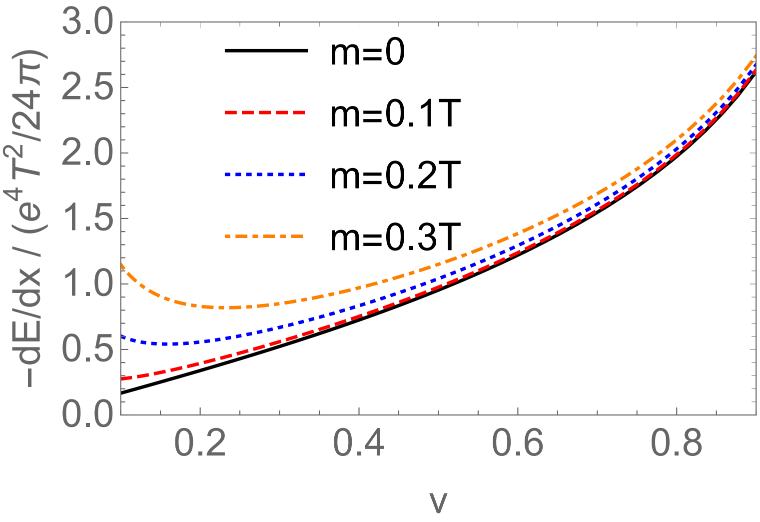

Figure 3.1: Values of the collisional energy loss in QED for different values of the mass of the plasma constituents. The black line corresponds to the massless case (BT), the red dashed line for $m = 0.1\,T$, the blue dashed line for $m = 0.2\,T$, and the orange dot-dashed line $m = 0.3\,T$.

We have evaluated the impact of including strange quark mass corrections to the collisional energy loss of a charm and bottom quark [41], when $T = 250$ MeV, and assuming that the strong fine structure constant is $\alpha_s = g^2/4\pi = 0.2$. Taking the strange quark mass as $m = 100$ MeV, so that $m = 0.4\,T$, we note that in this case the mass corrections are in the 1 to 2 percent level. The effect is certainly not as large as in QED case because of two reasons. First, the gauge coupling constant g is larger in QCD, and second, the contribution of one parton, no matter whether it is massless or massive, can never be too big as compared to the contribution associated to all partons.

In our third work [26] we successfully developed the OSEFT for photons. The formulation of the OSEFT for photons requires a careful treatment of the physical (transverse) and nonphysical (longitudinal and scalar) degrees of freedom of the gauge field. Notably, we showed that the OSEFT Lagrangian can be finally formulated in terms of a gauge invariant vector field without the need to introduce gauge-fixing. Specifically, the nonphysical degrees of freedom can be eliminated from the Lagrangian employing well established EFT techniques, such as integrating out and using local field redefinitions. In addition, we demonstrated the reparametrization invariance (RI) of the theory, which basically means that the theory is respectful with the Lorentz symmetry. Further, in this thesis we have also developed the following applications of the OSEFT for photons, summarized below:

1. By including interactions with soft and hard fermionic fields one can study properties of the EPP. For instance, one can reproduce the HTL fermion self-energy[2].

2. Together with the Schwigner-Keldysh (SK) formalism, the OSEFT can be used to construct a quantum kinetic theory for photons. We showed in [26] that the OSEFT allows to systematically compute quantum corrections to the classical Wigner function, in particular, we correctly reproduced the leading quantum correction ($\sim \hbar$) found in the literature.

3. Exploiting the RI symmetry of the OSEFT, we provided a first principles derivation of the so called side-jump effect, and checked that it coincides with that found in the literature.

4. We elaborated on a proper definition of the Stokes parameters [42] in the context of kinetic theory. The classical definition of the Stokes parameters needs to be modified in the presence of small (side-jump) quantum effects, so as to preserve the Lorentz invariance of the polarization ratios.

As we anticipated in the introduction, we also generalized the OSEFT by including an axion background. We then used the resulting EFT to construct a quantum kinetic theory for photons. However, as explained in Sec.(2), we decided to present in [27] the derivation from the full theory. In this last work, we computed the general Kadanoff-Baym equations obeyed by the photon Wigner function, assuming a collisionless medium. Then, resorting to a gradient expansion, we derived the classical limit of the Kadanoff-Baym equations. Subsequently, by decomposing the photon Wigner function onto a polarization basis, whose components can then be directly related to the Stokes parameters matrix, we derived the dispersion relation and transport equation satisfied by each polarization space component. These last step allowed us to check that the classical kinetic equations captured well known features of axion electrodynamics, such that right and left handed photons obey different dispersion relations and the rotation of the polarization plane, driven by the time evolution of the so called E and B modes. We commented on the

[2]This is not published in our works, but we elaborate it in App.A.

equivalence of our results with those obtained previously in the literature using other methods, and discussed on the suitability of our kinetic theory approach to the topic, as well as how it could be improved. Finally, by considering a high temperature EPP at thermal equilibrium, we addressed the impact of the axion background on the photon collective modes. As expected, the presence of the axion background breaks the degeneracy of the transverse collective modes, as it affects differently the right and left handed many-body excitations in the medium, while the plasmon mode remains unaffected.

Chapter 4

Conclusions

In a first stage of this thesis, we have studied the physical consequences of assuming that the masses of the fermionic constituents of an EPP or a QGP at high temperature and/or density are not strictly zero. As a first approach to address its impact, we have established in [23] how to include small mass corrections $m \ll T$ (and/or $m \ll \mu$) to the HTL photon/gluon polarization tensor. Then, in [25] we evaluated the impact of the mass corrections to the collisional energy loss experienced by a heavy fermion that traverses an EPP or a QGP. Our results indicate that the mass effects can have a significant impact on the collisional energy loss. Notably, we have also paved the way to assess the impact of assuming fermionic masses when these are not small compared to temperature and/or chemical potential, as our results suggest that the mass effects can be large in those regimes.

On the other hand, a certain theoretical methodology has been ubiquitous during the course of this thesis, that is the use of effective field theories. We have seen that these theoretical methods provide a robust framework for the study of the diverse phenomenology exhibited by high temperature and/or density plasmas. In particular, we learned that the effective degrees of freedom governing the physics at the hard scale of a plasma behave like quasiparticles of finite size, thus admitting a description in terms of the OSEFT. We gained expertise on employing the OSEFT for fermions to systematically determine key quantities, e.g the photon/gluon polarization tensor, that are necessary for the evaluation of many thermodynamic plasma properties. A remarkable goal that we achieved in this thesis is the construction of a new effective field theory: the OSEFT for photons [26]. In the context of an EPP, the OSEFT for photons can successfully characterize the effective bosonic degrees degrees of freedom operating at the hard scale. Applications of the OSEFT for photons in the context of an EPP have been presented, namely, in quantum kinetic theory and perturbative computations, which allows us to affirm the validity of the effective field theory. Remarkably, we also studied the effect of an axion background on the photon transport properties and the photon collective modes that occur in an EPP, employing the OSEFT for photons and also the full theory [27], leading to the same results in both cases. Thus, the OSEFT for photons can also have relevant applications in astrophysics and cosmology, as it provides an adequate framework to study the propagation of photons through the use of semi-classical transport equations.

An important objective that we had set ourselves at the beginning of this thesis is learning how to use and develop effective field theories in general, especially in the particular contexts where the medium effects are relevant. Thanks to the work carried out, we can therefore conclude that we have successfully achieved these objectives.

Appendix A

HTL fermion self-energy from the OSEFT

When constructing the OSEFT, one usually starts from the QED Lagrangian

$$\mathcal{L}_{\rm QED} = \overline{\psi}\left(i\not{D} - m\right)\psi - \frac{1}{4}F^{\mu\nu}F_{\mu\nu} \ , \tag{A.1}$$

where $\psi(x)$ is the fermion field and m its mass, also $\not{D} = \gamma^\mu D_\mu$ with $D^\mu = \partial^\mu - ieA^\mu$ the covariant derivative and $F^{\mu\nu} = \partial^\mu A^\nu - \partial^\nu A^\mu$, being A^μ the photon field. The fermion and photon fields are then split into hard and soft parts. In the HTL fermion-self energy (see Fig.(A.1)), the vertex contains a hard photon and both a hard and a soft fermion, so that the relevant Lagrangian for its derivation is

$$\mathcal{L}_{\rm EFT} = \overline{\psi}_v\left(i\not{\partial} - m\right)\psi_v - \frac{1}{4}(\partial^\mu A_v^\nu - \partial^\nu A_v^\mu)^2 + e\left(\overline{\eta}\not{A}_v\psi_v + \overline{\psi}_v\not{A}_v\eta\right) \ , \tag{A.2}$$

being $\eta(x)$ and $\psi_v(x)$ the soft and hard part of the fermion field respectively and $A_v^\mu(x)$ the hard part of the photon field. Then, for positive energies, one performs a momentum decomposition for the hard fields, e.g $K^\mu = Ev^\mu + k^\mu$ where E is the energy, v^μ a light-like vector and k^μ the residual momentum. Also, assuming that $Ev^\mu \gg k^\mu$, the dependence on the hard momenta can be factored out as $\psi_v(x) \sim e^{-iEv\cdot x}\Psi(x)$ and $A_v^\mu(x) \sim e^{-iEv\cdot x}\xi^\mu(x)$. This last expressions are plugged into the Lagrangian of Eq.(A.2) and then, by further decomposing the fields $\Psi(x)$

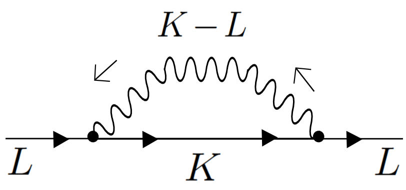

Figure A.1: Fermion-self energy diagram in QED. In the HTL approximation, $K \sim T$ is hard and $L \sim eT$ is soft.

and $\xi^\mu(x)$ using projectors, one can integrate out from the Lagrangian the heavier[1] components. Details on the construction of exact effective OSEFT Lagrangians can be found in [9, 26]. Here, we just need the leading order terms in the OSEFT Lagrangian, to derive the required effective vertex. For the positive energy sector, the leading order terms needed to reproduce the HTL fermion self energy are just

$$\mathcal{L}_{\text{EFT}} \approx \overline{\chi}_v \gamma^0 iv \cdot \partial \chi_v + E\tau^\dagger_{\perp,\mu} g^{\mu\nu} iv \cdot \partial \tau_{\perp,\nu} + e\left(\overline{\chi}_v \gamma^\mu_\perp \tau_{\perp,\mu} \eta + \overline{\eta} \gamma^\mu_\perp \tau^\dagger_{\perp,\mu} \chi_v\right) \;, \quad \text{(A.3)}$$

being $\chi_v(x)$ and $\tau^\mu_\perp(x)$ respectively the effective fermion and photon field. Note that in the above Lagrangian there are only transverse photons, which reflects the gauge invariance of the HTL fermion self-energy at leading order. Also, contrary to the computation of the HTL polarization tensor from the OSEFT, at this order there are no tadpole diagrams, which however appear at subsequent orders in the energy expansion. Let us explain the main steps in the computation. The general structure of the retarded fermion-self energy in the real time formalism can be found in [20, 29]. In the OSEFT, an analogous expression holds, obtained by replacing the full theory propagators and vertices with the corresponding ones in the OSEFT. Explicitly, one can write for the positive energy sector

$$\Sigma_{\text{OSEFT}}(L) = \frac{i}{2} \sum_{E,v} \int \frac{d^4k}{(2\pi)^4} V_\mu(k) \left[S_S(k) D^{\mu\nu}_A(p) + S_R(k) D^{\mu\nu}_S(p) \right] V_\nu(p) \;. \quad \text{(A.4)}$$

where $V_\mu(k)$ is an OSEFT vertex which generally depends on momentum, also $S_X(k)$ and $D^{\mu\nu}_X(p)$ with $X = A, R, S$ are the fermion and photon propagator components in the Keldysh representation respectively. Note that k^μ is the resiudal momenta and $p^\mu = k^\mu - L^\mu$ where L^μ is the external (soft) fermion momenta. The sum over all E and v^μ is needed because of the decomposition performed in the full theory

[1]Each projected component has different power counting in E^n $(n = 0, 1, 2 \ldots)$ and by heavier we mean those with the highest n.

momentum K^μ. The general form of the fermion propagators in the OSEFT can be found, for instance, in our first work [23] and the general expression for the thermal photon propagator in the OSEFT is [26]

$$D^{\mu\nu}_{A,R}(p) = -\frac{P^{\mu\nu}_\perp}{2E}\frac{1}{p_0 - f(\boldsymbol{p}) \mp i0^+} \ , \tag{A.5a}$$

$$D^{\mu\nu}_{S}(p) = \frac{P^{\mu\nu}_\perp}{2E} i2\pi\delta(p_0 - f(\boldsymbol{p}))[1 + 2n_B(E + p_0)] \ . \tag{A.5b}$$

where $P^{\mu\nu}_\perp$ is a transverse projector and $f(\boldsymbol{p})$ is the OSEFT dispersion relation. Although in practical computations the general expressions for the propagators need to be expanded at a fixed order in $1/E$, it is recommended to keep them unexpanded for the seek of general expressions for the self-energies [10]. Using the definitions of the OSEFT propagators one can write Eq.(A.4) as

$$\Sigma_{\rm OSEFT}(L) = \frac{i}{2}\sum_{E,v}\int \frac{d^4k}{(2\pi)^4} V_\mu(k)\frac{\not{v}}{2}P^{\mu\nu}_\perp V_\nu(p)$$
$$\times\frac{1}{2E}\left\{\frac{i2\pi\delta(k_0 - f(\boldsymbol{k},m))[1 - 2n_F(E + k_0)]}{p_0 - f(\boldsymbol{p}) - i0^+} + \frac{i2\pi\delta(p_0 - f(\boldsymbol{p}))[1 + 2n_B(E + p_0)]}{k_0 - f(\boldsymbol{k},m) + i0^+}\right\} . \tag{A.6}$$

The HTL fermion self-energy can be obtained by expanding the general vertex in $1/E$ and keeping the leading order term. Precisely

$$V^\mu(k) = V^\mu_{(0)} + \frac{1}{E}V^\mu_{(1)}(k) + \dots \ , \tag{A.7}$$

with $V^\mu_{(0)} = e\gamma^\mu_\perp$, as is derived from the Lagrangian in Eq.(A.3). Then, integrating over k_0 and subsequently expanding the expression inside the brackets of Eq.(A.6) to leading order, one reaches to

$$\Sigma^{\rm htl}_{\rm OSEFT}(L) = -\frac{e^2}{4}\sum_{E,v}\int \frac{d^3\boldsymbol{k}}{(2\pi)^3}\frac{n_F(E) + n_B(E)}{E}\frac{\gamma_{\perp,\mu}\not{v}\gamma^\mu_\perp}{v\cdot L} \ . \tag{A.8}$$

Resorting now to the general form of the fermion self-energy[2], one notes that there are only two independent scalar functions, given by

$$\mathrm{Tr}\left(\not{L}\Sigma^{\rm htl}_{\rm OSEFT}(L)\right) = 4e^2\sum_{E,v}\int\frac{d^3\boldsymbol{k}}{(2\pi)^3}\frac{n_F(E) + n_B(E)}{E} \ , \tag{A.9a}$$

[2]That is $\Sigma = A\not{L} + B\gamma^0$ [20], where the scalar functions $A = A(L^2)$ and $B = B(L^2)$ are given by $A = -\frac{1}{4\boldsymbol{\ell}^2}\left[\mathrm{Tr}\left(\not{L}\Sigma\right) - \ell_0\mathrm{Tr}\left(\gamma^0\Sigma\right)\right]$ and $B = -\frac{1}{4\boldsymbol{\ell}^2}\left[\boldsymbol{\ell}^2\mathrm{Tr}\left(\gamma^0\Sigma\right) - \ell_0\mathrm{Tr}\left(\not{L}\Sigma\right)\right]$ respectively.

$$\mathrm{Tr}\left(\gamma^0\Sigma^{\mathrm{htl}}_{\mathrm{OSEFT}}(L)\right) = 4e^2\sum_{E,v}\int\frac{d^3\boldsymbol{k}}{(2\pi)^3}\frac{n_F(E)+n_B(E)}{E}\frac{1}{v\cdot L}\ . \tag{A.9b}$$

Before computing the integrals, in the OSEFT one usually moves back to the full theory variables [9, 10]. At leading order in $1/E$ this step is trivial, for instance, using the notation $K^\mu = (K_0, \boldsymbol{K})$ for the full theory momentum, one has $E \approx E_K$, $v^\mu \approx v^\mu_K$ and $n_{F,B}(E) \approx n_{F,B}(E_K)$ being $E_K = |\boldsymbol{K}|$ and $v^\mu_K = (1, \boldsymbol{K}/E_K)$. In addition, one uses the association [10]

$$\sum_{E,v}\int\frac{d^3\boldsymbol{k}}{(2\pi)^3} \equiv \int\frac{d^3\boldsymbol{K}}{(2\pi)^3}\ . \tag{A.10}$$

After moving back to the full theory variables one can perform the required radial and angular integrals, which are finite at this order. Hence, after also adding the negative energy sector contribution, which gives an overall factor of two, one gets

$$\mathrm{Tr}\left(\not{L}\Sigma^{\mathrm{htl}}(L)\right) = 4m_F^2\ , \tag{A.11a}$$

$$\mathrm{Tr}\left(\gamma^0\Sigma^{\mathrm{htl}}(L)\right) = 2m_F^2\frac{1}{|\boldsymbol{\ell}|}\ln\left(\frac{\ell_0+|\boldsymbol{\ell}|}{\ell_0-|\boldsymbol{\ell}|}\right)\ , \tag{A.11b}$$

with $m_F^2 = e^2T^2/8$ the QED fermion thermal mass. The above result coincides with that found in the literature (see e.g [20, 29]). Recapitulating, we have shown that by including interactions with soft and hard fermionic fields to the OSEFT for photons one can reproduce the HTL fermion-self energy. Thus, we conclude that the OSEFT for photons can successfully characterize the effective photon degrees of freedom operating at the hard scale ($\sim T$) of an EPP.

Bibliography

[1] A. Bazavov et al. "The chiral and deconfinement aspects of the QCD transition". In: *Phys. Rev. D* 85 (2012), p. 054503. DOI: 10.1103/PhysRevD.85.054503. arXiv: 1111.1710 [hep-lat].

[2] Philippe de Forcrand. "Simulating QCD at finite density". In: *PoS* LAT2009 (2009). Ed. by Chuan Liu and Yu Zhu, p. 010. DOI: 10.22323/1.091.0010. arXiv: 1005.0539 [hep-lat].

[3] Luciano Rezzolla et al., eds. *The Physics and Astrophysics of Neutron Stars*. Vol. 457. Astrophysics and Space Science Library. Springer, 2018. ISBN: 978-3-319-97615-0, 978-3-319-97616-7. DOI: 10.1007/978-3-319-97616-7.

[4] Rod G. Greaves, Mark D. Tinkle, and C. M. Surko. "Creation and uses of positron plasmas". In: *Physics of Plasmas* 1 (1994), pp. 1439–1446. URL: https://api.semanticscholar.org/CorpusID:55023235.

[5] Edward W. Kolb. *The Early Universe*. Vol. 69. Taylor and Francis, May 2019. ISBN: 978-0-429-49286-0, 978-0-201-62674-2. DOI: 10.1201/9780429492860.

[6] Michael E. Peskin and Daniel V. Schroeder. *An Introduction to quantum field theory*. Reading, USA: Addison-Wesley, 1995. ISBN: 978-0-201-50397-5, 978-0-429-50355-9, 978-0-429-49417-8. DOI: 10.1201/9780429503559.

[7] A. V. Manohar. "Effective field theories". In: *Lect. Notes Phys.* 479 (1997). Ed. by H. Latal and W. Schweiger, pp. 311–362. DOI: 10.1007/BFb0104294. arXiv: hep-ph/9606222.

[8] Aneesh V. Manohar. "Introduction to Effective Field Theories". In: (Apr. 2018). Ed. by Sacha Davidson et al. DOI: 10.1093/oso/9780198855743.003.0002. arXiv: 1804.05863 [hep-ph].

[9] Cristina Manuel and Juan M. Torres-Rincon. "Chiral transport equation from the quantum Dirac Hamiltonian and the on-shell effective field theory". In: *Phys. Rev. D* 90.7 (2014), p. 076007. DOI: 10.1103/PhysRevD.90.076007. arXiv: 1404.6409 `[hep-ph]`.

[10] Cristina Manuel, Joan Soto, and Stephan Stetina. "On-shell effective field theory: A systematic tool to compute power corrections to the hard thermal loops". In: *Phys. Rev. D* 94.2 (2016). [Erratum: Phys.Rev.D 96, 129901 (2017)], p. 025017. DOI: 10.1103/PhysRevD.94.025017. arXiv: 1603.05514 `[hep-ph]`.

[11] W. E. Caswell and G. P. Lepage. "Effective Lagrangians for Bound State Problems in QED, QCD, and Other Field Theories". In: *Phys. Lett. B* 167 (1986), pp. 437–442. DOI: 10.1016/0370-2693(86)91297-9.

[12] G. P. Lepage and B. A. Thacker. "Effective Lagrangians for Simulating Heavy Quark Systems". In: *Nucl. Phys. B Proc. Suppl.* 4 (1988). Ed. by A. Billoire et al., p. 199. DOI: 10.1016/0920-5632(88)90102-8.

[13] Howard Georgi. "An Effective Field Theory for Heavy Quarks at Low-energies". In: *Phys. Lett. B* 240 (1990), pp. 447–450. DOI: 10.1016/0370-2693(90)91128-X.

[14] Nora Brambilla et al. "Potential NRQCD: An Effective theory for heavy quarkonium". In: *Nucl. Phys. B* 566 (2000), p. 275. DOI: 10.1016/S0550-3213(99)00693-8. arXiv: hep-ph/9907240.

[15] Christian W. Bauer et al. "An Effective field theory for collinear and soft gluons: Heavy to light decays". In: *Phys. Rev. D* 63 (2001), p. 114020. DOI: 10.1103/PhysRevD.63.114020. arXiv: hep-ph/0011336.

[16] Robert D. Pisarski. "Scattering amplitudes in hot gauge theories". In: *Phys. Rev. Lett.* 63 (11 Sept. 1989), pp. 1129–1132. DOI: 10.1103/PhysRevLett.63.1129. URL: https://link.aps.org/doi/10.1103/PhysRevLett.63.1129.

[17] Eric Braaten and Robert D. Pisarski. "Soft amplitudes in hot gauge theories: A general analysis". In: *Nuclear Physics B* 337.3 (1990), pp. 569–634. ISSN: 0550-3213. DOI: https://doi.org/10.1016/0550-3213(90)90508-B. URL: https://www.sciencedirect.com/science/article/pii/055032139090508B.

[18] J. Frenkel and J.C. Taylor. "High-temperature limit of thermal QCD". In: *Nuclear Physics B* 334.1 (1990), pp. 199–216. ISSN: 0550-3213. DOI: https://doi.org/10.1016/0550-3213(90)90661-V. URL: https://www.sciencedirect.com/science/article/pii/055032139090661V.

[19] J. I. Kapusta and Charles Gale. *Finite-temperature field theory: Principles and applications*. Cambridge Monographs on Mathematical Physics. Cambridge University Press, 2011. ISBN: 978-0-521-17322-3, 978-0-521-82082-0, 978-0-511-22280-1. DOI: 10.1017/CBO9780511535130.

[20] Michel Le Bellac. *Thermal Field Theory*. Cambridge Monographs on Mathematical Physics. Cambridge University Press, Mar. 2011. ISBN: 978-0-511-88506-8, 978-0-521-65477-7. DOI: 10.1017/CBO9780511721700.

[21] Mikko Laine and Aleksi Vuorinen. *Basics of Thermal Field Theory*. Vol. 925. Springer, 2016. DOI: 10.1007/978-3-319-31933-9. arXiv: 1701.01554 [hep-ph].

[22] Jacopo Ghiglieri et al. "Perturbative Thermal QCD: Formalism and Applications". In: *Phys. Rept.* 880 (2020), pp. 1–73. DOI: 10.1016/j.physrep.2020.07.004. arXiv: 2002.10188 [hep-ph].

[23] Marc Comadran and Cristina Manuel. "Mass corrections to the hard thermal or dense loops". In: *Phys. Rev. D* 104.7 (2021), p. 076006. DOI: 10.1103/PhysRevD.104.076006. arXiv: 2106.08904 [hep-ph].

[24] Cristina Manuel and Juan M. Torres-Rincon. "Chiral kinetic theory with small mass corrections and quantum coherent states". In: *Phys. Rev. D* 103.9 (2021), p. 096022. DOI: 10.1103/PhysRevD.103.096022. arXiv: 2101.05832 [hep-ph].

[25] Marc Comadran, Cristina Manuel, and Stefano Carignano. "Accounting for plasma constituent mass effects in heavy fermion energy loss calculations in hot QED and QCD". In: *Phys. Rev. D* 107.11 (2023), p. 116016. DOI: 10.1103/PhysRevD.107.116016. arXiv: 2304.14182 [hep-ph].

[26] Marc Comadran and Cristina Manuel. "On-shell effective field theory and quantum transport for hard photons". In: *Phys. Rev. D* 110 (9 Nov. 2024), p. 096024. DOI: 10.1103/PhysRevD.110.096024. URL: https://link.aps.org/doi/10.1103/PhysRevD.110.096024.

[27] Marc Comadran and Cristina Manuel. "Photon quantum kinetic equations and collective modes in an axion background". In: *Phys. Rev. D* 109.9 (2024), p. 096003. DOI: 10.1103/PhysRevD.109.096003. arXiv: 2402.18254 `[hep-ph]`.

[28] R. D. Peccei and Helen R. Quinn. "CP Conservation in the Presence of Instantons". In: *Phys. Rev. Lett.* 38 (1977), pp. 1440–1443. DOI: 10.1103/PhysRevLett.38.1440.

[29] Markus H. Thoma. "New developments and applications of thermal field theory". In: (Oct. 2000). arXiv: hep-ph/0010164.

[30] Jean-Paul Blaizot and Edmond Iancu. "The Quark gluon plasma: Collective dynamics and hard thermal loops". In: *Phys. Rept.* 359 (2002), pp. 355–528. DOI: 10.1016/S0370-1573(01)00061-8. arXiv: hep-ph/0101103.

[31] Stanislaw Mrowczynski, Bjoern Schenke, and Michael Strickland. "Color instabilities in the quark–gluon plasma". In: *Phys. Rept.* 682 (2017), pp. 1–97. DOI: 10.1016/j.physrep.2017.03.003. arXiv: 1603.08946 `[hep-ph]`.

[32] Eric Braaten and Robert D. Pisarski. "Resummation and Gauge Invariance of the Gluon Damping Rate in Hot QCD". In: *Phys. Rev. Lett.* 64 (1990), p. 1338. DOI: 10.1103/PhysRevLett.64.1338.

[33] Eric Braaten and Robert D. Pisarski. "Calculation of the gluon damping rate in hot QCD". In: *Phys. Rev. D* 42 (1990), pp. 2156–2160. DOI: 10.1103/PhysRevD.42.2156.

[34] Eric Braaten and Markus H. Thoma. "Energy loss of a heavy fermion in a hot plasma". In: *Phys. Rev. D* 44 (1991), pp. 1298–1310. DOI: 10.1103/PhysRevD.44.1298.

[35] Stefano Carignano, Cristina Manuel, and Joan Soto. "Power corrections to the HTL effective Lagrangian of QED". In: *Phys. Lett. B* 780 (2018), pp. 308–312. DOI: 10.1016/j.physletb.2018.03.012. arXiv: 1712.07949 `[hep-ph]`.

[36] Julian S. Schwinger. "Brownian motion of a quantum oscillator". In: *J. Math. Phys.* 2 (1961), pp. 407–432. DOI: 10.1063/1.1703727.

[37] L. V. Keldysh. "Diagram technique for nonequilibrium processes". In: *Zh. Eksp. Teor. Fiz.* 47 (1964), pp. 1515–1527.

[38] L.P. Kadanoff and G. Baym. *Quantum Statistical Mechanics*. New York: W.A. Benjamin Inc., 1962.

[39] Stefano Carignano and Cristina Manuel. "Measuring chiral imbalance with collisional energy loss". In: *Phys. Rev. D* 103.11 (2021), p. 116002. DOI: 10.1103/PhysRevD.103.116002. arXiv: 2103.02491 [hep-ph].

[40] Stephane Peigne and Andre Peshier. "Collisional Energy Loss of a Fast Muon in a Hot QED Plasma". In: *Phys. Rev. D* 77 (2008), p. 014015. DOI: 10.1103/PhysRevD.77.014015. arXiv: 0710.1266 [hep-ph].

[41] Eric Braaten and Markus H. Thoma. "Energy loss of a heavy quark in the quark - gluon plasma". In: *Phys. Rev. D* 44.9 (1991), R2625. DOI: 10.1103/PhysRevD.44.R2625.

[42] John David Jackson. *Classical Electrodynamics*. Wiley, 1998. ISBN: 978-0-471-30932-1.